

UNCLASSIFIED

A117F

F19628-76-C-0040

NL

1 OF 2
AD A049260

AD
A049260

100

RADC-TR-77-345



RADC-TR-77-345
Final Technical Report
October 1977

Handwritten signature

(2)



PERSPECTIVE NAVIGATION SYSTEM

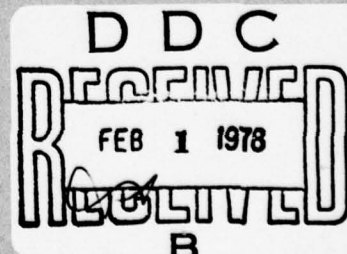
Proteon Associates, Inc.

AD A 0 49260

Approved for public release; distribution unlimited.

AD *initials*
DDC FILE COPY

ROME AIR DEVELOPMENT CENTER
AIR FORCE SYSTEMS COMMAND
GRIFFISS AIR FORCE BASE, NEW YORK 13441



This report has been reviewed by the RADC Information Office (OI) and is releasable to the National Technical Information Service (NTIS). At NTIS it will be releasable to the general public, including foreign nations.

APPROVED:

Uve H. W. Lammers

UVE H. W. LAMMERS
Contract Monitor
Propagation Branch
Electromagnetic Sciences Division

APPROVED:

Edward A. Lewis

EDWARD LEWIS, Chief
Propagation Branch
Electromagnetic Sciences Division

APPROVED:

Allan C. Schell

ALLAN C. SCHELL
Acting Chief
Electromagnetic Sciences Division

FOR THE COMMANDER:

John P. Huss

19 REPORT DOCUMENTATION PAGE		READ INSTRUCTIONS BEFORE COMPLETING FORM	
1. REPORT NUMBER RADC-TR-77-345	2. GOVT ACCESSION NO.	3. RECIPIENT'S CATALOG NUMBER	
4. TITLE (and Subtitle) PERSPECTIVE NAVIGATION SYSTEM.		5. TYPE OF REPORT & PERIOD COVERED Final rept. Aug 75 - May 77	
7. AUTHOR(s) Howard Salwen Henry Arbour		6. PERFORMING ORG. REPORT NUMBER A117F	
9. PERFORMING ORGANIZATION NAME AND ADDRESS Proteon Associates, Inc. 24 Crescent St. Waltham, MA 02154		10. PROGRAM ELEMENT, PROJECT, TASK AREA & WORK UNIT NUMBER 62101F 86820602	
11. CONTROLLING OFFICE NAME AND ADDRESS Deputy for Electronic Technology (RADC) Hanscom AFB, MA 01731 Contract Monitor: Uve H.W. Lammers/ETEN		12. REPORT DATE Oct 77	
14. MONITORING AGENCY NAME & ADDRESS (if different from Controlling Office)		13. NUMBER OF PAGES 110	
16. DISTRIBUTION STATEMENT (of this Report) Approved for Public Release; Distribution Unlimited		15. SECURITY CLASS. (of this report) unclassified	
17. DISTRIBUTION STATEMENT (of the abstract entered in Block 20, if different from Report)		15a. DECLASSIFICATION/DOWNGRADING SCHEDULE	
18. SUPPLEMENTARY NOTES			
19. KEY WORDS (Continue on reverse side if necessary and identify by block number) Navigation Interferometer Multipath			
20. ABSTRACT (Continue on reverse side if necessary and identify by block number) This report describes a perspective navigation system which employs a K-band interferometer mounted on an aircraft or similar platform. The interferometer measures angle of arrival of signals from an array of six ground mounted transmitters. The angle measurement data is processed by a least-squares algorithm which computes the position and orientation of the ground array relative to the interferometer coordinate system. A perspective display of the ground array is generated based on the derived position/orientation data. (Continued)			

DD FORM 1 JAN 73 1473

EDITION OF 1 NOV 65 IS OBSOLETE

unclassified

SECURITY CLASSIFICATION OF THIS PAGE (When Data Entered)

391 719

Hw

DDC
RECEIVED
FEB 1 1978
B

unclassified

SECURITY CLASSIFICATION OF THIS PAGE(When Data Entered)

The system is designed to operate at extremely low elevation angles where multipath is the dominant problem. An experimental effort was carried out to demonstrate the techniques. The results obtained are included in the report. System errors were shown to be small enough to allow aircraft landing based on the perspective display data under worst-case conditions.

ACCESSION for	
NTIS	White Section <input checked="" type="checkbox"/>
DDC	Buff Section <input type="checkbox"/>
UNANNOUNCED	<input type="checkbox"/>
JUSTIFICATION _____	
BY _____	
DISTRIBUTION/AVAILABILITY CODES	
AVAIL. and/or SPECIAL	
11	

unclassified

SECURITY CLASSIFICATION OF THIS PAGE(When Data Entered)

EVALUATION

F19628-76-C-0040

1. This document is the Final Report under this contract. It describes the second phase of a program to develop a precision microwave navigation system capable of the perspective display of the positions of a series of reference transmitters on-board a navigating vehicle. The motivation for this research was the need to develop an Independent Landing Monitor System (ILM), suitable as a future independent landing aid in conjunction with the Microwave Landing System (MLS) to provide a perspective high resolution display of the runway outline to the pilot under adverse weather conditions. In more general terms this research was intended to provide precision position and attitude information under severe multipath and GDOP conditions.

2. The first phase of the work under contract F19628-75-C-0087 addressed the feasibility of microwave interferometric measurements under multipath conditions and ambiguity resolution techniques of long-base line microwave interferometers. The second phase dealt with the implementation of an advanced system consisting of 6 reference transmitters and a complete receiving system to make precision angular measurements in azimuth and elevation of the reference transmitter positions, and to process and display this information into a perspective view of the transmitter network. Actual measurements in the field were performed.

3. The contract was completely successful in demonstrating the feasibility of the concept. In simulated landing situations (the receiving system was suspended on the side of a 100-foot tower and viewed the spatial layout of

transmitters from various heights and under various tilt angles) the proper perspective displays could be demonstrated. In its present form, however, the system is not and could not be intended to be suitable for actual flight-testing. The contractor has lined out the necessary steps that have to be taken to reach this stage. Current funding does not allow the continuation of this program.

Uve H. W. Lammers
UVE H. W. LAMMERS
Contract Monitor
Propagation Branch
Electromagnetic Sciences Division

TABLE OF CONTENTS

	<u>Page</u>
1. INTRODUCTION	
1.1 Background	1
1.2 Objective	1
1.3 Contents of the Report	2
2. THEORY OF OPERATION	4
2.1 Basic System Configuration	4
2.2 System Design Criteria	7
2.2.1 Noise and Dynamic Errors	8
2.2.2 Multipath Errors	12
2.2.3 Geometric Dilution of Precision	12
2.3 Processing Alternatives	12
2.4 Other System Configurations and Applications	13
3. HARDWARE DESCRIPTION OF THE TEST SYSTEM	14
3.1 Overall System Description and Specifications	14
3.2 Transmitting System	16
3.2.1 Transmitter Sequencing Box	18
3.2.2 Remote Transmitters	21
3.3 Receiving System	21
3.3.1 Microwave Front End	23
3.3.2 First IF	25
3.3.3 Signal Limiter	25
3.3.4 Phase-Locked Loop	26
3.3.5 System Timing Card	31
3.3.6 Local Oscillators	32
3.3.7 Power Supplies	34
3.4 Data Processing and Display System	34
3.4.1 Microprocessor Operating Program	35
3.4.2 Least Squares Estimation	46
3.4.3 Perspective Display Program	46
4. EXPERIMENTATION	52
4.1 Objectives of the Experiment	52
4.1.1 Multipath Effects	52
4.1.2 Performance Capabilities	52
4.2 Experimental Set-Up and Procedure	53
4.2.1 Experiment Configuration	53
4.2.2 Output Monitoring and Recording	54
4.2.3 Startup and Calibration Procedures	54
4.2.4 Experimental Procedure	55
4.3 Test Results	57
4.3.1 Calibration Results	57
4.3.2 Multipath Results	58
4.3.3 Shaped Beam Improved Results	61

4.4	Performance Demonstration Results	63
4.4.1	Demonstration Configuration	63
4.4.2	Demonstration Procedure	63
4.4.3	Display Output and Test Results	64
4.5	Conclusion	6
5.	CONCLUSIONS	68
5.1	Results of the Program	68
5.1.1	Basic Measurement Accuracy	68
5.1.2	Multipath Performance	69
5.1.3	Perspective Display	69
5.2	Recommendations	69
5.2.1	Hardware Improvements	70
5.2.2	Software Improvements	70
5.2.3	Display Equipment	71
5.2.4	Other Applications	71
APPENDIX A.	SCHEMATIC DIAGRAMS	A1
APPENDIX B.	SDK 80 OPERATING PROGRAM	B1
APPENDIX C.	PERSPECTIVE DISPLAY PROGRAM	C1

LIST OF FIGURES

Fig. 2.1. System Geometric Configuration	5
Fig. 2.2. Overall System Block Diagram	6
Fig. 3.1. Overall Block Diagram of Test System	15
Fig. 3.2. Transmitter Block Diagram	17
Fig. 3.3. TDM Timing Diagram	19
Fig. 3.4. Receiver Block Diagram	22
Fig. 3.5. Receiving Horn Antenna Configuration	24
Fig. 3.6. Limiter Signal D.C. Output	27
Fig. 3.7. PLL Block Diagram	28
Fig. 3.8. L.O. System Block Diagram	33
Fig. 3.9. Microprocessor Routines Block Diagram	37
Fig. 3.10. Translation Coordinates	40
Fig. 3.11. Rotation Sense	41
Fig. 3.12. Beacon Geometry and Coordinates	44
Fig. 4.1. Slotted Array Gain/Angle Plot	56
Fig. 4.2. Diffuse Multipath Data Errors	59
Fig. 4.3. Specular Multipath Data Errors	60
Fig. 4.4. Shaped Beam Specular Multipath Data Errors	62

LIST OF TABLES

Table 3.1. Least-Squares Coordinate Estimation Errors	47
Table 4.1. Observed Solution Coordinate Errors	65

1. INTRODUCTION

This document constitutes the Final Report prepared by Proteon Associates, Inc., Waltham, Massachusetts for the Deputy for Electronic Technology (RADC), Hanscom Air Force Base, Massachusetts under Contract No. F19628-76-C-0040 entitled Perspective Navigation System.

1.1 Background

Under Contract No. F19628-75-C-0087, experiments were conducted in cooperation with AFCRL personnel which validated an interferometer measurement scheme for application in a perspective display navigation/landing system. The scheme employs a crossed-baseline K-band interferometer mounted on-board the aircraft which measures the angles to a number of beacon transmitters located around the perimeter of the runway. The data collected is processed to generate a perspective display of the runway and a horizon reference line.

1.2 Objective

The objective of this effort is to develop equipment which demonstrates the feasibility of the perspective display concept. The equipment developed under the first phase of this contract included 3 beacon transmitters, a single interferometer receiver and phase data extractor, a digital data processing system, and a display subsystem. The effort also included field tests and demonstrations at RADC/ET, Hanscom AFB, Massachusetts.

Under Contract Modification P00001 the transmitting system was increased to six transmitters and the receiving system was increased to provide both horizontal and vertical interferometers simultaneously. This increase in system capability allowed for the generation of a perspective display of the 3-dimensional configuration of the beacon transmitters. In other words, the interferometer system collects sufficient data to determine its position relative to the beacon array which is mounted on the ground. In addition, the interferometer data also determines the

orientation of the interferometer coordinate system relative to the ground coordinate system. The system is thus useful for the implementation of an independent landing monitor which incorporates a cockpit mounted heads-up display. The system may also be used for any application in which it is desired to obtain vehicle orientation data in addition to vehicle position data.

It is typical that systems of the type described in this report must contend with severe multipath problems. The usual methods for discrimination against multipath such as antenna pattern shaping, doppler discrimination, or time delay discrimination, do not work well in the landing system configuration. In particular, the angle-of-arrival of the multipath signal is too close to the angle-of-arrival of the desired signal to allow antenna discrimination. Similarly, the time delay difference and the doppler difference between the desired signal and the multipath signal are too small to allow these means of multipath discrimination. The system under consideration in this report utilizes redundancy to combat the multipath problem. That is, a sufficient number of measurements are carried out per measurements cycle to allow for an overdetermined solution for the position and orientation of the vehicle relative to the ground coordinate system. In this way, The digital processing of the measurement data can incorporate a data screening algorithm which rejects measurements which are obviously corrupted by multipath. One of the important objectives of the experimental effort described in this report was to demonstrate that the interferometer system using overdetermined solutions for position and orientation of the vehicle provides a means for multipath rejection.

1.3 Contents of the Report

Section 2 contains a discussion of the theory of operation of the perspective display navigation system. The discussion emphasizes the design trade-offs leading to a working operational system. It also gives consideration to the design of the demonstration test-bed produced under this contractual effort. Section 3 presents a detailed hardware and software description of the demonstration system. Extensive discussions of the receiving system, the data processing system and the display systems are given. Section 4 describes the experimental effort carried out during the course of this contractual effort. The experimental set-up and procedures are described in detail. The results obtained are described. It is shown that the

system does in fact provide high accuracy position and orientation data and is not significantly affected by multipath. Section 5 contains a summary of conclusions derived during the course of the program and recommendations for future activities in this area.

2. THEORY OF OPERATION

This section presents a brief discussion of the theory of operation of the perspective navigation system. The discussion begins with a review of the system consideration. Then system design trade-offs are reviewed.

2.1 Basic System Configuration

The basic system configuration is shown in Fig. 2.1. We have chosen to use 6 ground transmitters in a hexagon array. The transmitters are interconnected such that they transmit in sequence, one following the other. In addition, a coherent reference generated at one of the transmitter modules is supplied to all the others so that the transmitter outputs are coherent. The transmitted carrier frequency is nominally 15 GHz. The sequencing rate is a function of mission constraints.

The airborne portion of the system employs a crossed baseline interferometer. We have chosen to use an interferometer which employs two antenna separations. The closer pairs measure coarse angles while the wider separated antenna pairs make fine angle measurements. The fine measurements are accurate but ambiguous. The coarse measurements are used to resolve the fine measurement ambiguities. This operation is carried out for both vertical and horizontal angular measurements as indicated in Fig. 2.1.

The interferometer antenna outputs are processed by an RF-IF system as shown in Fig. 2.2. The RF-IF subsystem as shown in Fig. 2.2 also includes phase measurements circuitry which measures the relative phases between the master antenna, denoted by "REF" in Fig. 2.1 and the coarse and fine vertical and horizontal antennas. Four relative phase measurements are produced in this way during each cycle of transmission from each of the ground beacon transmitters. The 4 measurements are read-out by a preprocessor subsystem. The preprocessor provides a number of important functions. First, by monitoring the RF-IF circuitry it establishes synchronism between the operations carried out in the phase measurement circuitry and the transmission sequence. This synchronism is established by detecting and tracking a gap between the transmission of transmitter F in Fig. 2.1 and transmitter A. There is no gap between the other transmissions. This operation

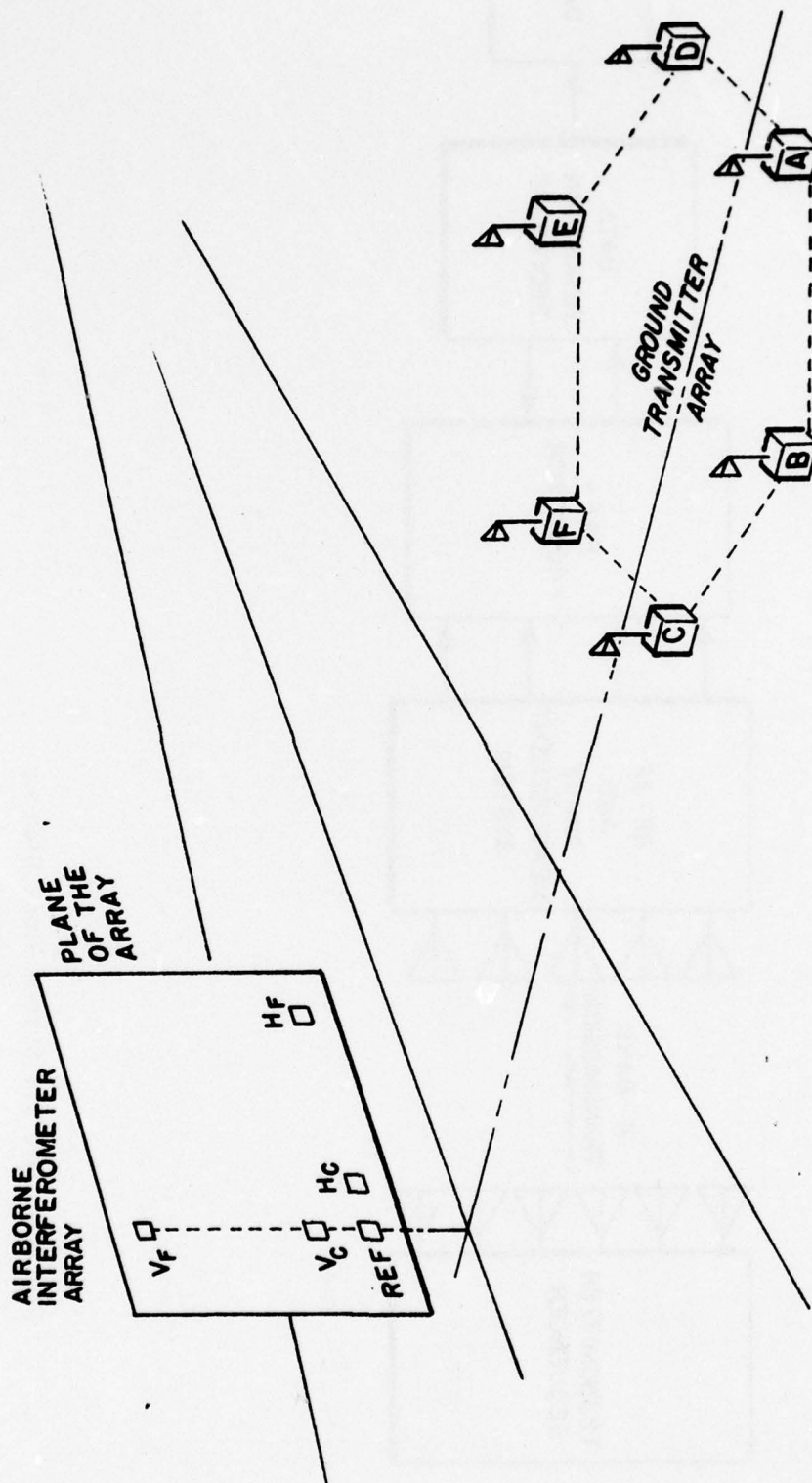


Fig. 2.1. System Geometric Configuration

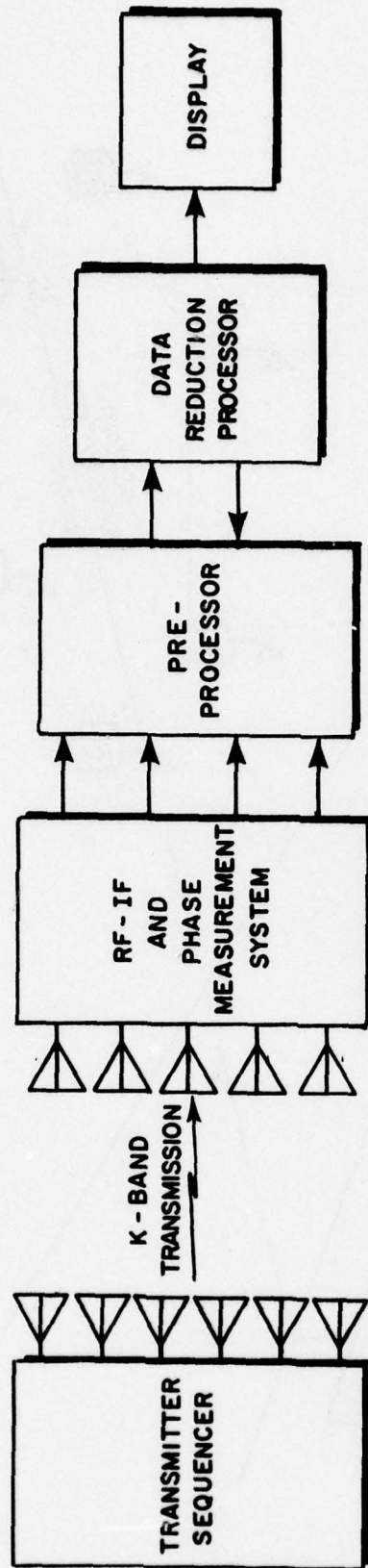


Fig.2.2. Overall System Block Diagram

is discussed in more detail in Section 3. The preprocessor, having established synchronism between the transmission and reception processes reads the phase measurement data created by each transmission cycle. The data consists of a coarse and fine angle measurement for the vertical and horizontal interferometers. The preprocessor uses an ambiguity resolution algorithm to combine the coarse and fine data. Next, The preprocessor smooths the ambiguity resolved data by forming a weighted average of past angle estimates and the current angle estimates.

The preprocessor interrupts the data reduction processor when ambiguity resolved data becomes available. This data consists of 12 measurements. In particular, there are vertical and horizontal angular measurements computed for each of the 6 ground beacon transmissions. The data reduction processor uses these 12 measurements per transmission sequence to compute 6 position and orientation unknowns. These are the range azimuth and elevation of the center of the ground array coordinate system relative to the coordinate system of the airborne array and the roll, pitch, and yaw of the ground array configuration relative to the airborne interferometer coordinate system. As currently configured, the data reduction processor uses a straightforward least-squares reduction procedure to derive the position and orientation data from the angle data. However, recursive formulations and the Kalman-Bucy filtering approach are suitable for this application. The results of the data reduction procedure are displayed in terms of a perspective view of the ground transmitter array. The perspective view is varied as a function of the position and orientation of the interferometer array relative to the ground transmitter coordinate system. The experimental system described in this report utilized an Intel SDK-80 as the preprocessor. A Wang 2200S calculator was employed for data reduction processing and for the perspective display.

2.2 System Design Criteria

This section discusses some of the design trade-offs associated with the perspective navigation system technique. The discussion is intended to be general so that it could be used for the design of operational systems with variable

performance requirements and constraints. On the other hand, the discussion of Section 3 is directed toward the implementation of a feasibility test system.

2.2.1 Noise and Dynamic Errors

The phase measurement circuitry of the system employs phase locked loops to filter the signals received by the interferometer array antennas. The tracking bandwidths of these phase locked loops determine the noise error on the basic interferometer angle measurements before processing. These bandwidths can also be the limiting factors on dynamic performance of the system and on the transmitter sequencing rate. Thus it is clear that the phase lock loop tracking bandwidths are basic design parameters.

The operation of the interferometer system is illustrated as follows: Assume an interferometer with antenna elements separated by 60 cm (30λ). The relationship between the electrical angle measured, ϕ_e , and the spatial angle of arrival, θ_s , of the K-band signal is repeated here for convenience. Namely,

$$\phi_e = \frac{2\pi D}{\lambda} \sin \theta_s \quad (2.1)$$

where λ is the carrier wavelength and D is the antenna separation. Now, with $D = 30\lambda$ and $\theta_s \ll 1$, Eq. (3.1) can be approximated by

$$\phi_e \approx 60\pi \theta_s \quad (2.2)$$

Assume that the electrical measurement error is $\Delta\phi_e = 0.2$ radians. This implies a spatial angular error given approximately by $0.2/60\pi \approx 1.06$ mrad. = 0.061 degrees. Of course θ_s is ambiguous every $1/30$ rad = 1.9 degrees. The role of the shorter baseline interferometer is to provide some ambiguity resolution. The electrical measurement error is probably independent of the interferometer baseline length. Thus, in general, the spatial angle measurement error is approximated by

$$\Delta\theta_s = \lambda\Delta\phi_e/2\pi D = 0.2/\pi D \quad (2.3)$$

where it is assumed that $\Delta\theta_e = 0.2$ rad. and $\lambda = 2$ cm in the latter expression.

The maximum unambiguous angle is a function of the separation of the coarse interferometer antennas, D_c . In particular

$$\theta_{s_{\max}} = \frac{\lambda}{D_c} = \frac{2}{D_c} \quad (2.4)$$

with D_c expressed in cm. Using Eq. (2.3) and (2.4) we can choose a shorter baseline length as follows: First, we note that Eq. (2.3) gives the r.m.s. error. It is typical in systems like these to choose parameter values so that ambiguity resolution is highly reliable. Therefore we should choose D_c in Eq. (2.3) such that the 3σ value of the error is equal to the long baseline interferometer ambiguity. In that case, the measurements on the shorter baseline interferometer will provide valid ambiguity resolution of the long baseline data 99% of the time. Thus, let

$$1/30 \geq (3)(.2)/\pi D_s \quad (2.5)$$

or, the short baseline length should be

$$D_s \geq 5.73 \text{ cm} \quad (2.6)$$

It may not be possible to place the antennas much closer together anyway if moderate gain (15 dB) horns are used. We will therefore assume that the short baseline length is $6 \text{ cm} = \lambda$. This is adequate to reliably resolve the longer baseline data but it is ambiguous itself. In particular, with $D_s = 3\lambda$, the short baseline data is ambiguous every $1/3$ radian $\approx 20^\circ$. This data is usable as is provided that the initial location and orientation of interferometer array are known with sufficient accuracy, a priori. Alternatively the six station solution may be used to help resolve a gross ambiguity error on the order of 20° . That is, the solutions obtained using data with improperly resolved ambiguities may be impossible or so unlikely that they can be rejected or corrected via computer processing.

The discussion above shows that for the selected configuration, the electrical noise error in each of the phase locked tracking loops must be less than 0.2 rad. The relationship between received carrier power, received noise density, loop tracking bandwidth, and phase noise error is given by

$$\sigma_{\phi_e} = \left[\frac{2C}{N_0 B_n} \right]^{-1/2} \quad (2.7)$$

where

C is received carrier power

N_0 is noise density $= k T_{eq}$

and

B_n is the tracking noise bandwidth (double-sided).

Equation (2.7) shows that the tracking error is reduced by decreasing the tracking noise bandwidth. However reduction of the tracking noise bandwidth degrades the dynamic performance of the tracking loop and lengthens the acquisition time. The latter factor has an impact on the transmitter sequency rate and hence on the update rate of the computer processed solution for the position and orientation

of the interferometer array relative to the ground transmitter array.

Let us assume for example that it is desired to establish a computer update every 50 ms. Given that 6 beacon transmitters are used, roughly 7.5 ms per transmission would be available. This means that the interferometer phase lock loops must be able to acquire and track a signal in under 7.5 ms. The transient response of a second order .707 damped phase locked loop is essentially complete in roughly $4.5/B_n$ seconds. Thus,

$$4.5/B_n \leq 7.5 \text{ ms} \quad (2.8)$$

or

$$B_n \geq 600 \text{ Hz}$$

With $B_n = 600 \text{ Hz}$, the received carrier noise density must be greater than 42 dB-Hz in order to insure that the electrical phase error is less than 0.2 rad.

The Servo lag error of the phase locked loop is also a function of the tracking noise bandwidth. In particular, assuming a second order .707 damped tracking loop, the steady-state error due to acceleration is given by

$$\Delta\phi_{\text{lag}} = \frac{2\pi a}{\lambda B_n^2} \quad (2.9)$$

where a is the acceleration. Thus with $B_n = 600 \text{ Hz}$ a lag error of less than 0.1 rad. is produced in the presence of radial accelerations of less than 12 g's. This should be adequate for most applications.

2.2.2 Multipath Errors

The analysis and experimentation carried under Contract F19628-75-C-0087 has shown that an interferometer system of the type implemented for the perspective navigation system can provide valid measurements in the presence of multipath. In particular, it was shown that in the presence of deep multipath induced nulls worst case spatial angular error was on the order of 0.25° . Typically it should be expected based on the results of that experimentation that peak angular errors will be around 0.1° given reasonable beacon transmitter antenna design.

2.2.3 Geometric Dilution of Precision

The interferometer measurement errors are related to the position and orientation output parameters through GDOP factors. These factors are a function of the ground array configuration and the position of the interferometer array relative to the ground transmitter array. The discussion of Section 3 includes consideration of the output parameter estimation errors in terms of the measurement errors. In particular, Table 3.1 gives parameter estimation errors assuming that spatial angular errors are 0.11° . This level of error is commensurate with experimental results presented in Section 4 of this report. The table shows that given a well-designed transmitter configuration, very low position and orientation errors can be achieved even under extremely poor GDOP conditions. For example, given that the interferometer array is at an altitude of 500 meters with range to the center of the transmitter array set at 10,000 meters, i.e. elevation angle equals less than 3 degrees, the altitude estimation error is less than 30 meters. The system error is much smaller under more favorable geometric conditions.

2.3 Processing Alternatives

The system which was implemented for this program uses a straightforward least-squares solution for the position and orientation parameters. An operational system should be programmed with a more efficient algorithm such as a Kalman filter or a recursive least-squares formulation. It should be recognized that since the measurement of 12 parameters is used to determine only 6 output parameters then it is possible to reject some of the measured variables if they

appear to be corrupted by multipath or other sources of error.

2.4 Other System Configurations and Applications

The perspective navigation system is easily adapted to other missions and system requirements. It is possible for example to use this system for airborne experiment monitoring and control. In such a mode, a digital recording facility can be readily interfaced with the preprocessor subsystem so that measured data from the interferometer system along with time tags can be recorded in real-time. The digital data recorded in this way can be reduced via post-flight data reduction algorithms which are more powerful than those which could be implemented for the real-time data processor and display subsystem. In fact, in some applications, the data reduction processor and display may not be needed at all.

The particular system configuration described in this report was designed specifically to provide high performance at very low elevation angles where multipath is the predominant problem. As noted above, under less severe geometric constraints, higher performance can be obtained because GDOP is smaller and because the multipath problem is less severe. In such cases it is reasonable to assume that the system configuration would employ interferometer arrays with smaller antenna separations because extremely high precision spatial angular measurement is not required.

3. HARDWARE DESCRIPTION OF THE TEST SYSTEM

This section describes the hardware of the test system in sufficient detail to provide an understanding of the signal processing and how that relates to the measurements which were made using the test system. Much of the hardware is either a modification or an outgrowth of that produced on Contract F19628-75-C-0087 and which was reported on in Reference 1 (report number AFCRL-TR-75-0526 entitled "Phase Derived Navigation Studies" dated 30 September 75). We will not attempt to describe the details of each circuit except where they are pertinent to the overall understanding or are critical to the performance. Details are shown in the accompanying schematics in Appendix A for reference and possible troubleshooting.

3.1 Overall System Description and Specifications

The overall block diagram of the complete test system is shown in Fig. 3-1. The test system consists of three principal sections: the transmitting system, the receiving system and the data processing and display system. The transmitting system consists of a master transmitter and five remote satellite transmitters which are operated in a timed sequence so that only one is on at a time. The five channel receiving system is configured to produce a two-dimensional interferometer with coarse and fine angular resolution both horizontally and vertically. The outputs of the receiver are fed to the microprocessor which resolves the coarse/fine ambiguity and passes the resolved phase data to the Wang 2200S. It also performs receiver/transmitter synchronization and data transfer timing and control. The Wang decodes the data, calculates the least-squares estimate of the transmitter coordinate system location, and produces the required perspective display.

The basic specifications of the feasibility test system are as follows:

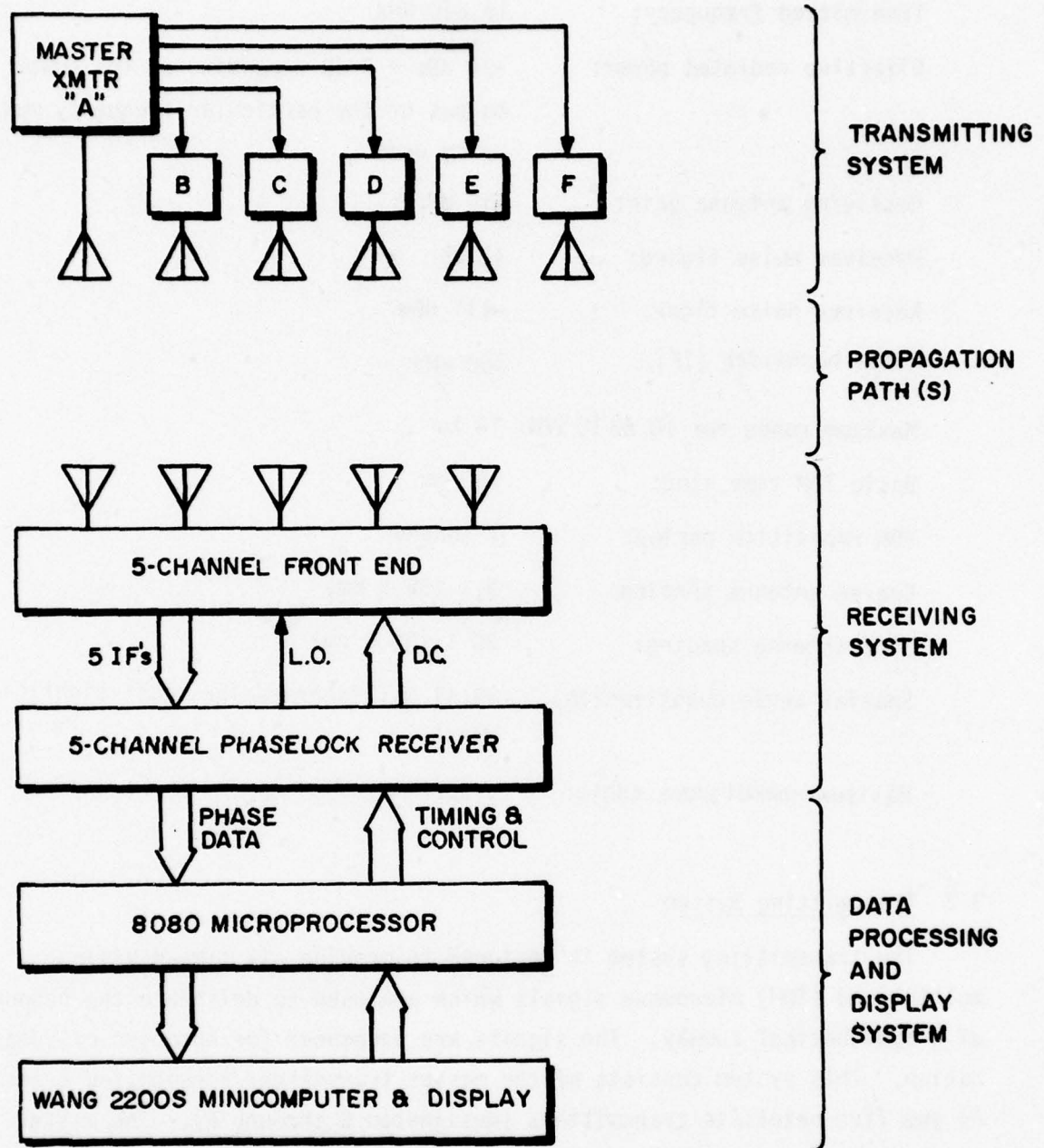


Fig. 3.1. Overall Block Diagram of Test System

Transmitted frequency:	15,840 MHz
Effective radiated power:	+24 dBm \pm 3 dB depending on the power output of the particular frequency multiplier being used
Receiving antenna gain:	+16 dB
Receiver noise figure:	12 dB
Receiver noise floor:	-111 dBm
Noise bandwidth (IF):	100 kHz
Maximum range for 10 dB IF S/N:	10 km
Basic TDM time slot:	100 ms
TDM repetition period:	1 second
Coarse antenna spacing:	3 λ (56.8 mm)
Fine antenna spacing:	30 λ (56.8 cm)
Spatial angle quantization:	19.47 millidegrees per least significant digit
Maximum unambiguous angle:	\pm 9.22°

3.2 Transmitting System

The transmitting system is designed to provide six time-division-multiplexed (TDM) microwave signals which are used to delineate the boundaries of a hypothetical runway. The signals are sequenced for purposes of identification. This system consists of the master transmitter (designated transmitter A) and five satellite transmitters (designated B through F). The master transmitter contains the system power, frequency standard, frequency synthesizer, timing system, and multiplex switching system. The block diagram is shown in Fig. 3.2.

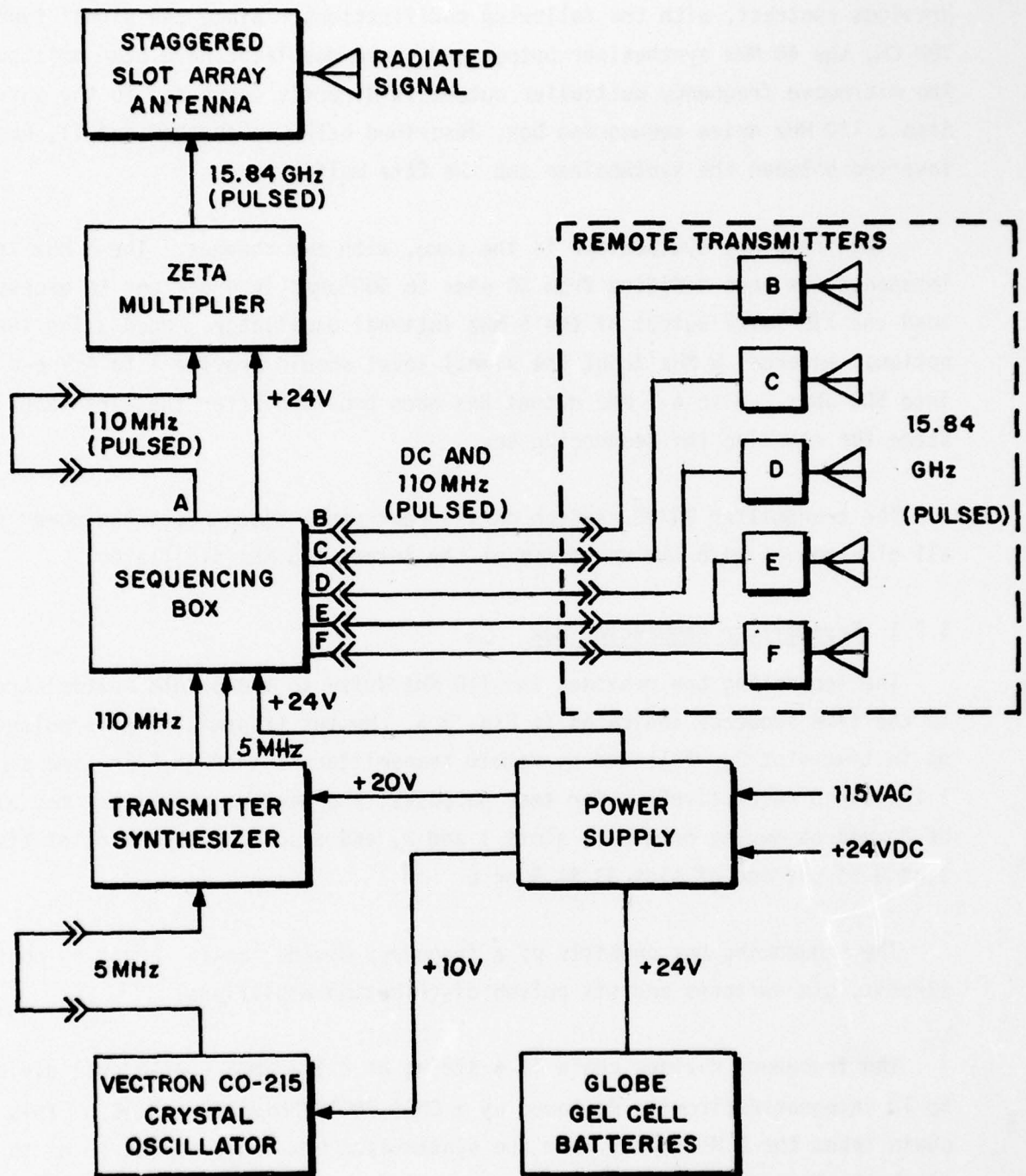


Fig. 3.2. Transmitter Block Diagram

The master transmitter is essentially the same as produced under the previous contract, with the following modifications. Since the signal type is TDM CW, the 40 MHz synthesizer output and phase modulator have been omitted. The microwave frequency multiplier output is directly connected to the antenna. Also a 110 MHz drive sequencing box, described below in further detail, has been inserted between the synthesizer and the Zeta multipliers.

The frequency synthesizer is the same, with two changes. The 5 MHz input impedance has been modified from 50 ohms to 500 ohms in order not to excessively load the TTL level output of the 5 MHz internal oscillator. When using the optional external 5 MHz input the signal level should provide 1 to 4 V p-p into 500 ohms. Also a 5 MHz output has been provided after the first amplifier stage for clocking the sequencing box.

The transmitter ON/OFF switch on the rear panel disconnects the power to all electronics with the exception of the internal 5 MHz oscillator.

3.2.1 Transmitter Sequencing Box

The sequencing box provides the 110 MHz drive to the 6 Zeta multipliers in the time sequence indicated in Fig. 3.3. Master transmitter A is pulsed on in time slot 0, followed by remote transmitters B through F in time slots 1 through 5 respectively. For test purposes, the master transmitter may also be turned on during both time slots 1 and 2, and also from the start of time slot 3 to the end of slot 3, 4, 5 or 6.

The sequencing box consists of a frequency divider chain, a gating control circuit, six switches and six pulsed distribution amplifiers.

The frequency divider chain is a string of 2 1/2 CMOS CD4518 dual divide by 10 integrated circuits followed by a CMOS 74C192 divide by 5 IC. This chain takes the 5 MHz input from the synthesizer box and produces 10 Hz to clock the gate control IC.

The gate control is a CMOS CD4017 Johnson decade counter which provides ten separate decoded sequential outputs which repeat each 10 clock cycles.

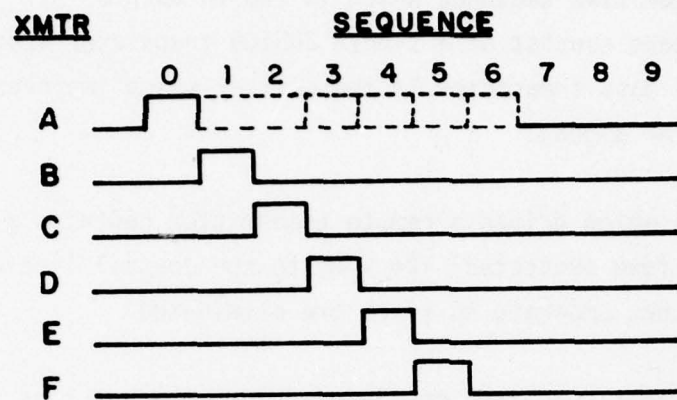


Fig. 3.3. TDM Timing Diagram

Each of the first 6 outputs, designated 0 through 5, drives one sixth of a CMOS CD4050 hex buffer, followed by a biasing diode, into the I port of its respective mixer which is used as an RF switch. The 110 MHz drive is applied in parallel to the L ports of each mixer. The output of each mixer is a pulsed RF signal in the proper time sequence which is fed to each of six distribution amplifiers. These consist of a single 2N5109 transistor stage, suitably enabled by a 2N3904 pass transistor in the emitter which improves the OFF isolation of the pulsed RF signal.

Each of the 5 amplifiers which drives a remote transmitter contains a combining circuit to add (a fuse protected) +24 V DC to the coaxial line along with the pulsed 110 MHz so that separate DC wires are eliminated.

In order to provide the test functions mentioned above, the input of the hex buffer which drives the channel A switch can also be connected to outputs 1 through 6 of the gate control circuit. Time slots 1 and 2 are enabled by a front panel toggle switch. Each of the time slots 3 through 6 are similarly enabled in sequence by a front panel rotary switch. Suitable diode and resistive dc isolation prevents cross coupling of the switching signals to the other channels.

Besides the two switches mentioned above, there are two other controls located outside the sequencing box. Provision has been made for manual or automatic clocking of the gate control circuit. A toggle switch on the front panel disconnects the divider chain output for manual operation. The gate control circuit may then be manually single stepped through its sequence by depressing a front panel push button, which has been followed by a debouncing circuit.

A buffered output from time slot nine provides a synchronous scope trigger signal at the front panel for test purposes.

All six pulsed RF outputs are brought to the front panel for distribution. The channel A output is normally connected back to the input of the master transmitter Zeta multiplier.

3.2.2 Remote Transmitters

The 5 remote transmitters consist of a circuit to separate the DC and 110 MHz components of the remote signal, a Zeta X144 multiplier and a staggered slot array antenna. The +24 VDC is fed to the DC input and the pulsed 110 MHz is fed to the RF input of the Zeta multiplier. The remote transmitters are connected to the main unit with up to 500 foot lengths of RG-8/U coaxial cable.

3.3 Receiving System

The receiving system is set up as a crossed baseline interferometer designed to measure phase differences between signals received at spatially separated antennas as a means of determining azimuth and elevation angles to the transmitting sources. It is composed of 5 channels--one reference channel together with coarse and fine resolution channels in both the horizontal and vertical directions.

The receiving system consists of a 5 channel microwave front end and the main receiver. The interconnecting cable between the front end and the rest of the receiver allows them to be separated by up to 30 meters. The main receiver cabinet contains the 5 first IF's, 5 signal limiters, 5 phase-locked loops (PLLs), a system timing card (STC), associated local oscillators (LOs), power supplies, and the SDK 80 microprocessor. The block diagram of the receiving, data processing and display systems is shown in Fig. 3.4.

The microwave front end mixes the received signals at 15.84 GHz with the 15.696 GHz LO to produce 144 MHz IFs with associated phase differences. The first IFs amplify and mix these signals with the 139 MHz second LO to produce 5 MHz second IF signals. These are then amplified/limited, mixed with the 4 MHz third LO to yield 1 MHz signals, and further amplified/limited to produce a constant amplitude signal for the PLLs. The limiters also produce a DC output proportional to the input signal level for the STC.

The phase data is extracted from each 1 MHz limited IF signal by means of a PLL. Its phase detector measures the difference in phase between the divided VCO frequency and the incoming 1 MHz signal and produces a signal

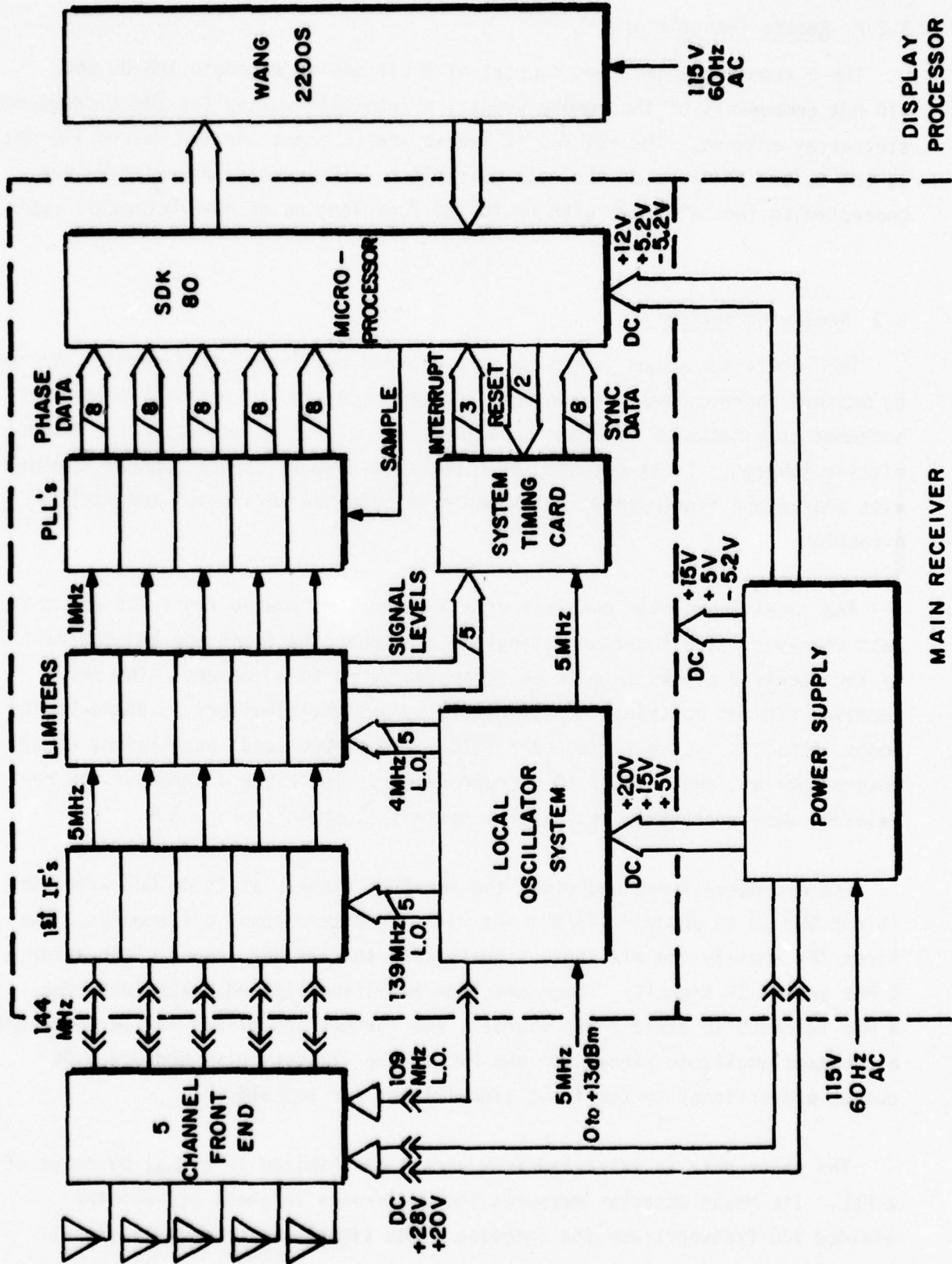


Fig. 3.4. Receiver Block Diagram

operated on by the loop filter to provide the VCO control voltage. As the VCO oscillates at 100 MHz, this produces an effective 100 times multiplication of the phase information. Therefore cycle counting of the VCO output in the PLL frequency divider is quantized in increments of 3.6 electrical degrees of the received microwave signal.

The 5 PLLs are simultaneously sampled by the microprocessor on interrupt from the system timing card once per transmitter time slot in order to determine the state of the digital divider for phase comparison. The STC provides 10 interrupts per second to the microprocessor and provides for determination of signal presence. It also provides data on receiver/transmitter synchronization quality to the microprocessor in order to reinitialize synchronization, if necessary.

3.3.1 Microwave Front End

The microwave front end is mounted on an aluminum plate physically separate from the rest of the receiver. Interconnection is made by 6 coaxial cables and one 4 wire cable 30 m in length. One coax carries the 109 MHz LO up to the array and 5 coax cables carry the wideband IF down to the respective main receiver channels. The +28 VDC and +20 VDC power are carried on the 4 wire cable. The receiving horn layout is shown in Fig. 3.5.

The front end consists of 5 signal paths, an LO chain and a power supply. The signal paths consist of microwave receiving horns, adapters and cables, and RHG DMP 12-18WW97 mixer/amplifiers which mix the received 15.84 GHz signal with the 15.696 GHz LO to produce 144 MHz wideband IF, which it then amplifies.

The LO chain consists of a Zeta 4284-15.84 X144 amplifier multiplier, an Omni-Spectra A30565 injection-locked Gunn amplifier, and American 2089-6405 four-way and 2089-6205 two-way power dividers, all interconnected with SF-142B microwave coax cables selected for low VSWR and insertion loss. The Zeta multiplier takes the 109 MHz LO (at +3 dBm) from the main receiver and multiplies it up to 15.696 GHz. The Gunn amplifier takes the 15.696 GHz produced by the Zeta multiplier at approximately +12 dBm and amplifies it to a +20 dBm level to make up for losses incurred in power division. It is followed by the four-way power divider, producing 3 LO outputs at +13 dBm, then the two-way power divider, producing the remaining 2 LOs at +9 dBm.

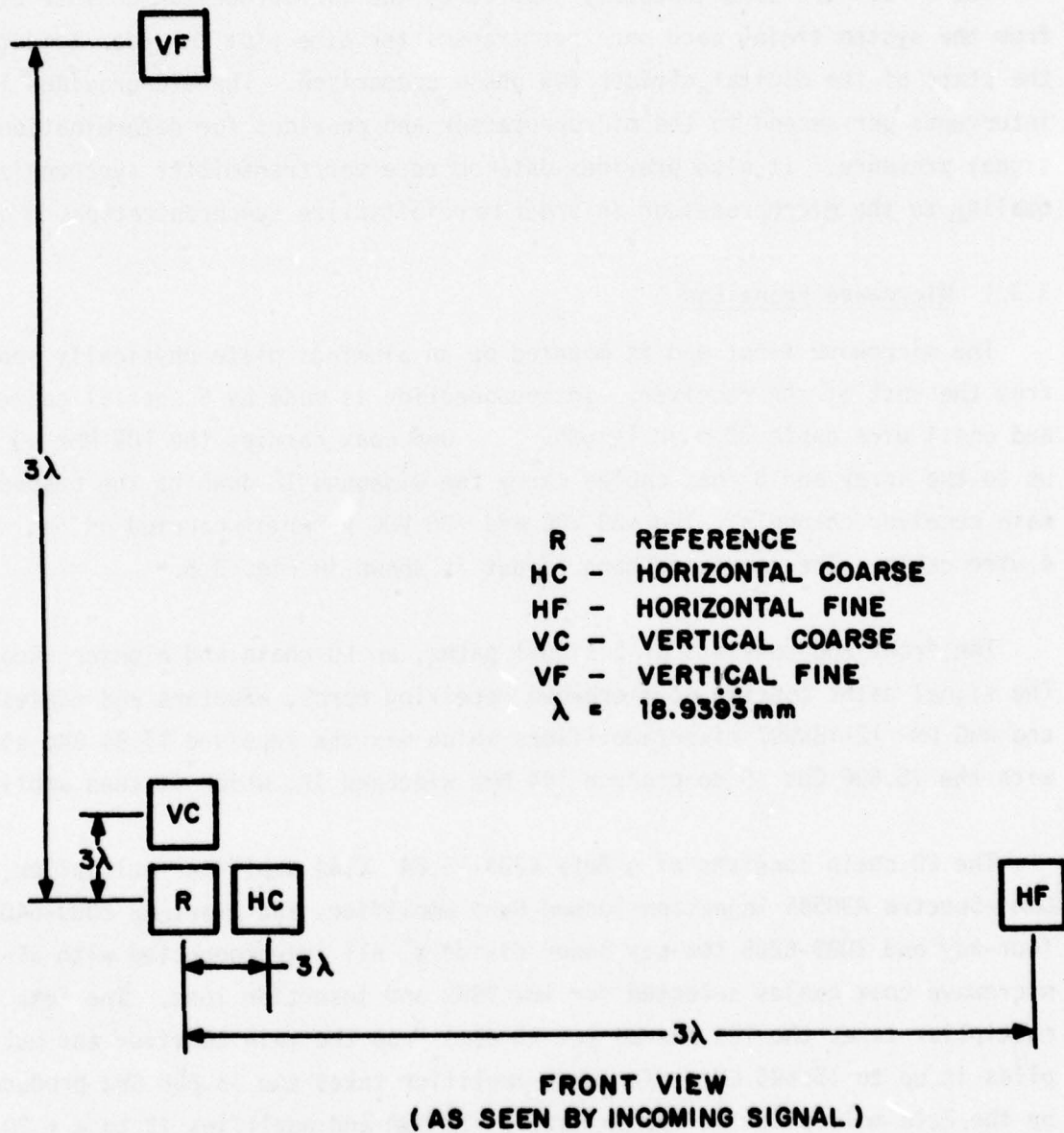


Fig. 3.5. Receiving Horn Antenna Configuration

The front end power supply consists of a National LM 340 T-15 regulator to produce +15 V for the mixers from the incoming +28 volts and a National LM 317 adjustable regulator circuit to produce +8 V at 1.2 A for the Gunn amplifier from the incoming +20 volt line.

3.3.2 First IF

The first IF consists of an RF amplifier at 144 MHz, followed by an Olektron R-CDB-224 mixer utilizing the 139 MHz LO to produce a 5 MHz signal. This is fed through a 3 pole passive bandpass filter to reject undesired mixer products.

The RF amplifier provides 2 stages of linear gain by utilizing a 40673 MOSFET operating in a common source configuration, followed by a 2N3646 transistor operating in a common base mode. Both stages employ selective LC filtering. Care has been taken to provide proper decoupling of the DC lines to prevent unwanted feedback which may cause oscillation. The net gain for the box is set to 15 to 20 dB with a gimmick connected from drain to input gate on the MOSFET. A front panel adjustment sets the bias on the MOSFET bias gate.

3.3.3 Signal Limiter

The signal limiter consists of 6 limiting amplifier stages at 5 MHz followed by a one pole 5 MHz LC filter, a mixer utilizing the 4 MHz LO to translate the signal to 1 MHz, a narrowband 1 MHz filter, 6 limiting amplifier stages at 1 MHz followed by a one pole 1 MHz LC filter and a hybrid, and a log detector circuit. The 1 and 5 MHz filters immediately following the limiters constrain the total noise power generated by the limiters. The final hybrid is an Olektron TO-HJ-302V two-way power divider used to provide an extra output as a monitor point for the 1 MHz signal going to the PLL. The mixer is an Olektron R-CDB-224.

The signal limiter features 100 dB net RF gain. Each 6 stage limiter is AC and DC feedback stabilized and provides low phase change with input amplitude variations. The narrowband 1 MHz filter following the mixer is a 3 pole LC circuit which sets the basic receiver noise bandwidth of 100 kHz.

Each 6 stage limiting amplifier utilizes two MC10116 ECL triple line receiver chips to provide 6 amplification stages in cascade. Each stage is operated in a balanced configuration and has resistive dual negative feedback. The 6 stage chain has overall DC feedback to stabilize the DC operating point. An input transformer provides single-ended to balanced input and impedance matching, while an output transformer performs the complementary function.

The log detector employs 12 RF diode detectors connected to the outputs of all 12 limiter stages, the outputs of which are summed according to operating frequency (in two groups of six) in 2 741 op amp chips connected as DC summing amplifiers. This yields an effective piecewise linear approximation to a log response. The two outputs are further summed in a third 741 similarly configured to provide the signal DC output which is inversely proportional to the log of the RF input level at 5 MHz. A typical performance curve is shown in Fig. 3.6.

The layout is critical due to the high gain and low phase change requirements of the circuit. Every attempt has been made to isolate outputs from inputs. The signal limiting path has been constrained to flow in one basic direction across the board. Individual parts placement has been adjusted for optimum performance and leads have been kept short.

3.3.4 Phase-Locked Loop

The PLL block diagram is shown in Fig. 3.7. It is composed of five major functional blocks--the phase detector, the loop filter amplifier, the VCO and frequency divider, the data converter and the lock indicator.

The phase detector is an Olektron R-CDB-224 analog mixer with about 0.14 volts/radian sensitivity. It measures the phase difference between the 1 MHz limited IF and the divided VCO frequency. The IF is fed through a single pole 1 MHz LC filter by an MC10116 ECL line receiver.

The loop filter amp is an analog 741 chip connected as an integrator. Both time constants are 7.5 milliseconds. A front panel push-to-lock button discharges the integrating capacitors through a 2N3646 NPN transistor held on

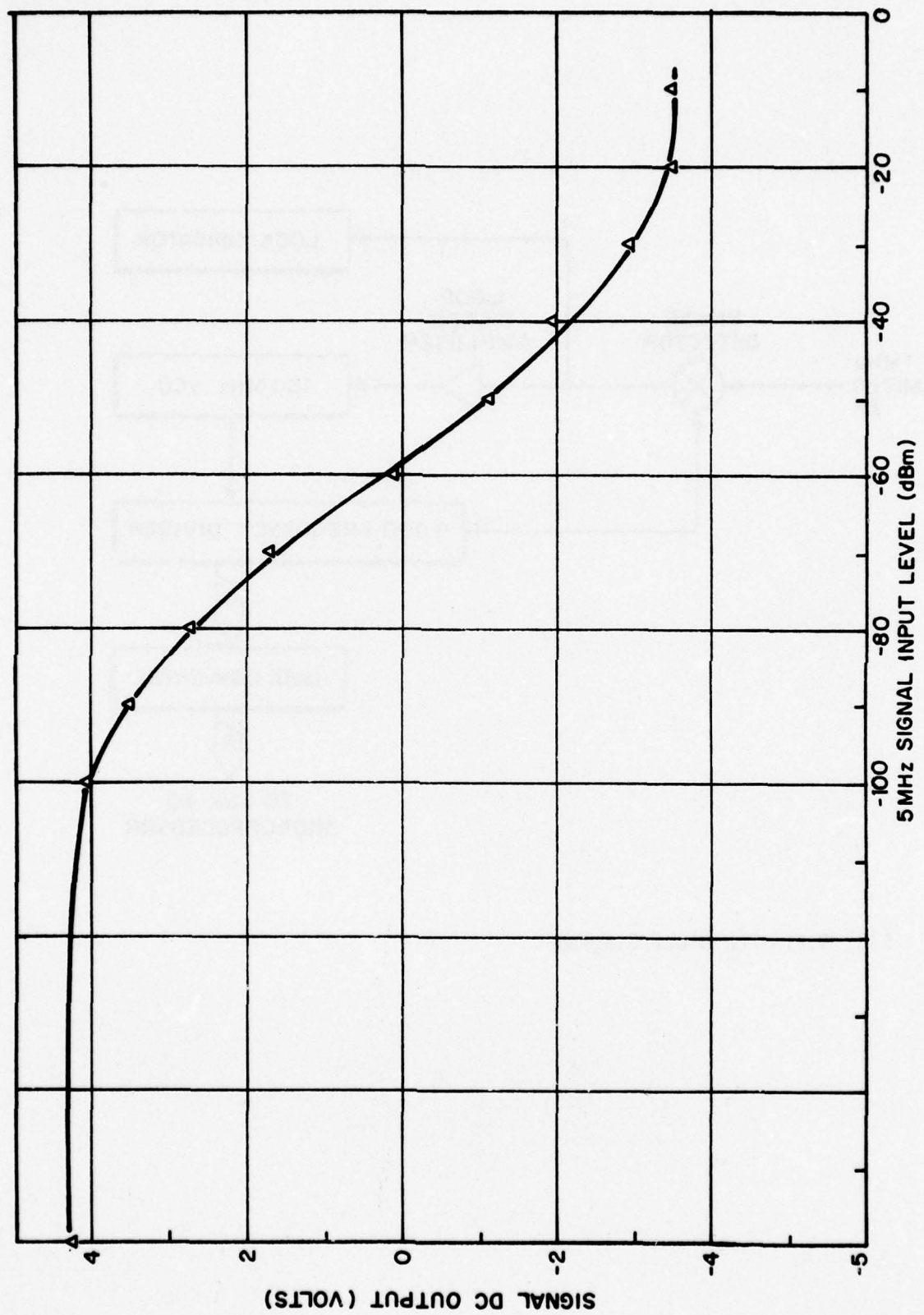


Fig. 3.6. Limiter Signal D.C. Output

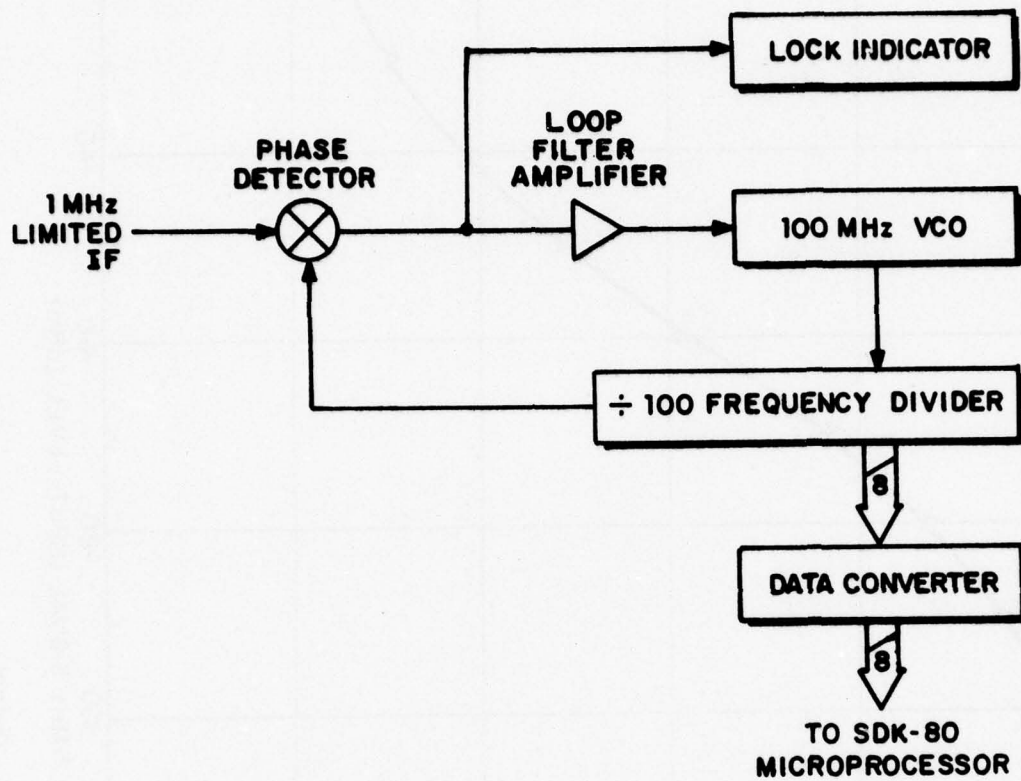


Fig. 3.7. PLL Block Diagram

for approximately one millisecond. Then, as long as the button remains depressed, the lock circuit pushes the integrator output upward. When the lock button is released, the VCO sweeps down until the input signal is acquired.

The VCO uses an MC1648P ECL oscillator with an MV3102 varicap in the tuning tank circuit. The varicap is driven by the 741 output to vary the VCO operating frequency. The circuit sensitivity is about 400 kHz/volt. The center frequency is about 100.2 MHz with 5 volts at the 741 output. The controlled oscillation frequency range is 97 to 103 MHz. The frequency divider consists of two MC10138 ECL divide by 10 counters in cascade, set up to count in BCD. The second counter feeds the phase detector through an MC10104 ECL AND gate used as a buffer for isolation of the data line.

The data converter consists of an MC10104 AND gate used to enable the 100 MHz VCO output to the frequency divider, and two MC10101 ECL OR gates switching the counter outputs into two MC10125 ECL to TTL converters. This gating prevents spurious system pickup occasioned by toggling of the TTL lines out of the PLL card. The enable lines on each card are driven by an MC10104 AND gate used for fan out capability. The ECL Loop Enables into each card are driven by an MC10124 TTL to ECL converter located on card number four. Care has been taken to use proper TTL pull-up and ECL pull-down and line driving resistors and twisted pair lines between the converter and all receiving MC10104s in order to achieve simultaneous sampling of all PLL counters. The TTL Enable signal is provided by the SDK 80 microprocessor. A logical high level holds the count and provides output on the TTL data lines to the microprocessor while a low level closes the loop and disconnects the output. At the ECL level, these logic levels are inverted.

The lock indicator consists of a 741 analog chip set up as a simple amplifier from the phase detector output to a 2N3646 transistor LED driver. The LED lights to indicate a large low frequency phase detector output when the loop is unlocked. (The LED will also glow when there is significant noise at the phase detector output due to very low input signal-to-noise ratio.)

Pull down resistors are included on all used ECL 10,000 series outputs (in most cases provided by Beckman 898-1-R1K resistor network chips). The DC power inputs are bypassed at the chips. All unused TTL inputs are grounded.

The PLL characteristics are as follows:

$$\begin{aligned} K_o \text{ (VCO sensitivity)} &= \frac{2\pi \cdot 400 \text{ kHz/volt}}{100} \\ &= 2.5 \times 10^4 \text{ rad./volt sec.} \end{aligned}$$

$$K_d \text{ (phase detector sensitivity)} = 0.14 \text{ volts/rad.}$$

$$\begin{aligned} \text{PLL gain} &= K_o K_d = 2.5 \times 10^4 \text{ rad./volt sec.} \cdot 0.14 \text{ volts/rad.} \\ &= 3.5 \times 10^3 / \text{sec.} \end{aligned}$$

$$\tau_1 = 7.5 \text{ msec.}$$

$$\omega_n = \left(\frac{K_o K_d}{\tau_1} \right)^{1/2} = \left(\frac{3.5 \times 10^3 / \text{sec.}}{7.5 \times 10^{-3} \text{ sec.}} \right)^{1/2} = 684 \text{ rad./sec.}$$

$$\tau_2 = 7.5 \text{ msec.}$$

$$\begin{aligned} \zeta(\text{damping}) &= \frac{\tau_2 \omega_n}{2} = \frac{7.5 \times 10^{-3} \text{ sec.} \cdot 684 \text{ rad./sec.}}{2} \\ &= 2.56 \end{aligned}$$

3.3.5 System Timing Card

The system timing card consists of a counter chain which generates interrupts to the microprocessor from the incoming 5 MHz L0 signal, a signal level summer and indicator which operates on the signal DC outputs from the 5 limiters, and a sync counter which provides a measure of sync quality.

The counter chain consists of a cascade of a 7490 TTL divide by 5 chip, a 4017 CMOS Johnson decade counter, 2 4518 CMOS dual BCD counters and one section of a 4013 CMOS dual D flip flop. The first 4 chips produce pulses at 1 MHz, 100 kHz, 1 kHz and 10 Hz respectively as their final output. The 10 Hz signal is used to clock the 4013 which, in conjunction with the Q_4 output of the 4017 on its reset line, produces 2200 μ sec. long interrupt pulses to the SDK 80 at a 10 Hz rate.

The signal level summer is a 741 op amp set up as an inverting summing amplifier. It provides an indication of signal presence to the microprocessor, clocks the sync counter and controls the signal indicator. This consists of a 2N3646 transistor LED driver and a front panel LED, which lights to indicate a received signal. There is also a front panel bias adjustment which sets the signal summer threshold.

The sync counter consists of the other section of the 4013 flip flop followed by a third 4518 CMOS dual BCD counter. When clocked by the signal summer at the onset of the received transmitter sequence, the flip flop is set, providing a rising edge representing signal edge to the microprocessor, and also disabling the third 4518 which has been counting the 1 kHz pulses provided by the first 4518 in the counter chain. This held count is then available to the microprocessor as a sync indication.

With the above mentioned inputs the SDK80 can, after system reset, calculate and wait the proper time before resetting the chips in the counter chain. The sync counter flip flop and counter are also reset by the microprocessor.

3.3.6 Local Oscillators

The block diagram of the local oscillator system is shown in Fig. 3.8. It consists of an LO synthesizer, two filters and three distribution amplifiers. The input 5 MHz bandpass filter is a passive 3 pole LC filter on the 5 MHz reference signal, followed by a two-way power divider hybrid which feeds both the LO synthesizer and the STC. The 5 MHz reference is connected on the front panel and should provide 0 to +14 dBm input level. The LO synthesizer is identical to that produced under the previous contract and operates on the filtered 5 MHz reference signal to produce 4 MHz for distribution, 10 MHz for further processing and 109 MHz for distribution.

The 4 MHz LO distribution amplifier is similar to that produced under the previous contract. However it employs two stages of linear gain rather than one, followed by a five-way power divider hybrid as opposed to two-way. It takes the 4 MHz LO from the synthesizer at -16 dBm and distributes it at +13 dBm to the 5 signal limiters as the third LO.

The other two synthesized frequencies, 10 and 109 MHz, are fed to the 109 MHz distribution amplifier, with the 109 MHz signal passing through a Cir-Q-Tel FBT/2-109/1-5/50-3A/3A filter for rejection of 5 MHz and above sidebands, as in the previous contract. The distribution amplifier is also similar to that of the previous contract except that the 4, 9 and 10 MHz distribution circuits have been eliminated, leaving only the 10 MHz tripler, 30 MHz filter, amp and hybrid and 109 MHz distribution circuit. Also both 30 and 109 MHz output hybrid circuits have been modified to produce single outputs at 50 ohms. This box provides the 109 MHz LO at +10 dBm for the microwave front end through a front panel connection and also feeds 30 and 109 MHz to the 139 MHz distribution amplifier.

The 139 MHz distribution amplifier consists of a PLL which generates 139 MHz from the 30 and 109 MHz inputs, an output buffer amplifier and output power divider. The PLL consists of a 12040 ECL phase detector IC which measures the phase between the incoming 30 MHz and that internally generated, the loop amplifier and filter employing a 741 op amp set up as a low pass filter, an ECL 1648 VCO operating at 139 MHz center frequency and controlled

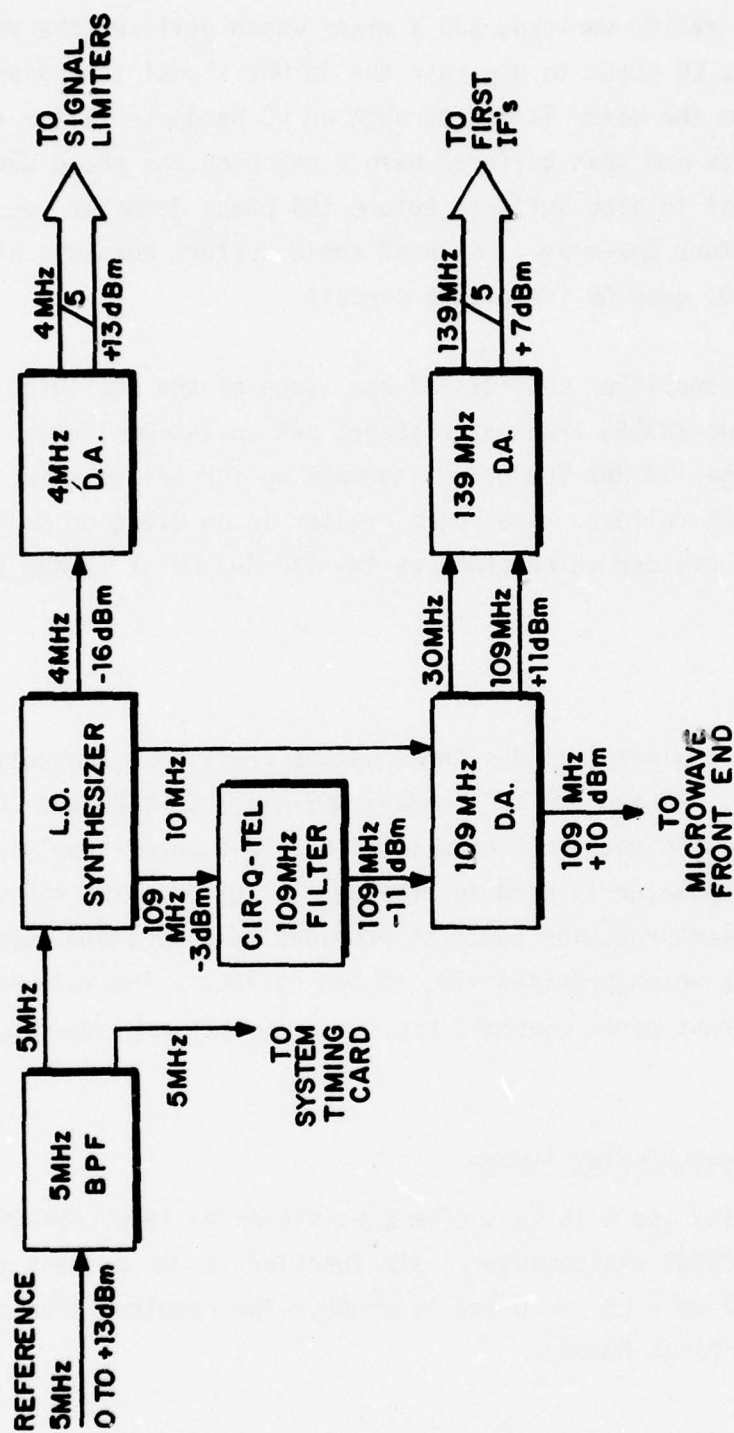


Fig. 3.8. L.O. System Block Diagram

by the 741 through an MV3102 varicap, and a mixer which utilizes the VCO output and the 109 MHz LO input to generate the 30 MHz signal for phase detection. The 30 MHz signal from the mixer is fed through an LC bandpass filter to reduce unwanted mixer products and then buffered before reaching the phase detector. The input 30 MHz signal is also buffered before the phase detector, as is the 139 MHz VCO output before the mixer. Each of these buffers consists of one section of an ECL 10101 quad OR integrated circuit.

The output buffer amplifier consists of one stage of the ECL 10101 integrated circuit followed by two 2N3563 transistor stages set up in a Darlington configuration. It amplifies the 139 MHz VCO output to make up for losses incurred in the power divider which follows. The power divider is an Oelektron R-HJ-305H hybrid five-way power divider which produces the 139 MHz LO at +7 dBm for the five first IFs.

3.3.7 Power Supplies

The main receiver cabinet includes three Lambda precision, low noise power supplies for +5, +20 and +28 VDC, models LCS-A-5, LCS-B-20 and LCS-A-28 respectively. It also includes an Elexon model OLV 30-5 power supply for -5 VDC. An LM 341P-15 regulator is used to provide +15 VDC from the +28 volt supply. The SDK 80 microprocessor power is provided by a separate supply, an Elexon model CKS-1 OVP which provides +12, +5 and -5 VDC. The main AC power switch on the front panel controls the inputs to all five supplies.

3.4 Data Processing and Display System

The data processing and display system consists of an Intel SDK-80 microprocessor and a Wang 2200S minicomputer. Its function is to process the phase data produced by the five PLLs in order to produce the required true perspective display of the hypothetical runway.

The microprocessor performs data conditioning for input to the Wang. It interrogates the PLLs on interrupt from the system timing card, and reads in the phase data in parallel. It then subtracts the reference channel phase from the horizontal and vertical phase data. The phase difference data is then processed to resolve the coarse/fine ambiguity. A constant is subtracted from the ambiguity resolved data to account for random hardware delays. This boresight correction factor is entered via the Wang keyboard. Following boresight correction, the conditioned data is transferred to the Wang in serial fashion.

The SDK-80 also operates as the master computer for the system. It sequences and controls PLL and system timing card data input and the Wang data I/O, for which it also provides timing. It also synchronizes the receiver to the transmitter TDM sequence after system reset via front panel pushbutton.

The Wang 2200S perspective display program inputs the resolved phase data, then unpacks and interprets it as the appropriate spatial angles. Then it calculates the least-squares estimate of the location of the transmitter coordinate system in aircraft space (i.e., relative to the interferometer coordinate system). It uses this solution to calculate the resultant estimate of the runway perspective display, using stored information about the location in the transmitter coordinate system of the object to be displayed (in this case the runway). This data is displayed together with an artificially generated horizon line.

3.4.1 Microprocessor Operating Program

The microprocessor operating program stored on PROM in the SDK-80 is written in assembly language. It provides for input of the phase data contained in the PLL frequency dividers on interrupt from the STC, phase comparison with the reference channel, boresight correction, ambiguity resolution and data transfer to the Wang 2200S display processor. It keeps track of the transmitter timing sequence in order to properly control data operations. It also provides for receiver/transmitter synchronization on initialization (system turn-on or front panel system reset pushbutton) by averaging 8 seconds of data from the STC sync counter and resetting the STC counter chain. It provides master system sequencing for all of these functions. A full listing of the operating

program may be found in Appendix B.

A block diagram of the program routines is shown in Fig. 3.9. The program consists of three major parts--an initial setup section, an interrupt processor which serves as the main program, and various subroutines. The subroutines, called by the interrupt processor or by a higher level subroutine, are the synchronization routine, the byte processor, the byte counter, the data input routine, an ambiguity resolution routine and the Wang I/O. The synchronization routine and byte processor are called by the interrupt processor. The byte processor calls all other subroutines except ambiguity resolution, which is called by the data input routine.

The setup section equates variables, defines input, output and timing ports and control words and organizes RAM data storage locations. Entered once at system turn on or system reset, it clears program control words and initializes the stack pointer, Wang I/O control and the STC counter chain, then waits for interrupt. All interrupts from the STC are handled by the interrupt processor.

The interrupt processor performs the main executive functions of the microprocessor. It saves the contents of all register pairs in order to retain original program status and calls either the synchronization routine (on the first interrupt after system turn on or system reset) or the byte processor. After byte processor completion it restores register pair contents and returns to the original program task at the time of interrupt.

The synchronization subroutine serves to synchronize the receiver to the transmitter. It first increments the byte counter by calling the byte counter subroutine, as is done for each STC interrupt. It then checks for the signal edge occurring in the same time slot. When this is found it inputs and stores 8 seconds of sync data from the STC, one data word per second. After it has input 8 measurements it averages them and resets the (STC) sync data counter. It also sets the beginning switch so that the interrupt processor will no longer call the sync routine unless the system is reset. Then it calculates and waits the required delay before resetting the STC counter chain. This accomplishes the required receiver/transmitter synchronization. The

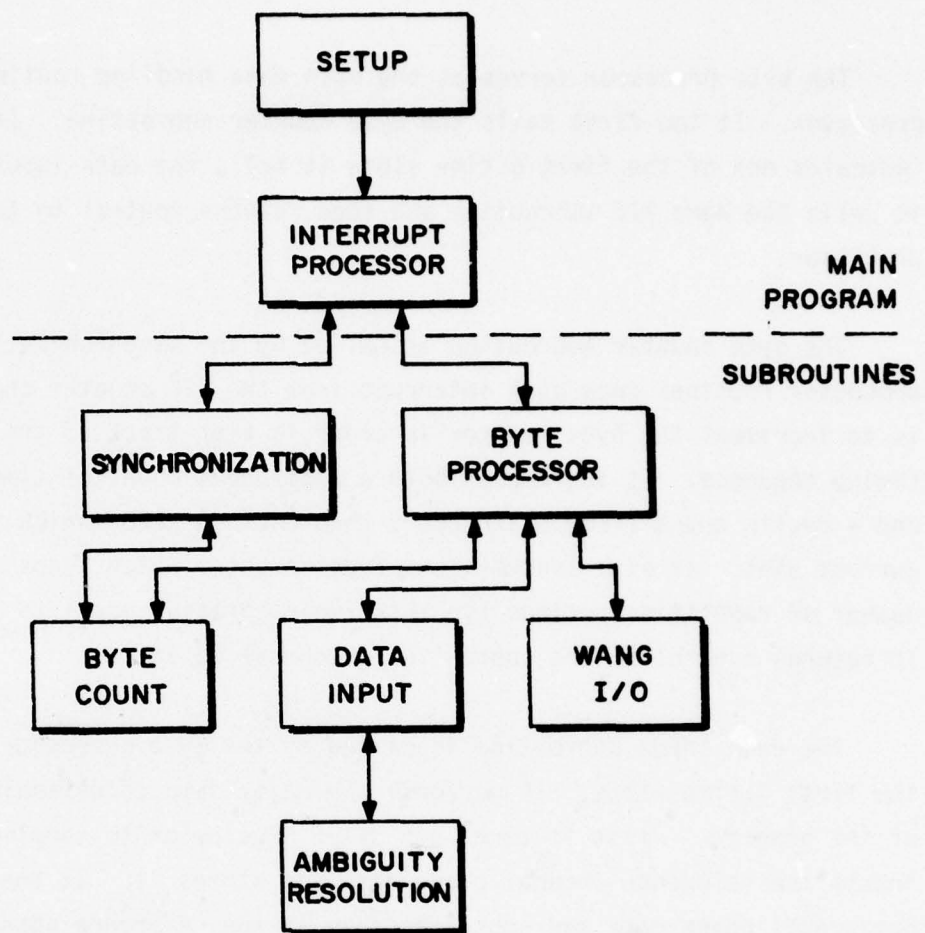


Fig. 3.9. Microprocessor Routines Block Diagram

routine then stores the proper sequence count in the byte counter to keep track of the transmitter timing sequence and waits for interrupt.

The byte processor serves as the main data handling routine for the micro-processor. It too first calls the byte counter subroutine. If the byte count indicates one of the first 6 time slots it calls the data input routine. Lastly it calls the Wang I/O subroutine and then returns control to the interrupt processor.

The byte counter subroutine is called by the synchronization or byte processor routines once each interrupt from the STC counter chain. Its function is to increment the byte counter in order to keep track of the transmitter timing sequence. It increments both a continuous count of time slots elapsed and a cyclic count (from 0 through 9 then back to zero) which identifies the current slot. It also increments a frame counter which keeps track of the number of repetition periods (in this implementation equal to seconds) elapsed. It returns control to the subroutine which called it.

The data input subroutine is called by the byte processor during one of the first 6 time slots. It performs the major data conditioning functions of the program. First it turns off all 5 PLLs prior to sampling. Then it inputs the reference channel phase data and stores it. It then inputs the horizontal phase data and subtracts from it the reference phase. Next it adds the boresight correction factor and calls the ambiguity resolution subroutine. When this is complete it stores the resolved phase data in RAM for output to the Wang. It repeats the input, subtraction, addition, resolution and storage sequence for the vertical phase data, turns the 5 PLLs back on and returns control to the byte processor.

The ambiguity resolution subroutine resolves the ambiguity in the most significant digit (MSD) of the processed phase data resulting from the fact that it contains contributions by both the least significant digit (LSD) of the coarse channel data and the most significant digit of the fine channel data. This is due to the fact that the two digit data from both coarse and fine channels,

in decimal form, represent spatial angle information in a ten-to-one ratio, resulting from the microwave antenna spacing ratio. The routine subtracts the fine channel MSD from the coarse channel LSD and compares the absolute value of the result to five. If it is less than five it sets the resolved MSD equal to the original coarse MSD; if it is greater than or equal to five it then compares the coarse LSD to five. If this is less than five, it sets the resolved MSD equal to the original coarse MSD minus one; if it is greater than or equal to five it sets the resolved MSD to the original coarse MSD plus one. The routine is then complete, with the resolved MSD determined as described above, the second MSD equal to the original fine MSD and the resolved LSD equal to the original fine LSD. It returns this three digit number to the data input subroutine for storage.

The Wang I/O subroutine handles data transfer to and from the Wang 2200S. It counts the elements of the input and output data strings as they are transferred, strobes the appropriate control lines and provides the proper delay between byte transfers. It outputs data to the Wang before inputting data from it and provides the proper delay between these operations. It returns control to the byte processor routine, from which it was called.

3.4.2 Least Squares Estimation

It is desired to apply least-squares estimation techniques to improve the accuracy of the system display. This is equivalent to improving the estimate of the position and orientation of the runway coordinate system. In this case the classic least-squares formulation may be written as

$$A\vec{x} = b \quad (3.1)$$

where \vec{x} is the unknown solution vector $(x_0, y_0, z_0, \theta, \beta, \phi)$ consisting of the 3 translational and 3 rotational coordinates of the runway with respect to the aircraft as shown in Figs. 3.10 and 3.11, b is the noisy measurement vector consisting of azimuth and elevation angles to the 6 beacon transmitters, and A is the coefficient matrix. The perspective display is derived by coordinate

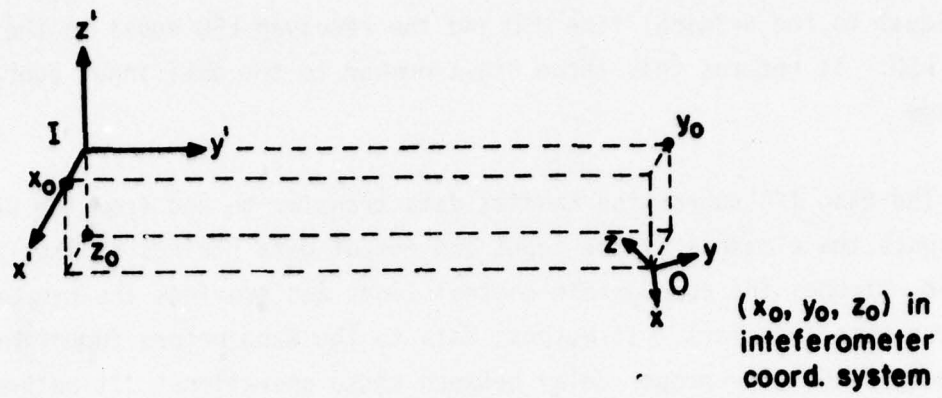


Fig. 3.10. Translation Coordinates

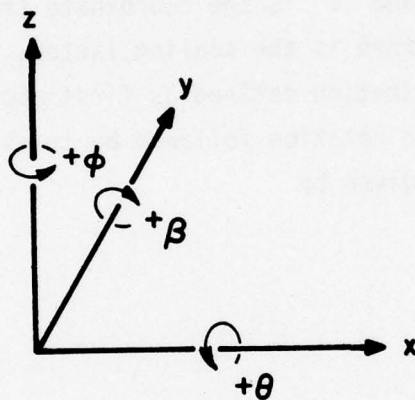


Fig. 3.11. Rotation Sense

transformation of the coordinates of the scene to be displayed as a function of the solution variables, followed by a projection transformation.

For the system geometry shown in Fig. 3.10 the coordinate transformation is given by

$$P' = P T (\vec{x}) \quad (3.2)$$

where P' is the coordinate vector $(x', y', z', 1)$ to point p in the aircraft coordinate system, P is the coordinate vector $(x, y, z, 1)$ in the runway coordinate system and T is the coordinate transformation matrix. The fourth element in the vectors is the scaling factor, set equal to 1. For the sequence of rotation application defined as first about the x -axis, then about y and finally z , and with rotation followed by translation, the coordinate transformation matrix is given by

$$T(x_0, y_0, z_0, \theta, \beta, \phi) =$$

$$\begin{bmatrix} \cos \beta \cos \phi & \cos \beta \sin \phi & -\sin \beta & 0 \\ (\sin \theta \sin \beta \cos \phi - \cos \theta \sin \phi) & (\sin \theta \sin \beta \sin \phi + \cos \theta \cos \phi) & \sin \theta \cos \beta & 0 \\ (\cos \theta \sin \beta \cos \phi + \sin \theta \sin \phi) & (\cos \theta \sin \beta \sin \phi - \sin \theta \cos \phi) & \cos \theta \cos \beta & 0 \\ x_0 & y_0 & z_0 & 1 \end{bmatrix}$$

(3.3)

where θ , β and ϕ are angles of rotation about the x , y and z runway axes respectively, with the sense of rotation as indicated in Fig. 3.11, and x_0 , y_0

and z_0 are the coordinates of the runway center relative to the aircraft centered coordinate system.

The interferometer measurement angles for the k th beacon are given by

$$\begin{aligned} b_{Hk} &= \tan^{-1} \left(\frac{x'_k}{y'_k} \right) + e_{Hk} \\ b_{Vk} &= \tan^{-1} \left(\frac{z'_k}{y'_k} \right) + e_{Vk} \end{aligned} \quad k = 1, 6 \quad (3.4)$$

where x' , y' , z' are Cartesian coordinates of the 6 beacon transmitters in the aircraft (interferometer) coordinate system, and e_H and e_V are the horizontal and vertical measurement errors. Thus, from Eq. (3.2)

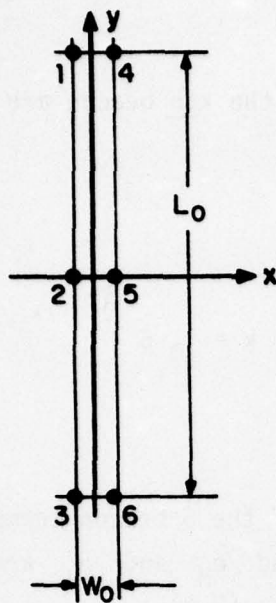
$$b_i(P'_k) = b_i(P_k T(\vec{x})) + e_i \quad \begin{aligned} i &= 1, 12 \\ k &= 1, 6 \end{aligned} \quad (3.5)$$

gives the functional dependence of the measurements in terms of the beacon ground coordinates P_k and the solution coordinates $\vec{x} = (x_0, y_0, z_0, \theta, \beta, \phi)$. The beacon transmitter geometry and coordinates are given in Fig. 3.12.

The resulting Eq. (3.5) must first be linearized before applying the least-squares method. This may be accomplished by expanding the 12 equations in a Taylor series about the assumed interferometer position, retaining only first order terms. This yields 6 coefficients for each equation, associated with the first differences with respect to the 6 assumed position variables. Thus

$$b_i - b_i^0 = \sum_{j=1}^6 \frac{\partial b_i}{\partial x_j} (x_j - x_j^0) + e_i \quad i = 1, 12 \quad (3.6)$$

Rectangular Array



$$P_1 = (-1, L, 0, 1)$$

$$P_2 = (-1, 0, 0, 1)$$

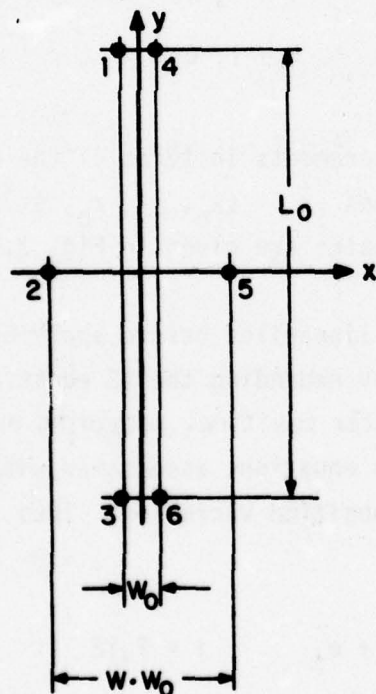
$$P_3 = (-1, -L, 0, 1)$$

$$P_4 = (1, L, 0, 1)$$

$$P_5 = (1, 0, 0, 1)$$

$$P_6 = (1, -L, 0, 1)$$

Hexagonal Array



$$P_1 = (-1, L, 0, 1)$$

$$P_2 = (-W, 0, 0, 1)$$

$$P_3 = (-1, -L, 0, 1)$$

$$P_4 = (1, L, 0, 1)$$

$$P_5 = (W, 0, 0, 1)$$

$$P_6 = (1, -L, 0, 1)$$

SCALING:

$$\frac{W_0}{2} = 1 \text{ UNIT}$$

$$L = \frac{L_0}{W_0}$$

Fig. 3.12. Beacon Geometry and Coordinates

where b_i^0 is the true measurement angle at the assumed position, x_j are the solution vector elements and x_j^0 are the assumed position coordinates. In matrix notation

$$b_{\text{noisy}} - b^0 = A(\vec{x} - \vec{x}^0) + e$$

or

$$b = A \vec{x}$$

as desired in Eq. (3.1), where A is the 12×6 coefficient matrix of partial derivatives.

The well known least-squares solution is given by

$$\vec{x} = (A^t A)^{-1} A^t b. \quad (3.8)$$

For simplicity of evaluation, Eq. (3.4) are first approximated by

$$\tan^{-1} a \approx a \quad (3.9)$$

a small angle approximation valid for this system since the maximum unambiguous angle from boresight resolvable is about ± 9.5 degrees.

It is assumed that all measurement errors e are zero mean random variables with equal variance σ^2 . Thus the measurement covariance matrix C is given by

$$C = \sigma^2 (A^t A)^{-1} \quad (3.10)$$

the major diagonal elements of which are the variances in estimating the solution variables \vec{x} .

A computer program was written to determine these estimation errors as a function of aircraft location and beacon geometry. It was assumed σ^2 was equal to 0.002 radians spatial angular error. This is commensurate with experimental results presented later in this report. Table 3.1 gives the resulting coordinate estimation errors as a function of aircraft position, given in terms of the aircraft coordinate system. Note that the last line gives the equivalent aircraft position.

Next the elements of matrix A were recalculated by a succession of approximations to investigate the approximation sensitivity. The first approximation was $\sin a = a$, the next was $\cos \theta = 1$, and finally $\cos \beta = 1$. The first is a small angle approximation reasonably valid for acceptable landing configurations. The second is quite good due to the small difference angle θ between attack angle and glide slope. The third approximation is good for low bank angles. Upon application of all 3 approximations, it was found to affect neither the A matrix, the b vector, nor the estimation variances to any significant degree. Nor was the computation time reduced noticeably. Thus it was decided to implement the exact solution.

3.4.3 Perspective Display Program

By similar triangles the plot coordinates for display are given by

$$\begin{aligned} X_k &= D \frac{x'_k}{y'_k} \\ Z_k &= D \frac{z'_k}{y'_k} \end{aligned} \quad k = 1, 6 \quad (3.11)$$

where X_k is the horizontal display coordinate of beacon k, Z_k is the vertical display coordinate, D is the forward (y) distance to the plotting screen from the observer's eye times any necessary scaling terms, and x'_k , y'_k and z'_k are the beacon coordinates in the aircraft coordinate system as given by Eq. (3.2). Positive X is plotted to the right and positive Z is plotted upward.

Table 3.1
LEAST-SQUARES COORDINATE ESTIMATION ERRORS

Beacon Geometry			Aircraft Position ($x_0, y_0, z_0, \theta, \beta, \phi$)					
			R.M.S. Errors are in Parentheses					
L_0 (KM)	W_0 (M)	W -	x_0^0 (M)	y_0^0 (M)	z_0^0 (M)	θ^0 (°)	β^0 (°)	ϕ^0 (°)
3	100	1	-500 (76.4)	10,000 (1495.8)	-500 (76.4)	0 (0.59)	0 (9.15)	0 (0.58)
3	500	1	-500 (17.4)	10,000 (302.0)	-500 (17.4)	0 (0.39)	0 (1.83)	0 (0.39)
3	500	1	-250 (5.3)	5,000 (60.0)	-250 (5.3)	0 (0.19)	0 (0.85)	0 (0.19)
Hex. Pattern -								
3	100	5	-500 (28.5)	10,000 (537.4)	-500 (28.5)	0 (0.41)	0 (3.11)	0 (0.41)
3	100	5	-250 (8.1)	5,000 (129.1)	-250 (8.1)	0 (0.21)	0 (1.54)	0 (0.21)
3	100	5	-125 (2.7)	2,500 (21.6)	-125 (2.7)	0 (0.10)	0 (0.72)	0 (0.10)
3	100	5	-625 (5.8)	2,424 (19.3)	-113.6 (2.5)	0 (0.099)	2.865 (0.70)	11.46 (0.096)
Runway Coords. →			125	-2,500	125			

The perspective display program stored on tape cassette for use in the Want 2200S is written in BASIC. It provides for input and interpretation of the resolved phase data, calculation of the least-squares solution for the ground coordinate system and generation and plotting of a true perspective view of the runway and horizon line. A full listing of the program may be found in Appendix C.

As indicated from Eq. (3.7) and (3.8) in the previous section, it is desired to generate a least-squares solution as follows:

$$(x - x^0) = (A^t A)^{-1} A^t (b - b^0)$$

or

(3.12)

$$x = (A^t A)^{-1} A^t (b - b^0) + x^0$$

where x is the solution vector for the ground coordinate system location, A is the first-order partial derivative coefficient matrix, b is the measured beacon angle vector, b^0 is the expected measurement angle vector and x^0 is the assumed solution vector. In this implementation b^0 is calculated as a function of x^0 as indicated by Eq. (3.2) through (3.5), and x^0 is taken to be the previous least-squares solution.

The perspective display program consists of six major sections. The first is a dimension and setup section which provides for input of physical system parameters such as beacon configuration variables and assumed initial solution. The second calculates display and expected measurement angles. The third section uses the calculated display angles to generate and plot the display. The fourth or input section reads the data from the SDK 80, interprets it as spatial angles and subtracts from them the expected angles. The fifth section generates the elements of the Taylor coefficient matrix. And the last section generates the least-squares solution as indicated in Eq. (3.12). The program then loops

back to the second section for angle calculations based on the latest solution iteration.

On running the program, the setup section requests input of the beacon configuration length to width ratio L and the hex pattern width ratio W . These symbols are indicated in Fig. 3.12 on beacon geometry. Suggested values (for both physical and numeric configurations, of course) are $L = 30$ and $W = 5$. For a non-hexagonal array, the value for W is, of course, 1. Also requested is the distance to the screen in millimeters. A suggested value is 300. Another input quantity is the "G factor" or boresight correction factor. This is a four digit number determined from the boresight program.

The first section also requires input of an initial solution. All six variables are measured relative to the interferometer coordinate system. Coordinates for rotation of the beacon array about its own coordinate system are angles theta, beta and phi, measured in radians, about the x, y and z axes respectively. As indicated in Fig. 3.11, positive rotation sense is determined by the right-hand rule, with the thumb pointing in the positive direction along the axis of rotation. Facing the beacon array in the direction the interferometer does, positive x is defined to the viewer's right, positive y is away from the viewer (the direction the interferometer faces), and positive z is upward. Translational coordinates are measured in units of half the beacon array minor width (W_0 in Fig. 3.12), along the positive axes mentioned above, from the interferometer to the array center, as indicated in Fig. 3.10.

The order of application of rotation, namely first about the x axis, then about the y and z axes, respectively, must be borne in mind when entering initial rotation conditions. Thus, a positive angle theta, representing a rotation of the array about its x axis, indicates a difference in heading between the beacon and interferometer axes which implies that the interferometer (or aircraft) is nosed down toward the array, corresponding most closely to a pitch angle. Similarly, positive beta, being a rotation about the already pitched y axis, corresponds most closely to a bank angle to the right for the runway, or a bank to the left by the aircraft. And a positive angle phi corresponds most closely to a crab angle and indicates the aircraft is headed

to the right of the runway centerline (a positive clockwise crab angle as viewed from above).

Typical rotational coordinates might be 0.2 radians or less, particularly with respect to the pitch angle theta. For a 100 meter wide beacon spacing, typical translational coordinates might be

$$\begin{aligned} |x| &< 5 \\ y &= 100 \\ z &= -5 \end{aligned} \tag{3.13}$$

indicating a runway center less than 250 meters to the right or left of the aircraft heading, 5 kilometers in front of and 250 meters below the aircraft, corresponding to roughly a three degree glide slope. Note that these conditions are unrealizable with the present system due to insufficient remote transmitter cable lengths.

The coordinate transformation of Eq. (3.2), yielding the coordinates of the beacons in the aircraft coordinate system, is calculated first since it is necessary prior to both display calculation and expected angle calculation. This section consists of a calculation of the elements of the transformation matrix as functions of the estimated (or initially assumed) solution coordinates, a statement of the beacon ground coordinates, and subsequent matrix multiplications. This is followed by projection transformations which produce the tangents of the expected measurement angles, as indicated in Eq. (3.4).

The third section calculates the display points by scaling the tangents of the display angles as given in Eq. (3.11). Then it determines the two vanishing points using the angular solution variables. Next it calculates, crops and plots the horizon line joining the two vanishing points. It is plotted from right to left to avoid possible erasure by the TAB function on succeeding points. Lastly, it crops and plots the display points. For the

plotting operation, boresight zero has been defined to be the center of the Wang CRT screen.

The fourth section inputs the resolved phase data from and outputs the boresight correction factor to the SDK 80 using the GIO instruction. Next it unpacks and stores the data prior to interpretation as spatial angles and subtraction of the expected angles calculated in the second section. Lastly, it zeros temporary storage locations.

The fifth section first calculates common terms for use in the matrix element generator. Next it calculates the coefficient matrix elements, first the lines corresponding to azimuth angles, then those corresponding to elevation angles.

The last section performs the calculation indicated in Eq. (3.12) to generate the least squares solution variables for the orientation and location of the beacon coordinate system. The order of matrix operations is chosen to minimize intermediate step data storage requirements. This prevents errors generated by table overflow since the perspective display program utilizes nearly all the memory storage capability of the Wang 2200S. The program then loops back to angle calculation.

Note that the program has been modified to handle data overranging. Available program space dictated use of a simple algorithm which adds or subtracts a fixed amount to incoming data outside of the range from -500 to +500. As a result, the program functions properly but is intolerant of input from beacons outside the maximum unambiguous angle from boresight.

4. EXPERIMENTATION

This section describes the multipath experiments carried out during the course of this contract. First the objectives of the experimentation are outlined. Then the experiments are described and the results presented.

4.1 Objectives of the Experiment

The primary objective of the experimental effort was to demonstrate the performance capabilities of the K-band interferometer based navigation/landing system and to determine the effect of multipath on the accuracy of the resolved angle data transferred to the display processor. The second objective is to determine the resulting accuracy of the least-squares coordinate solution and evaluate the true perspective display output.

4.1.1 Multipath Effects

The objective of this portion of the experimental effort was to locate transmitter, propagation path, and receiver configurations producing strong multipath effects on the received signal (particularly positions near strong nulls), and study the resultant effects on the data quality after ambiguity resolution. This was done in order to obtain an indication of the statistical accuracy of the spatial angle measurements presented to the display processor prior to least-squares estimation and perspective display.

4.1.2 Performance Capabilities

The objective of this segment of the experimental evaluation was to display the six sequenced transmitters in a scaled-down version of a landing beacon array, locate the microwave front end to simulate actual landing configurations and study the static and dynamic performance of the least-squares estimation routine. This was done in order to determine the accuracy limits and response characteristics of the coordinate solution and to evaluate the capabilities of the perspective display.

4.2 Experimental Set-Up and Procedure

The three general configurations employed for data generation were a short range calibration setup, with vertical polarization, horizontal interferometer orientation and minimal diffuse multipath reflection; and two longer range configurations with horizontal polarization, vertical orientation of the interferometer and low angle multipath interference consisting of either specular or diffuse reflection.

4.2.1 Experiment Configuration

All experiments were performed in an open field behind the Air Force Geophysics Laboratory building at Hanscom Air Force Base, Mass. The receiver microwave front end was mounted on a platform which ran on a vertical track up the side of the antenna range tower at one end of the field. For the calibration configuration, the main transmitter and two remote transmitters were all placed at three successive locations with path lengths of approximately 31, 128, and 160 meters, respectively, and the microwave front end was at a local elevation of 8.4 meters. Because of terrain conditions the effective elevation angles were approximately 15.6, 0.2 and 0.1 degrees, respectively. Also, since the main transmitter was located on top of a hill in the last configuration, its effective depression angle to the receiver array was -2.86 degrees. The propagation path was over grass, which provided the minimal multipath reflection.

For the two multipath configurations, the receiver front end height was adjustable from 1.5 to 25.3 meters local elevation, which resulted in -6.5 to 17.3 meters effective elevation with respect to the transmitter locations. For the specular multipath case, the three transmitters were located on the far side of a road running along the far side of the field from the antenna range tower. The specular reflection zone consisted of the asphalt surface of the road and the concrete curbstones. The path length was approximately 160 meters. In the diffuse multipath case, the three transmitters were located on the near side of the road, at a path length of about 140 meters. The diffuse reflection zone consisted of the grassy slope from the transmitter to the receiving array.

4.2.2 Output Monitoring and Recording

The system provides six indicators for monitoring system conditions. These are the five PLL lock indicators and the STC signal indicator. The PLL LEDs were monitored to assure that the PLLs were locked, as indicated by an unlit condition. The STC LED was monitored to assure that a proper signal was being received, as indicated by a blinking condition with a one second repetition rate and a duty cycle equivalent to the transmitted signal ON duty cycle.

The three major data outputs consisted of, first, the three digit resolved phase data for each transmitter displayed on the Wang CRT; second, the magnitude of the received signal at the 5 MHz IF level as monitored on an HP 141/8552/8553 spectrum analyzer; and third, the difference between the resolved elevation angle data for the master transmitter (A) and one of the remotes (B), also displayed on the Wang CRT.

The three digit resolved phase data is, of course, directly proportional to the measured spatial angle to the appropriate transmitter from the interferometer after boresight correction. This is particularly useful in calibrating the interferometer and comparing this to the expected results. It is also used as a direct indication of the statistical effects of multipath interference on the display data input.

The 5 MHz IF signal level monitor was used to locate the receiving array heights associated with strong multipath interference. It provided data on both the location and depth of the signal nulls. The master/remote resolved elevation angle difference readout was used in conjunction with two transmitters located at the same elevation. This was done to produce a zero mean expected reading in order to cancel the effect of the absolute elevation angles at different receiver array heights for data-taking purposes, i.e. an automatic detrending operation. This facilitates statistical analysis of the multipath effects under the various reflection conditions. It also provides a filter on the effects of wind on the microwave antenna array platform since it essentially provides data sampling at a 0.1 second rate with a one second refresh rate.

4.2.3 Startup and Calibration Procedures

After setting up the equipment in the calibration configurations indicated above and accomplishing all necessary system interconnections indicated in the

hardware section, startup procedures were initiated. These consist of power turn on of the main transmitter, receiver, Wang CPU and operator console; momentary depression of each of the five PLL push-to-lock buttons (after ascertaining signal reception via STC LED as indicated above); loading and running the appropriate Wang operating program; and depressing the microprocessor reset button. The synchronization routine requires eight seconds to complete before data can be passed to the Wang for display. The first program to be run is the boresight routine, which determines the boresight correction, or "G," factor to be input via keyboard.

For the calibration portion of the effort, the main transmitter was placed in the field near boresight zero of the horizontal interferometer array, and the two remote transmitters were placed at various measured distances to either side. The calibration operating program provided display of the six digit resolved data for each transmitter. In this way, data was taken to correlate resolved phase data with actual measured spatial angles. The remote readouts were compared to the main readout to determine relative data.

4.2.4 Experimental Procedure

For the multipath portion of the experiment, the equipment was first installed and started up as indicated above. The objective of locating regions of strong multipath influence and studying the effect on the data was then easily accomplished. The receiving antenna platform was moved up and down the tower, with the interferometer in a vertical orientation, and the 5 MHz IF signal level was monitored to search for a minimum level. Then near positions of strong multipath effect, data was taken on the individual transmitter or master/remote difference angle readouts (displayed on the Wang CRT by the multipath operating program) as a function of height and signal level, for both specular and diffuse reflection.

For the improved multipath conditions portion of the experiment the transmitters were equipped with horizontally polarized staggered slot array antennas to effect shaped beam transmission. The master and remote transmitters were placed in the specular reflection configuration described above. The 5 MHz signal level was then monitored as a function of receiver antenna height to determine the depth of the multipath nulls and the transmitting antenna depression angles were adjusted for minimal cancellation. It was found that a 10 degree depression angle yielded the best results. The slotted array gain/angle plots are shown in Fig. 4.1.

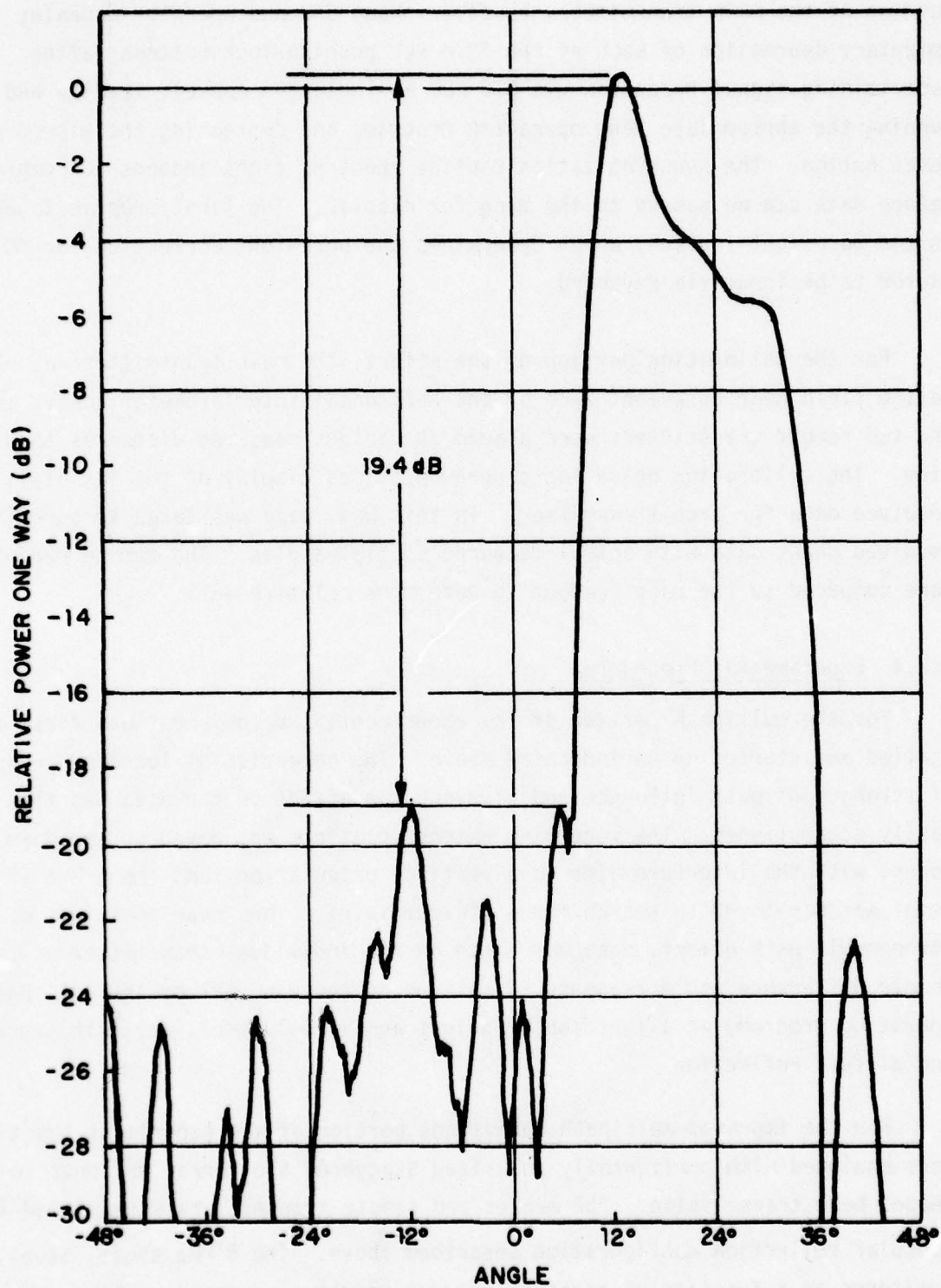


Fig. 4.1 Slotted Array Gain/Angle Plot

4.3 Test Results

This section presents the results of the multipath test effort to determine the quality of the data entering the display processor. It includes calibration accuracy results and multipath interference results.

4.3.1 Calibration Results

For the calibration portion of the experiment, the recorded readouts were compared to the expected readings. From the measured slant range and transmitter spacings, the differential readouts were calculated according to the following formulas. The interferometer gain is given by

$$\theta_e = 2\pi \frac{d}{\lambda} \sin \theta_s \quad (4.1)$$

where θ_e is electrical phase difference in radians, d is the receiving antenna spacing, λ is the transmitted wavelength and θ_s is the spatial angle from the interferometer boresight to the transmitter. Since the phase data is quantized in terms of one hundredth of an electrical cycle, the readout is given by

$$R = \frac{100}{2\pi} \theta_e \quad (4.2)$$

where R is the CRT readout. For the calibration configuration

$$\frac{d}{\lambda} = \frac{1000 \text{ mm}}{18.9393 \text{ mm}} = 52.8 \quad (4.3)$$

Therefore,

$$R = \frac{100}{2\pi} \cdot 2\pi \cdot 52.8 \sin \theta_s = 5280 \sin \theta_s \quad (4.4)$$

From this equation and the measured spatial angles, it was determined that the worst case error amounted to +3.62% of the expected reading and the average magnitude of the error amounted to 2.54% of the expected readings. This was within the experimental and readout digit quantization error expected. This confirms the high accuracy of the K-band cycle counter. From Eq. (4.4), readout quantization is given by

$$\theta_s = \sin^{-1} \frac{1}{5280} \quad (4.5)$$

which equals 10.92 millidegrees for the initial configuration. No multipath effects were observed in this segment of the experiment.

For the improved multipath portion, it should be noted that the microwave receiving antenna spacing was changed to 30.0 wavelengths. By similar calculations, readout quantization for this spacing is found to be 19.471 millidegrees, or 0.34 milliradians of spatial angle.

4.3.2 Multipath Results

The results achieved in the multipath tests are shown in Fig. 4.2 and 4.3. Figure 4.2 graphs the average readings of the master/remote difference angle readout as a function of receiving array height for diffuse reflection. Recall that a zero mean readout was expected. It was found that multipath fading was on the order of 6 dB worst case, with nulls occurring at heights between 19 and 23 feet, for both the master and remote transmitters. At this point the average difference angle readout goes through its maximum change of 10 digits from -3 to +7, representing a worst case spatial error of 0.11 degrees or 1.9 milliradians, and a peak error of 0.076 degrees or 1.33 milliradians.

Figure 4.3 graphs the reading of the master/remote difference angle readout for specular reflection as a function of array height. In this case it was found that multipath fading was on the order of 17 dB for the main transmitter and 14 dB for the remote transmitter, worst case. These nulls were also more sharply defined as a function of location. Because of vertical interferometer orientation and physical separation of the receiving antennas, the reference and coarse antennas passed through a null at a different array height than did the fine antenna. Thus the main transmitter null produced effects at both 23 and 20 feet, and the remote transmitter null occurred at both 20 and 17 feet.

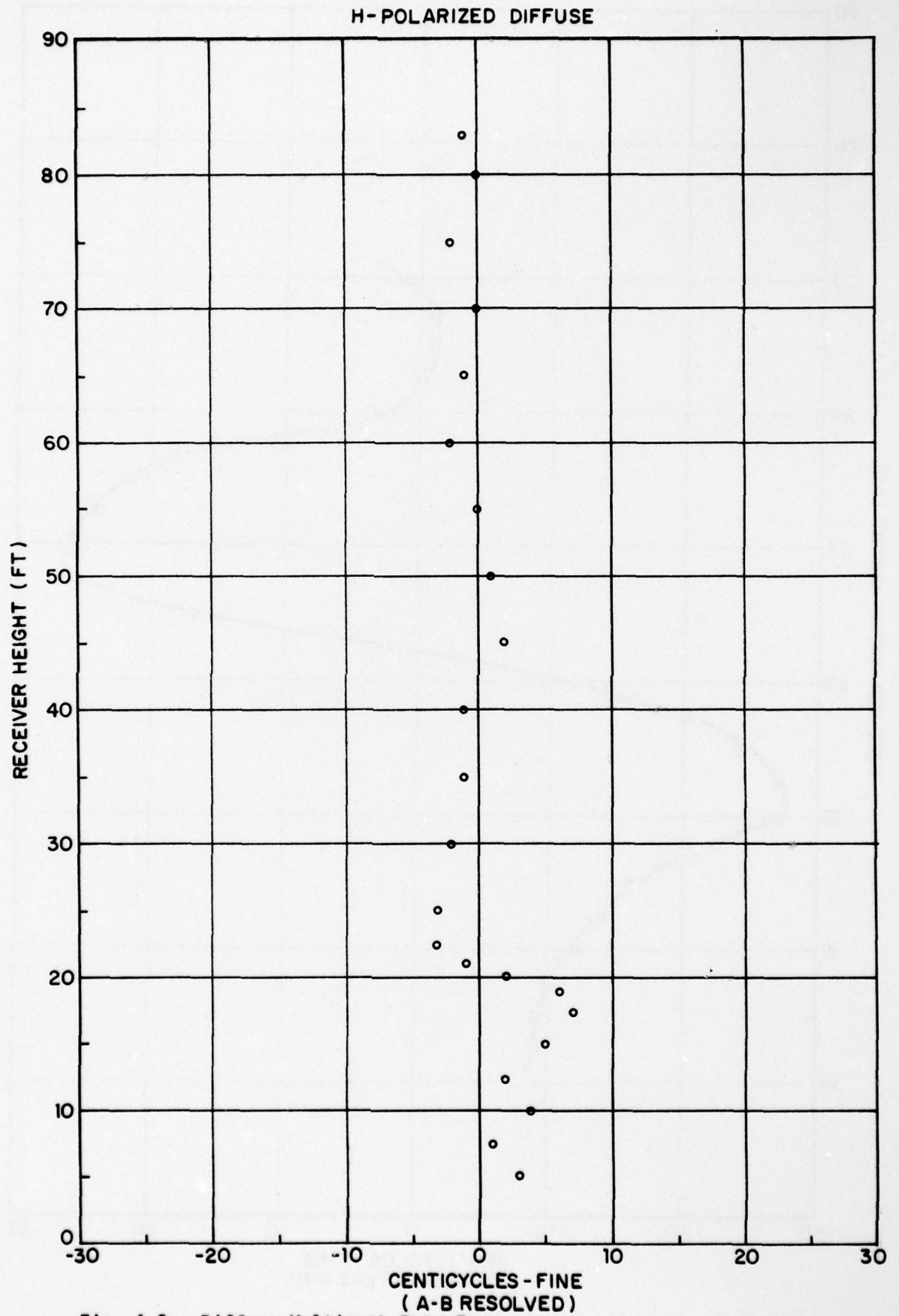


Fig. 4.2. Diffuse Multipath Data Errors

60
H - POLARIZED SPECULAR

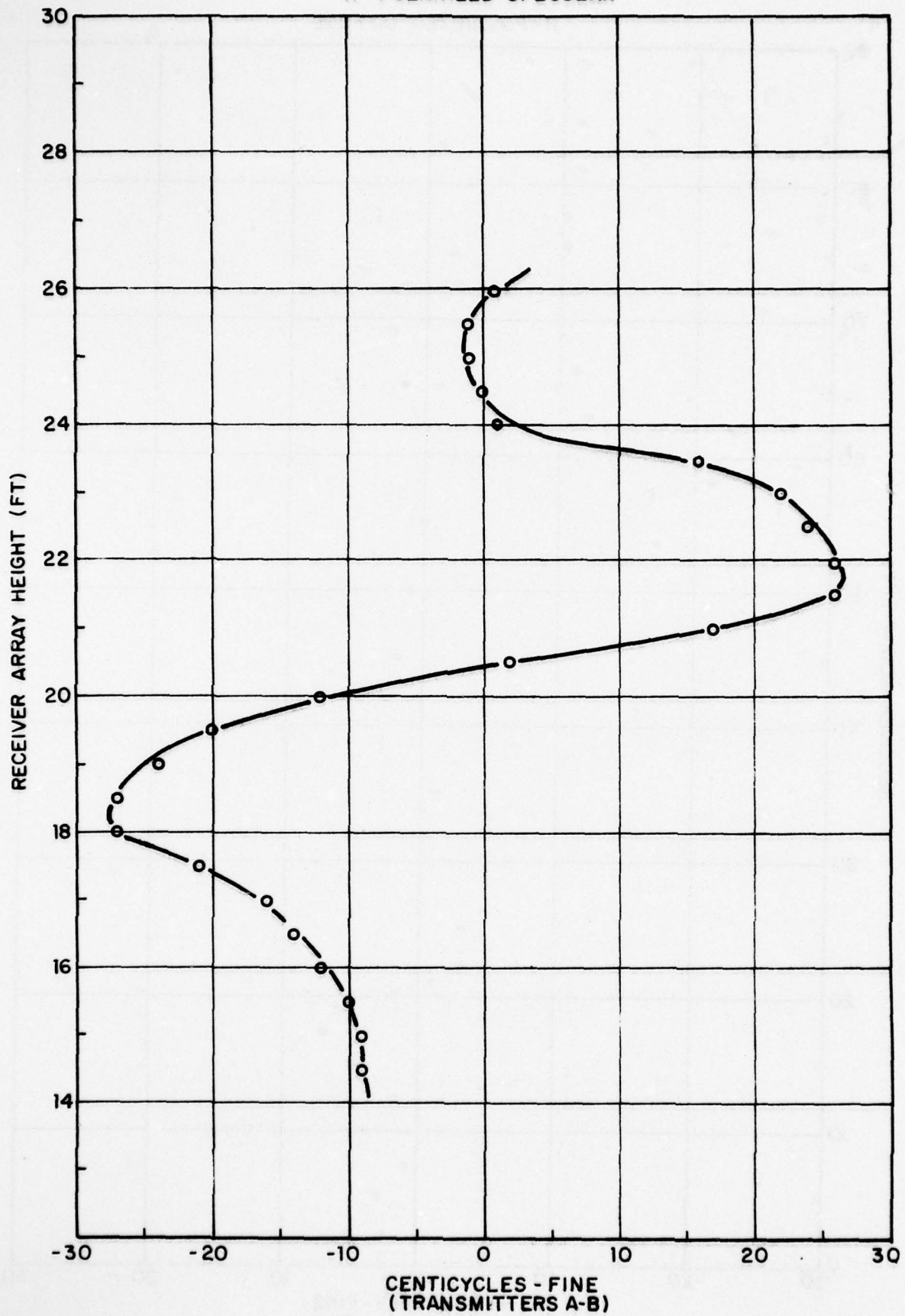


Fig. 4.3. Specular Multipath Data Errors

As shown in the graph the difference angle readout experiences a change of 59 digits, worst case, near the 20 foot nulls. This represents a spatial angular error of 0.64 degrees (11.2 milliradians) peak-to-peak, or 0.23 degrees (4 milliradians) rms for a worst case condition consisting of two coincident null effects. The apparent effect of a single null (as indicated by the readout change near the 23 and 17 ft. levels) is approximately half this amount. This does not take into account the improvements which may be made by utilizing shaped beam transmitting antennas and microwave absorbing material in the reflection zone.

Not indicated in the figure are the errors resulting from incorrect ambiguity resolution. These were experienced just above the 23 ft. level, and indicate that the sharpness of the effective multipath zone at the receiving array was sufficient to produce anomalous effects at the two (coarse and fine) separated antennas. Due to specular reflection from the horizontal surface of the runway, it is expected that this will have significant effect only upon the vertical data. This effect is also expected to be reduced or eliminated by the employment of shaped beam transmission and microwave absorber.

4.3.3 Shaped Beam Improved Results

The results obtained for shaped beam transmission over a specular reflection zone are shown in Fig. 4.4. Average readings of vertical master/remote difference angle readouts are graphed as a function of receiving array height. Multipath fading was on the order of 2 dB. The graph shows a 7.5 digit p-p error, representing a worst case spatial error of 0.146 degrees or 2.54 milliradians peak-to-peak.

It should be noted that the 30 wavelength fine antenna spacing used for this portion of the experiment reduces the precision of the interferometer and increases the effect of multipath phase errors. However, since the digit error is close to unity, a smaller antenna spacing tends to increase the relative effect of digit quantization error.

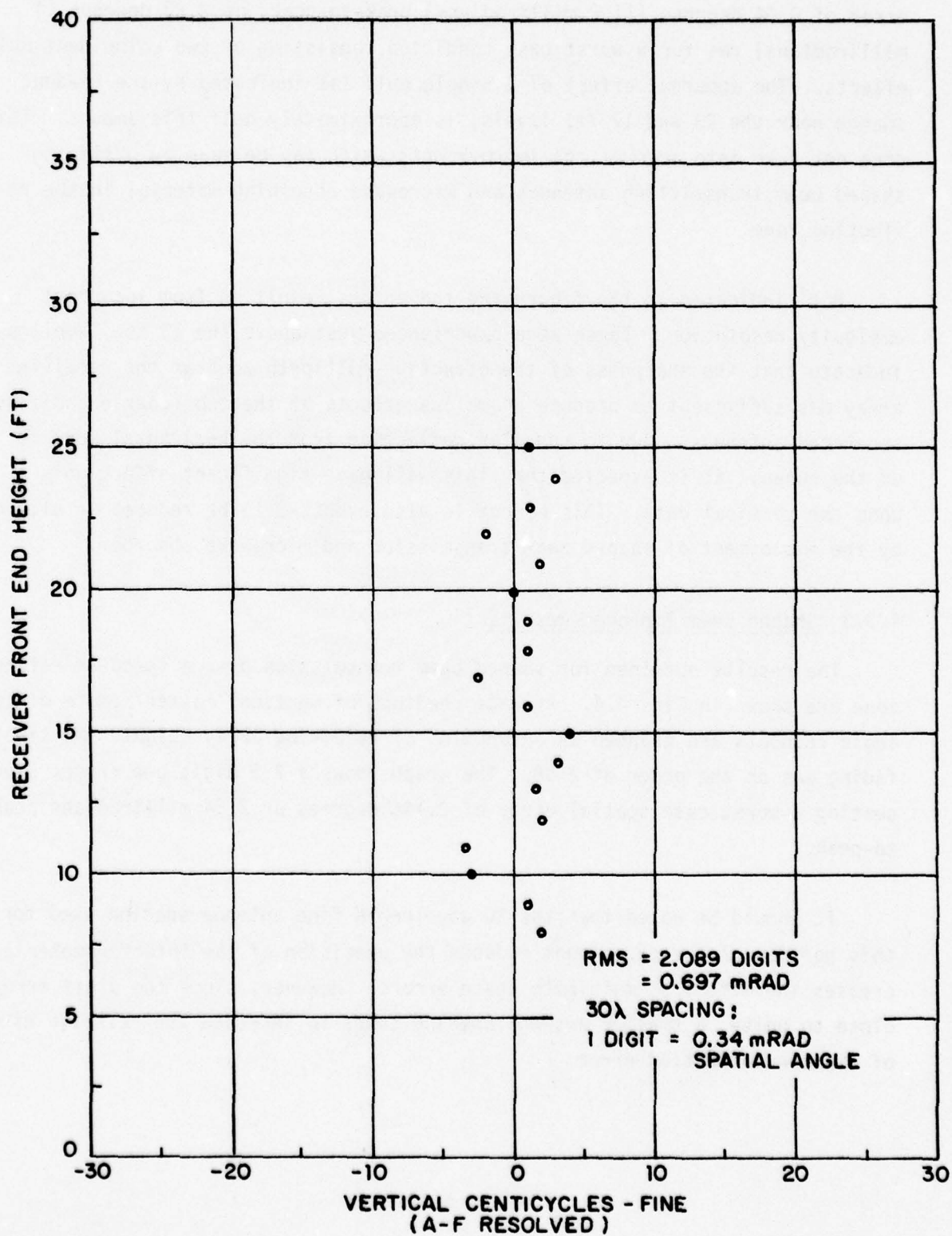


Fig. 4.4. Shaped Beam Specular Multipath Data Errors

One positive result of a closer antenna spacing is the increased spatial acceptance angle. For the 52.8 wavelength spacing, the acceptance angle is ± 5.36 degrees, whereas for the 30 wavelength spacing it is ± 9.22 degrees.

No ambiguity resolution errors were noted for shaped beam transmission.

4.4 Performance Demonstration Results

This section presents the results of the study of the performance characteristics of the least-squares estimation routine under live data input conditions in a simulated scaled-down landing configuration. It includes static and dynamic performance results, coordinate solution error data and comments on perspective display capabilities.

4.4.1 Demonstration Configuration

For the demonstration phase of the effort, the six transmitters were deployed in the field next to the antenna range tower in the hexagonal geometry indicated in Fig. 3.12. The array width, W_0 , was 6 feet; the length, L_0 , was 180 feet. The center pair separation width was 30 feet, giving a hex width factor of 5. The center of the array was 210 feet directly in front of the receiver microwave front end. The staggered slot array transmitting antennas were used with a 10 degree depression angle.

The front end height was adjustable from 5 to 20 feet. In addition, it was possible to introduce rotation about the three major axes of the front end array.

4.4.2 Demonstration Procedure

The equipment was first installed and started up as indicated above. Then the boresight program was run to determine the boresight factors for entry into the least-squares routine. Then the least-squares estimate perspective display program was run.

The coordinate solutions were then studied for accuracy and error statistics. Dynamic variation was introduced into the simulated landing configuration by way of adjustments to the microwave front end height and discrete rotations about its axes, as indicated above. The coordinate solutions and perspective display were studied for response characteristics and accuracy. The Wang runway perspective and horizon line display was studied for capabilities and limitations.

4.4.3 Display Output and Test Results

The coordinate solution accuracy was tested with the above-mentioned adjustments to front end height and orientation. Using the coordinate convention indicated in Chapter 2, with the x axis to the right, y forward and z upward, measurable rotation about the x and z axes were obtainable. A close correspondence was noted between the measured front end rotation and the corresponding display solution coordinates (θ and ϕ) due to relative rotation of the beacon pattern as seen by the interferometer. Close correspondence was also noted between the consequent changes induced in the translational (z and x) solution coordinates and the calculated values. Rotation about the y axis produced the expected rotation of the pattern perspective display and horizon line. The z coordinate solution was found to be a quite accurate indicator of front end height. This close correspondence can be explained by the relatively high precision to which the actual height was measured.

The solution response characteristics were studied by way of step changes introduced in the front end height and orientation. Convergence on the new solution was usually noted after one or two iterations. Solution response was also probed by means of intentional misinitialization of program solution variables. The solution was found to converge within one to four iterations.

The display accuracy was gauged by eye. The runway perspective display and horizon line were noted to properly indicate all of the above-mentioned adjustments to the front end. Because of the long time (approximately 20 seconds) necessary for each solution/plot iteration, the display was completely discrete in time, and its response characteristics were equivalent to those of the coordinate solution. Display vertical quantization, stemming from the spaced

line format of the Wang, was most limiting. Horizontal (adjacent character) quantization was less noticeable.

The coordinate solution error statistics observed are presented in Table 4.1. The translational quantities presented have been scaled up for direct comparison with the expected results presented in Chapter 3. This is for a runway width of 100 meters. It should also be noted that the height (Z_0) given is the position of the beacon array center in the interferometer coordinate system, and is not necessarily the aircraft altitude. For the first two cases, because of elevation angle rotation, the actual altitudes are 400 and 259 meters respectively.

Table 4.1
OBSERVED SOLUTION COORDINATE ERRORS

Aircraft Position (R.M.S. Errors in Parentheses)					
x_0 (m)	y_0 (m)	z_0 (m)	θ (°)	β (°)	ϕ (°)
0 (3)	3500 (13)	-205 (2.8)	3.15 (0.036)	0 (1.3)	-0.6 (0.06)
0 (13.5)	3500 (152)	-66 (3)	3.15 (0.216)	0 (0.24)	-0.6 (0.36)
0 (3.64)	3500 (39.55)	-200 (3.61)	0 (0.102)	0 (0.195)	-1.2 (0.378)

In the first case, the solution errors are well within expected values for similar geometries. For the other two cases, however, not all of the variables exhibit lower errors. Some are as much as twice what might be expected, particularly x , y and ϕ . These discrepancies are for the most part due to insufficient mechanical stabilization of the interferometer platform against the effects of wind, which caused random changes in its orientation, particularly with respect to rotation about the vertical axis. This instability, together with the much less than instantaneous sample time of 0.6 seconds imposed by the transmitter sequencing rate, introduced observable error into the raw data entering the least-squares routine. Here it is coupled by the matrix inversion process into other solution variables, although it affects the more obvious quantities to a greater extent. This condition caused a much smaller effect in the first case due to the fact that this position was much closer to the point at which the interferometer angles were constrained. Without these constraints it was noted that the solution r.m.s. errors were larger. These errors would be much smaller if the transmitter cycle rate was faster.

This points to more general observations regarding the interferometer display system. It is inherently quite sensitive, with 0.33 milliradian data quantization. This sensitivity, together with the small unambiguous acceptance angle of $\pm 9.22^\circ$ leads to problems of data overranging and consequent grossly erroneous solutions. This points out the need for further data processing such as bad point rejection and prediction routines for overrange ambiguity resolution. Simple routines may well be adequate for landing system requirements, but were not feasible in this demonstration experiment due to a shortage of memory space in the Wang and the slow computation rate of the Wang calculator.

4.5 Conclusion

The experimental effort has shown that satisfactory system performance can be achieved to yield accuracies equal to or better than those predicted in Table 3.1. It has also shown that, with shaped beam transmission techniques, multipath phase errors can be kept near or below the 2 milliradian r.m.s. level used to predict those accuracies, even under the more severe conditions of transmission over a large reflective asphalt surface. Hence it can be expected

that satisfactory performance can be achieved for actual runway environments.

The perspective display and horizon line showed satisfactory static and dynamic performance within the limitations of the Wang output format. This was found to be the most significant limitation on actual visual output due to the tremendous imbalance between the format display capabilities and the solution accuracies. This fact, coupled with the slow (approximately 12 second) data processing speed of the Wang, indicate that this part of the system is the greatest obstacle to a workable landing display. Faster processing and a more suitable display format should eliminate this obstacle and yield a system with dynamic dependence mainly on PLL tracking characteristics, transmitter sequencing rate, and available signal-to-noise ratio.

5. CONCLUSIONS

This section summarizes the conclusions derived from the experimental program. Recommendations for future efforts in connection with the perspective navigation technique are presented.

5.1 Results of the Program

The experimental effort described in this report demonstrated that a perspective navigation system utilizing a crossed-baseline interferometer can provide reliable, high accuracy performance.

Previous efforts in this area were not entirely successful because low elevation angle operation was severely degraded by multipath reflections. For example, the Microvision System created by the Bendix Corporation does not provide high accuracy display under low elevation angle conditions. The perspective navigation system described in this report is similar to the Bendix approach. However, the measurement and signal processing is substantially different. In particular, the approach employed for the perspective navigation system was designed and developed from the outset with the multipath problem in mind.

Concurrent landing monitor efforts carried out at M.I.T. Lincoln Laboratories (Beacon Radar Precision Altitude and Landing Monitor, J. E. Evans, et al.) provide high accuracy in the presence of multipath at low elevation angles. However, the operation of the Lincoln Labs. system is ground based. As such, it does not make independent measurements of aircraft orientation. Rather, it provides accurate position information only. The perspective navigation system is intended to provide independent monitoring of both position and orientation of the aircraft relative to the runway coordinate system.

5.1.1 Basic Measurement Accuracy

The interferometer measurement/least squares processor technique was shown to yield high accuracy aircraft position and orientation estimates. Specifically, the most sensitive (and most critical) parameter is aircraft altitude. Under very severe GDOP conditions, the r.m.s. error in this parameter was approximately

5 percent. Under more typical landing conditions, it was 1-2 percent. Similarly the critical elevation angle had an r.m.s. error of roughly 10 percent under poor GDOP conditions and roughly 1 percent under average landing conditions.

5.1.2 Multipath Performance

Worst-case spatial error in the presence of multipath was roughly 2.5 milliradians peak-to-peak and no ambiguity resolution errors were observed. Shaped beam antenna and horizontal polarized transmission were employed for the experimentation. These results are sufficient for the purposes of the perspective navigation system. Even better performance can be obtained using shaped beam antennas which utilize vertical polarization. However, antennas of this type were not readily available during the experimental effort.

5.1.3 Perspective Display

The feasibility of a perspective display system based on the technology developed during the course of the contractual effort was clearly demonstrated. However, the perspective display performance was limited by Wang processor speed and the relatively crude pictorial display capabilities of the Wang 2200S 16 x 64 alpha-numeric CRT readout system. The Wang 2200S offered significant flexibility and cost advantages for the development program. The unit served as both an analytical tool and an experiment monitor. However, it was not ideally suited for the perspective display role. Nonetheless, a perspective display of the beacon transmitter array and an artificially derived horizon line were generated by the least-squares estimation processed interferometer data. The display update rate was once per 20 seconds. This rate was limited by the Wang calculator capabilities.

5.2 Recommendations

The experimental effort conducted under this contract produced uniformly positive results. Thus, it is recommended that further development of the system should proceed. This section presents specific areas where further effort is required. The discussion also includes consideration of other applications for the system.

5.2.1 Hardware Improvements

The implementation currently uses 1 sequence per second. The hardware in its present form is capable of transmitted sequence rates on the order of 10 per second. Even faster sequencing rates are feasible with minor hardware modifications. In fact, the only limit on sequencing rate is determined by PLL bandwidth. The bandwidth is selected such that sufficiently low noise error is achieved at a given signal-to-noise ratio. The current system was designed to provide 13 dB of margin at a range of 10 km with +10 dBm transmitted by each beacon through low gain antennas. Clearly, higher transmitted EIRP's are easily achieved. Thus, it is reasonable to conclude that update rates well in excess of 10 per second could be achieved with the same general hardware configuration.

Even better multipath performance can be obtained through the use of vertically polarized antennas. It is recommended that consideration be given to the use of shaped beam vertically polarized antennas for future development systems.

5.2.2 Software Improvements

Future development systems should employ computer subsystems which are tailored to the perspective navigation system requirements provided that real-time rapid update performance is desired. The basic matrix least-square solution should be replaced by a recursive formulation of the least-squares solution or by a Kalman-Bucy recursive estimation algorithm. Use of a more suitable computer subsystem and recursive estimation procedures should result in a more rapid update rate capability.

The added computation speed capability should also be used to allow the addition of important system features which were not included in the demonstration system. In particular, software should be implemented which extends the maximum unambiguous acceptance angle beyond that determined by the coarse interferometer antenna separation. This is achieved by recognizing $0-2\pi$ transitions in the measured electrical angle data from a given transmitter beacon.

Software should also be implemented to screen the data before least-squares (or Kalman-Bucy) processing. In this way, obviously erroneous data caused by

multipath or other phenomena can be rejected before the position/orientation algorithms. Since each solution is overdetermined, it is believed that several questionable points per sequence can be rejected without serious consequences.

5.2.3 Display Equipment

A number of relatively inexpensive CRT display systems have become available which should be considered for the perspective display application.

5.2.4 Other Applications

The position/orientation measurement capabilities of the perspective navigation system can be used to advantage for monitoring of airborne experiments. The system will provide unique capabilities under poor visibility conditions. Typically, such experiments do not require data in real-time. In that case, the system can be readily reconfigured so that the interferometer angle measurement data is formatted for digital recording on-board the test vehicle or for transmission to a ground based recording and/or processing system via an air/ground data link. The only modification required in the software is a change in the 8080 output algorithm.

Depending on the applications, it may also be desired to decrease the fine interferometer antenna separation in order to accommodate the packaging constraints. In this connection, it should be noted that the receiver RF-IF and PLL equipment can be repackaged to yield a more compact structure.

APPENDIX A

Schematic Diagrams

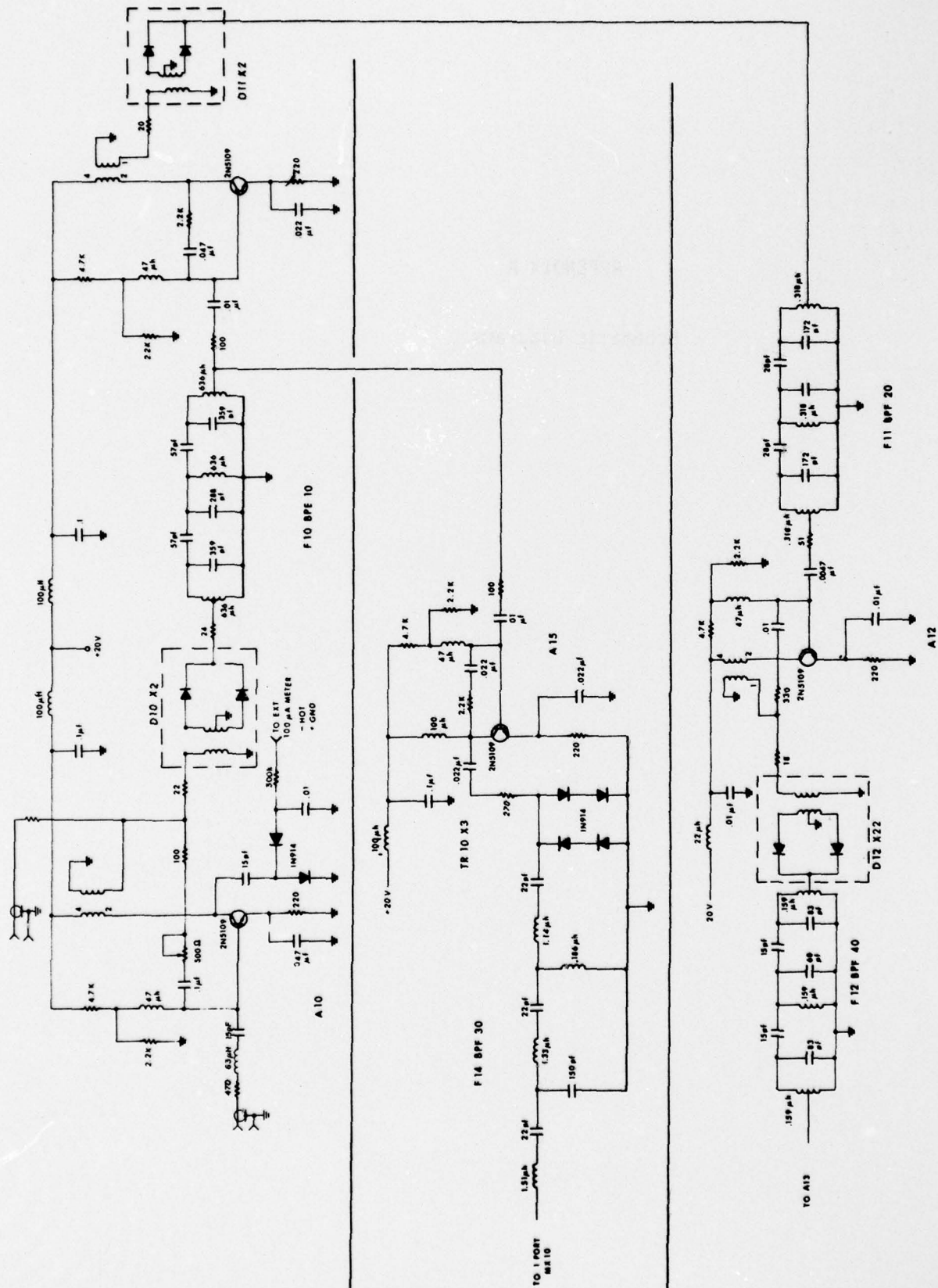


Fig. A-1A Transmitter Frequency Synthesizer (Sheet 1 of 2)

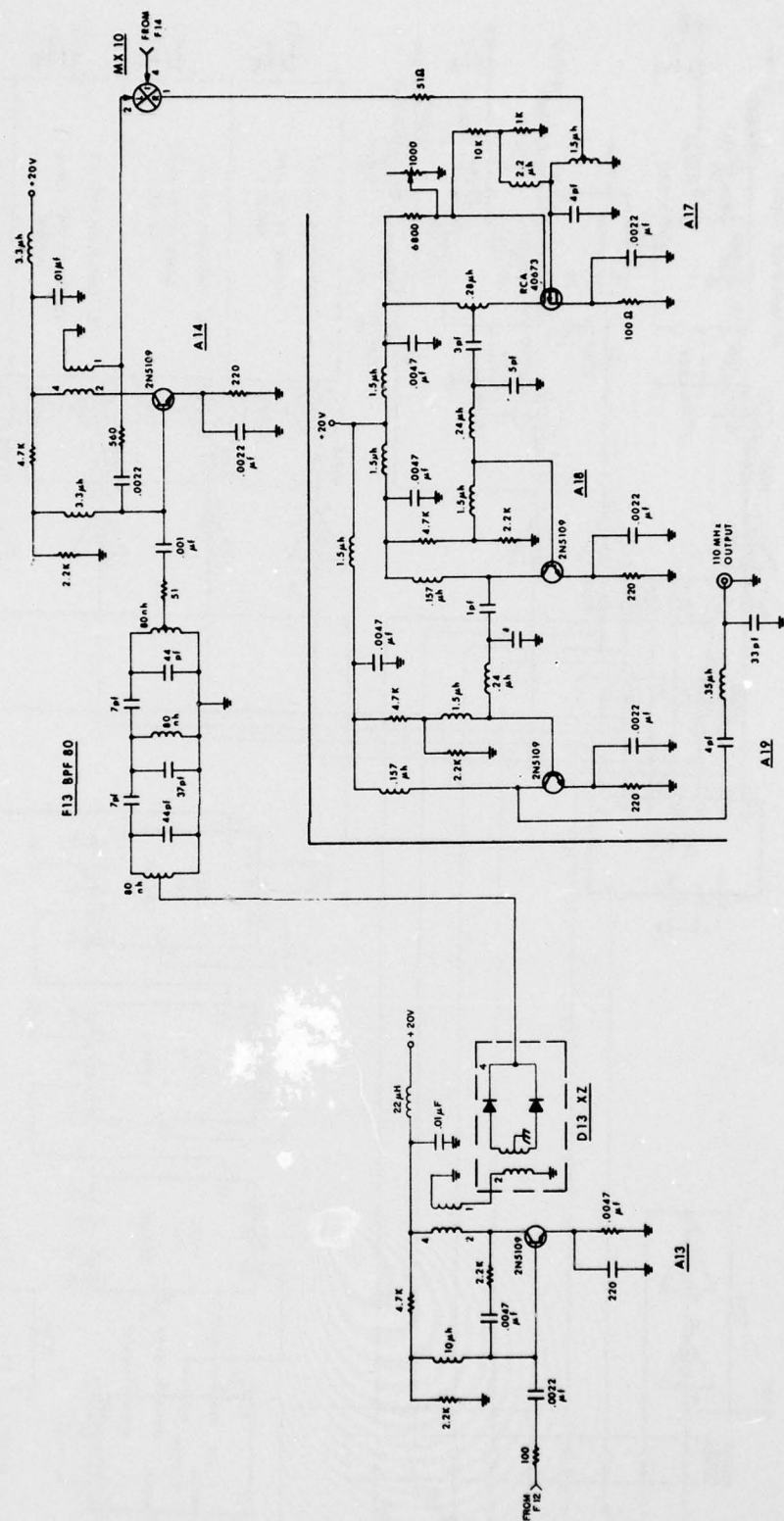


Fig. A-1B Transmitter Frequency Synthesizer (Sheet 2 of 2)

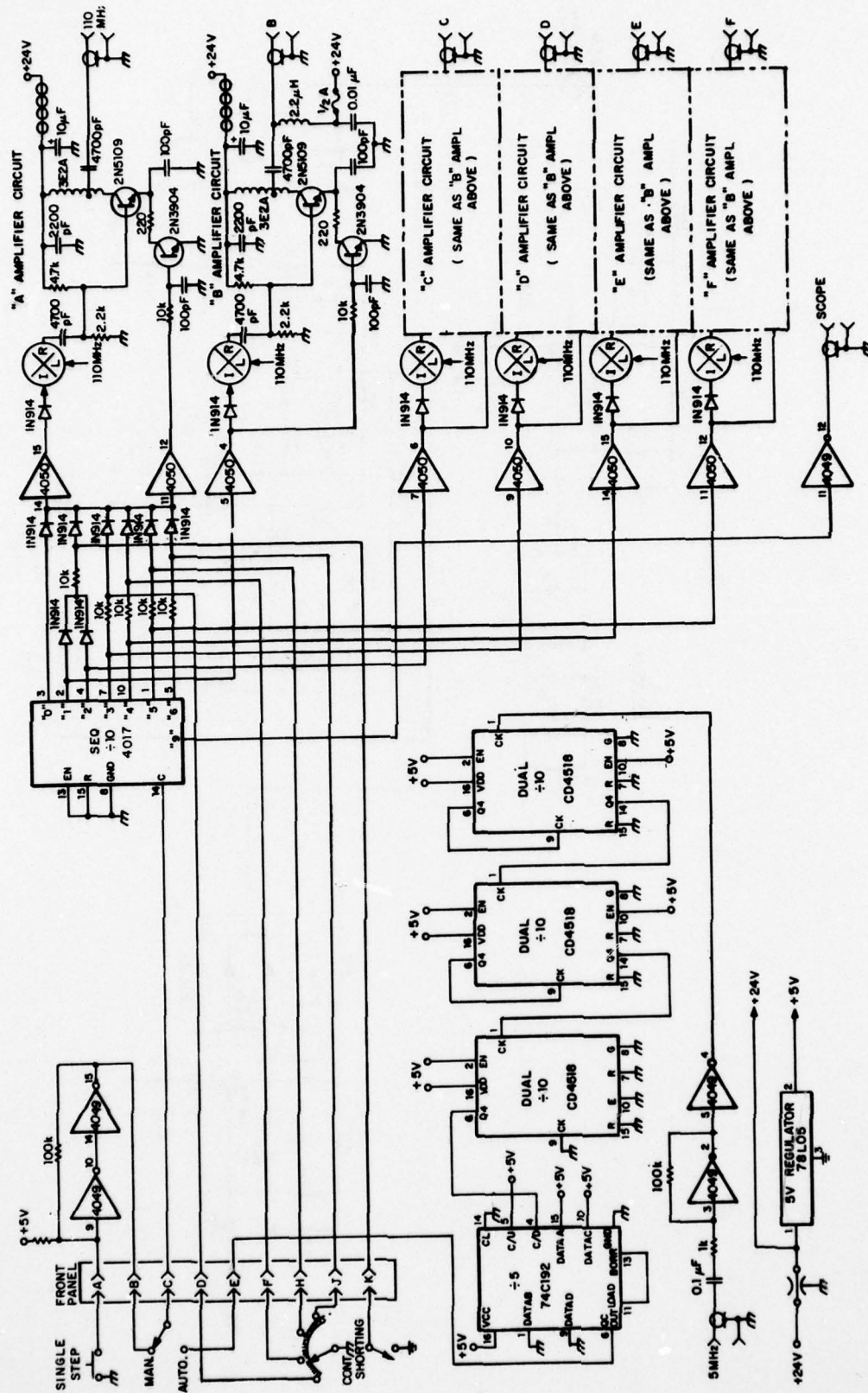
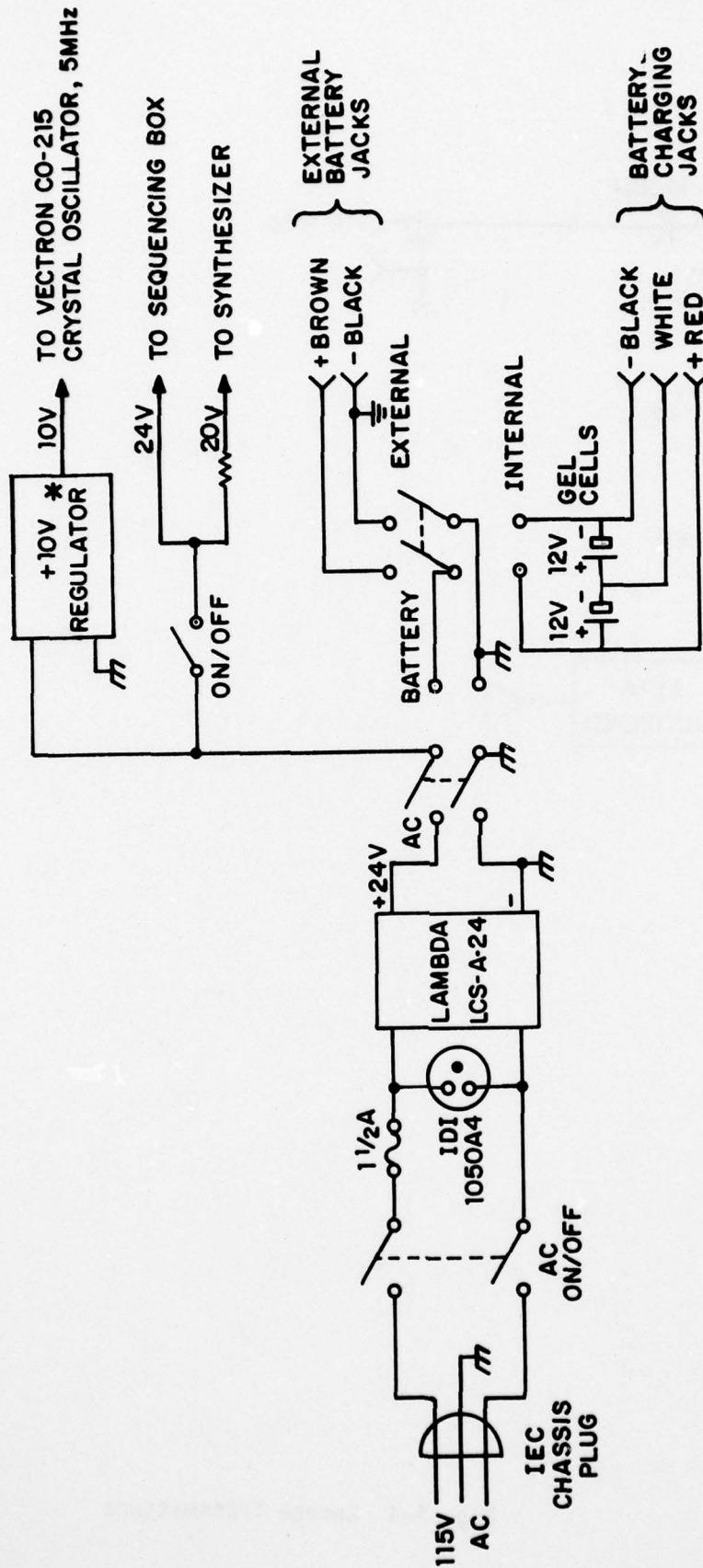


Fig. A-2 Transmitter Sequencing Box



* NOTE: SEE FIG. B-8 OF AFCRL-TR-75-0526

ALL SWITCHES, JACKS ON REAR PANEL.

Fig. A-3 Transmitter Power System

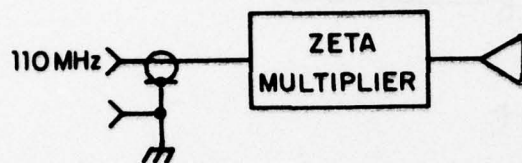
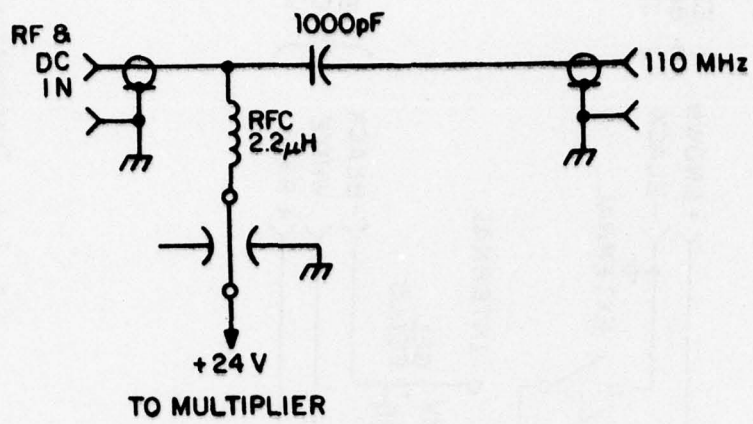


Fig. A-4 Remote Transmitters

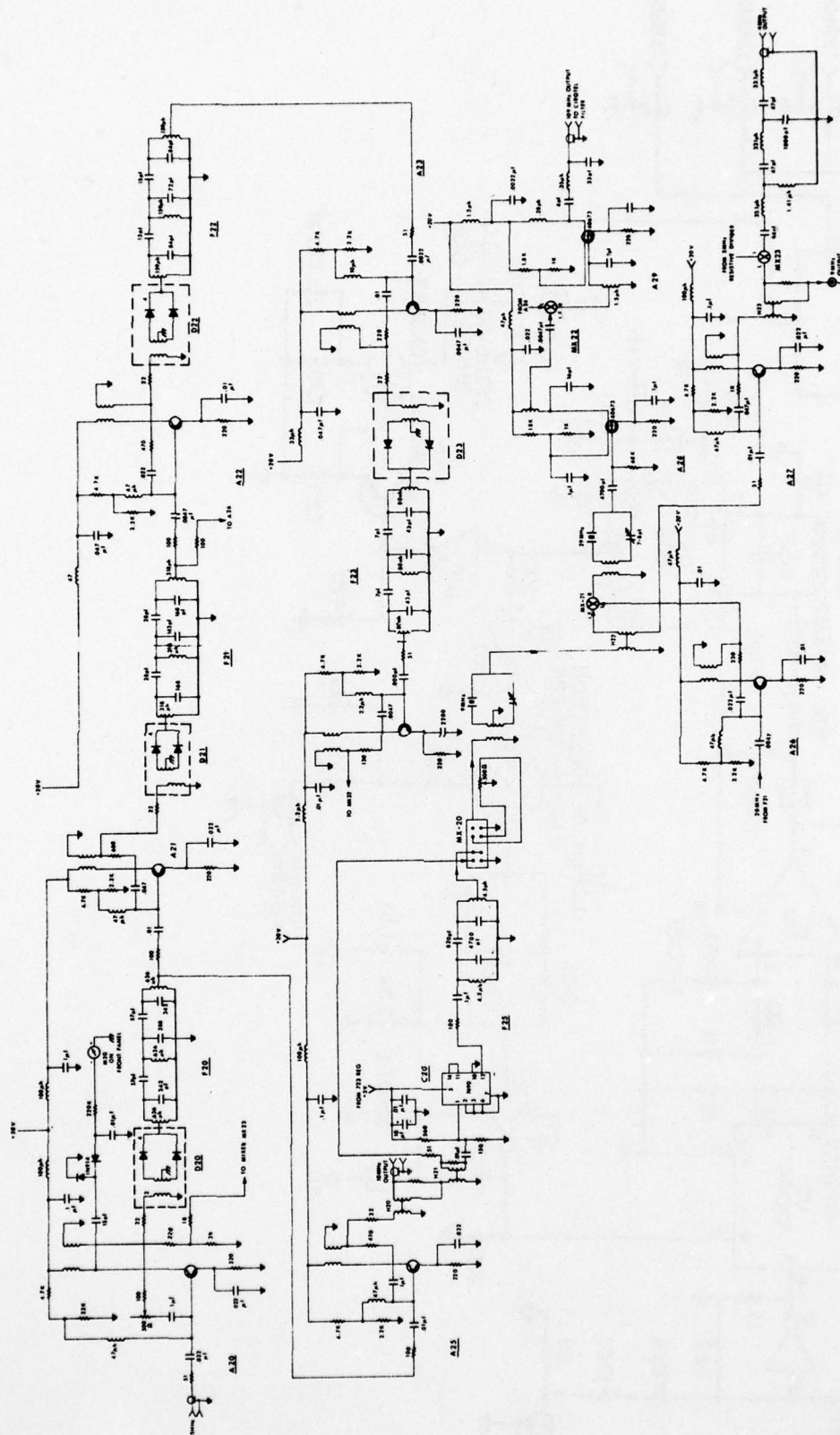


Fig. A-5 Receiver Local Oscillator Synthesizer

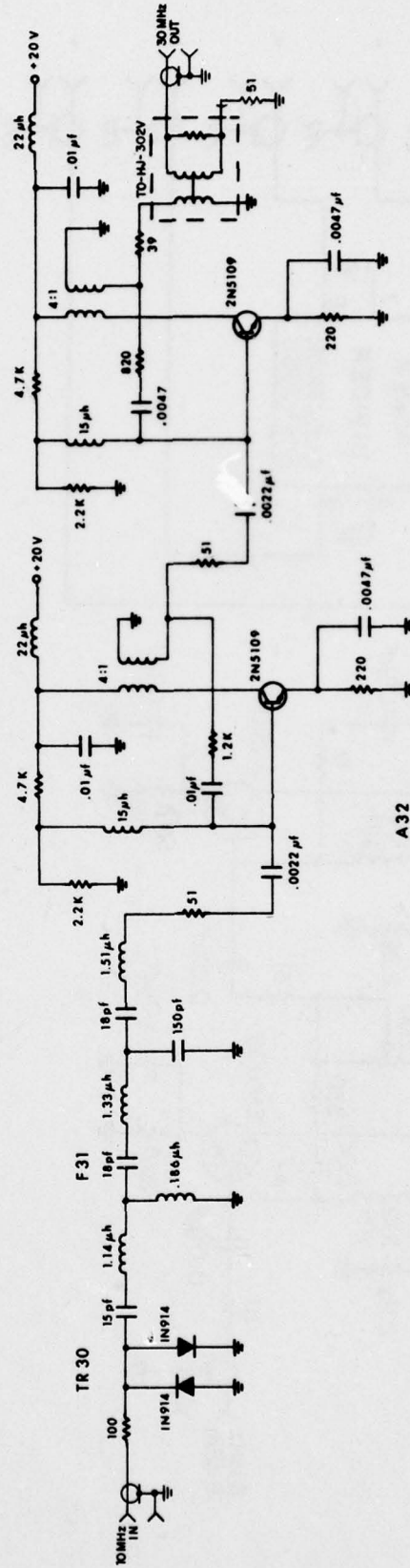
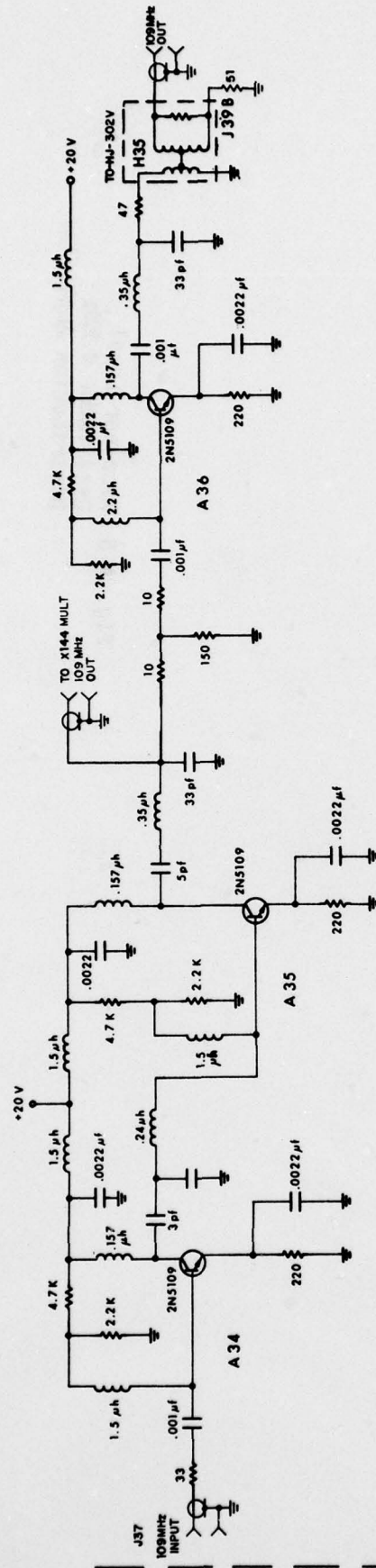
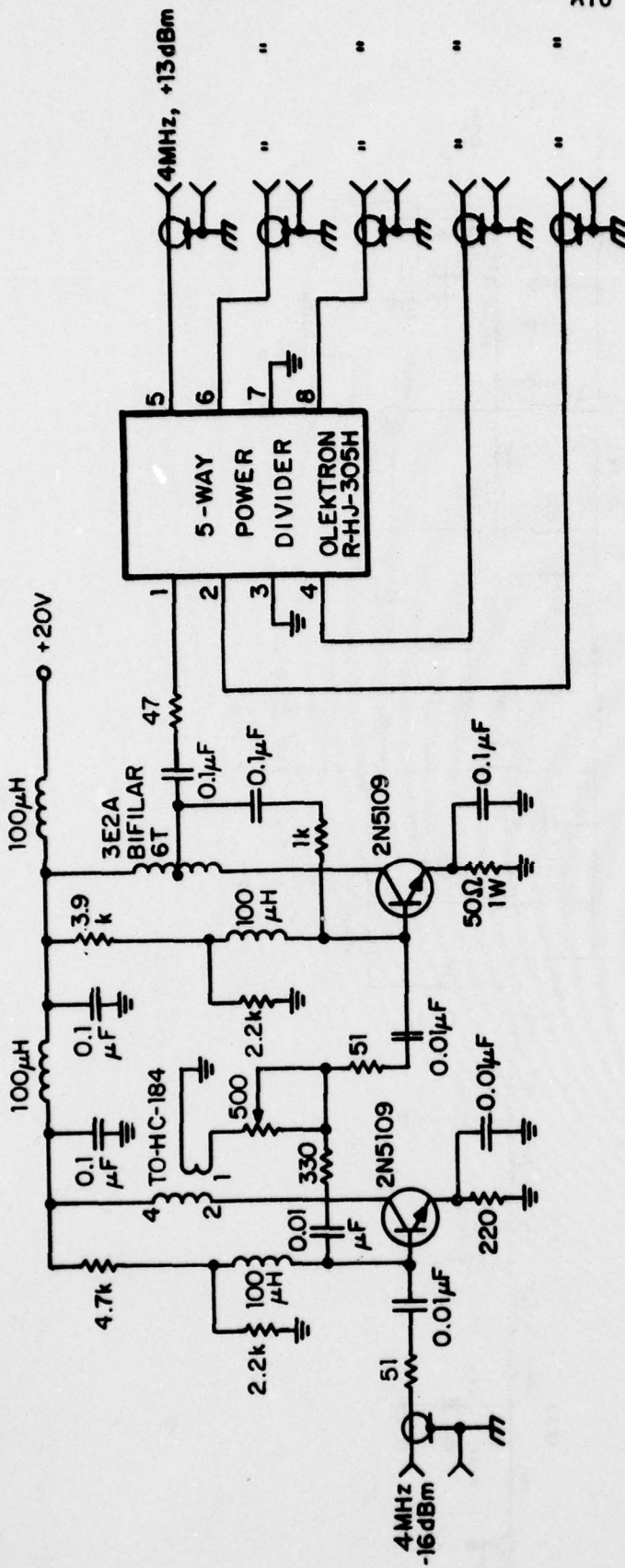


Fig. A-7 Receiver Local Oscillator 109 MHz Distribution Amplifier



A10

Fig. A-8 Receiver Local
Oscillator 4 MHz
Distribution Amplifier

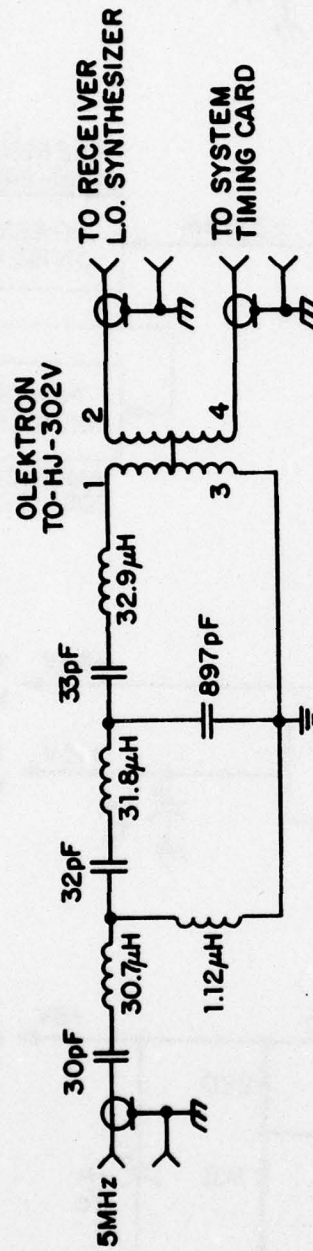


Fig. A-9 Receiver 5 MHz Input Filter

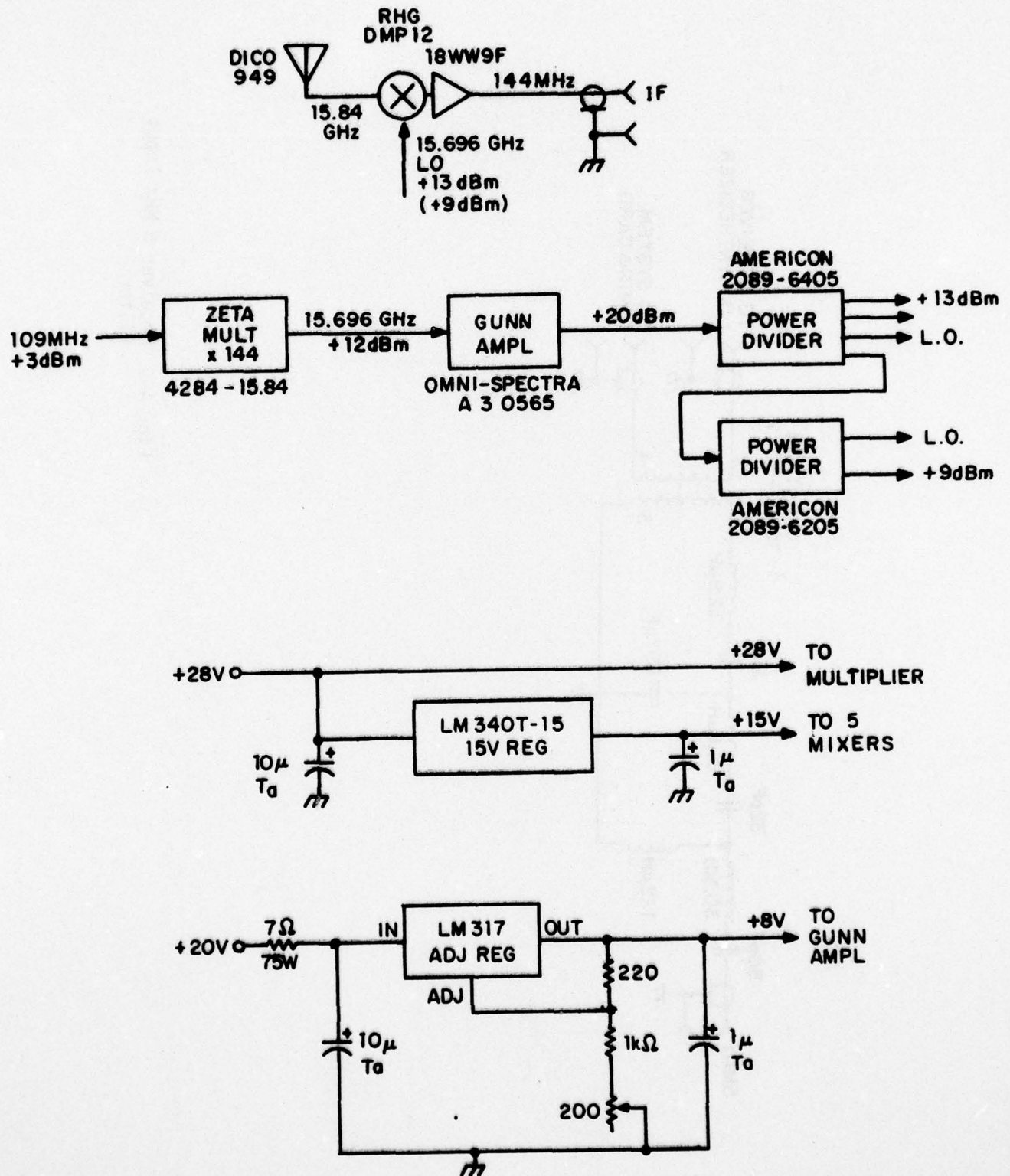


Fig. A-10 Receiver Microwave Front End

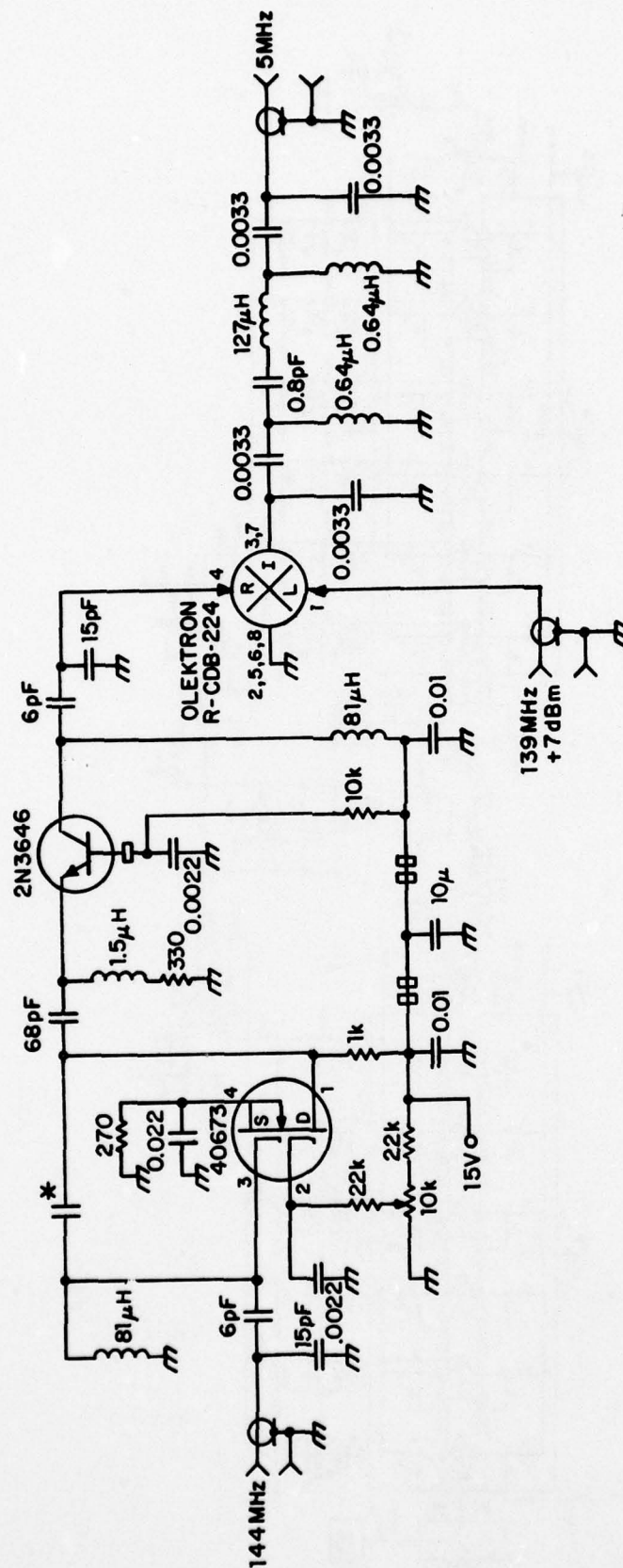


Fig. A-11 Receiver First IF

*** NEUTRALIZING FEEDBACK
GIMMICK CAPACITOR**

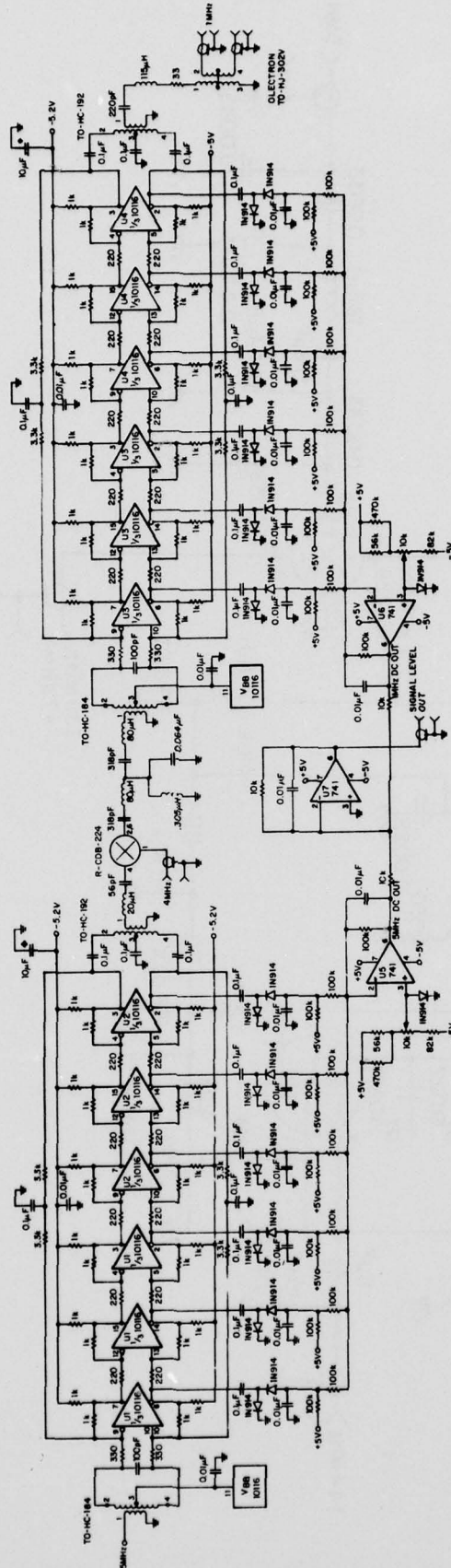


Fig. A-12 Receiver Signal Limiter

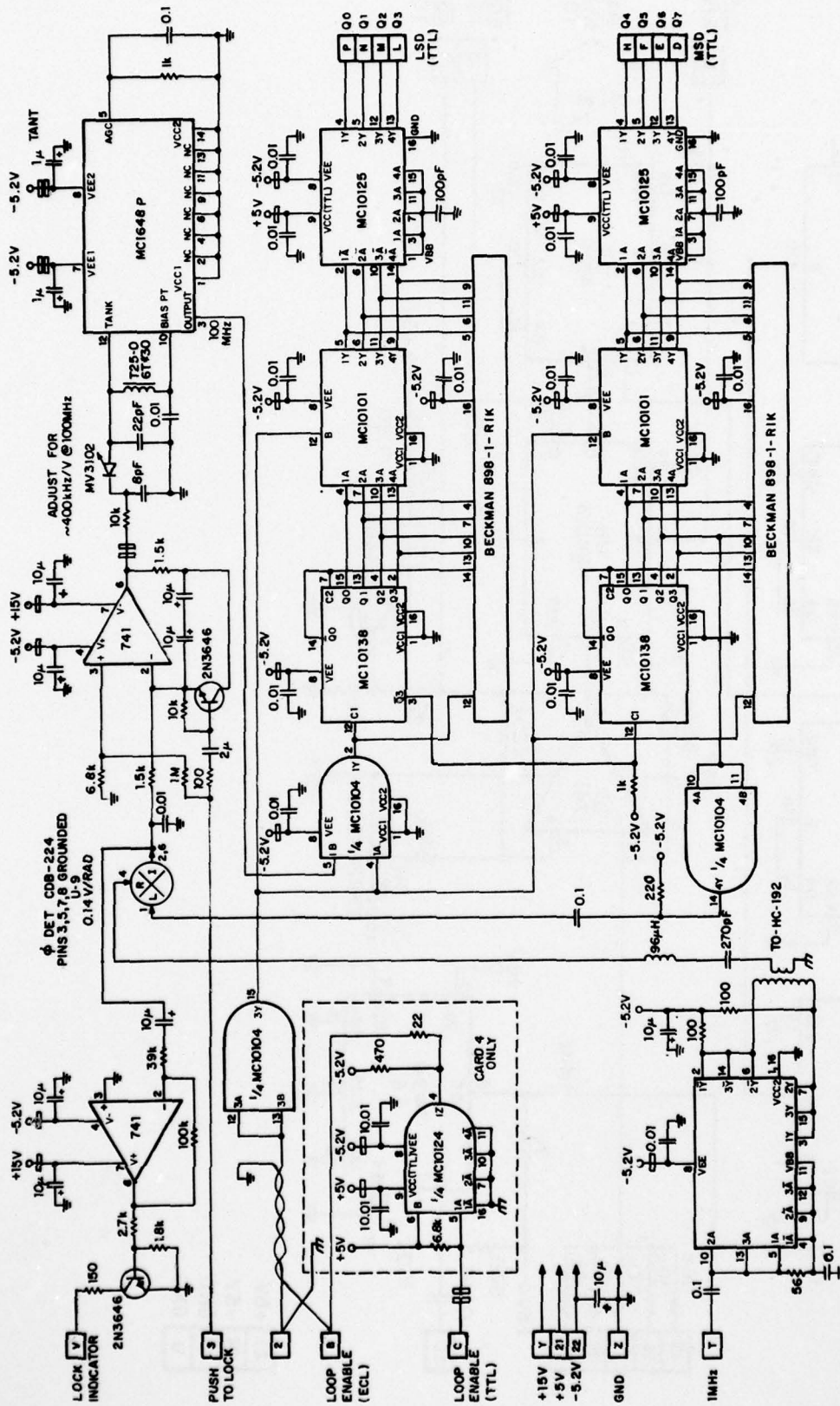


Fig. A-13 Receiver Phase Locked Loop

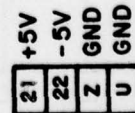


Fig. A-14 Receiver System Timing Card

AD-A049 260

PROTEON ASSOCIATES INC WALTHAM MASS
PERSPECTIVE NAVIGATION SYSTEM.(U)
OCT 77 H SALWEN, H ARBOUR

F/G 17/7

UNCLASSIFIED

A117F

RADC-TR-77-345

F19628-76-C-0040

NL

2 OF 2
AD
A049260



END
DATE
FILMED

3 - 78

DDC

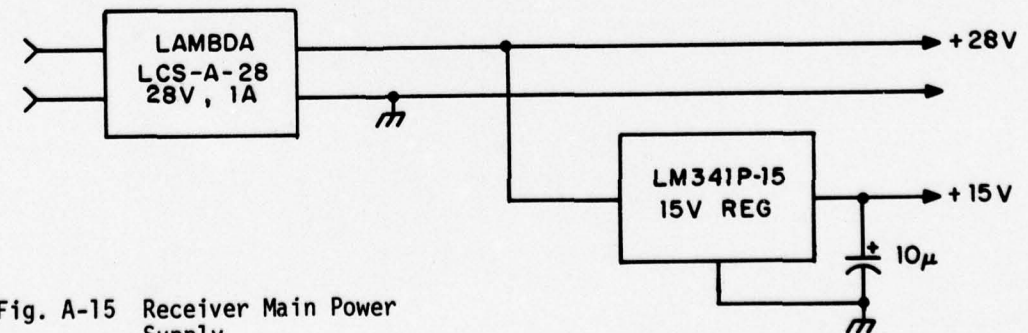
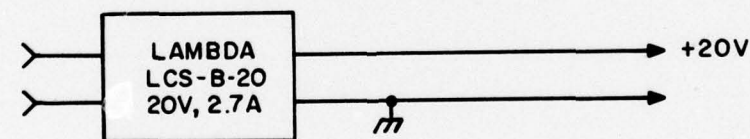
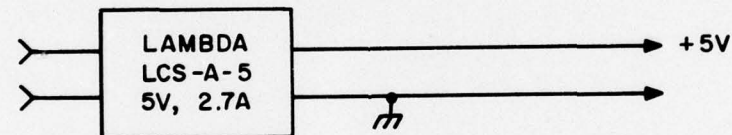
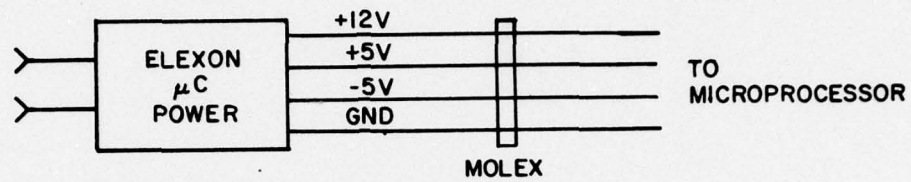
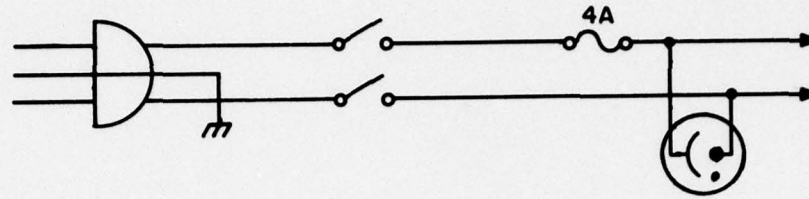


Fig. A-15 Receiver Main Power Supply

APPENDIX B
SDK 80 Operating Program

;A117 OPERATING PROGRAM
 ;REV 11 FROM VERSION - 1/19/77
 ; MOD FOR 6 TRANSMITTERS
 ; A C MARSHALL

;EQUATES

```

00F0      MSB      EQU 0F0H
000F      LSB      EQU 0FH
000F      LSD      EQU 0FH
0005      FIVE     EQU 5
0004      FOUR     EQU 4
0000      ZERO     EQU 0
0002      FINE     EQU D
0028      GETCM    EQU 02BH
0002      CPB      EQU 2          ;PC1
13FD      MSTAK    EQU 13EDH
13F2      ASAVE    EQU 13F2H
13F3      LSAVE    EQU 13F3H
13F7      SSAVE    EQU 13F7H
13F5      PSAVF    EQU 13F5H

;WANG
00F7      WNCTL    EQU 0F7H      ;WANG CONTROL
00F6      WNGIO    EQU 0F6H      ;PORT C
00F5      WNOTD    EQU 0F5H      ;PORT B
0091      WNMCD    EQU 91H        ;A IN, B OUT, H-C OUT, L-C IN
00F4      WNIET    EQU 0F4H      ;PORT A
0020      ACK      EQU 20H        ;PC5
0010      IBS      EQU 10H        ;PC4
0001      DORE     EQU 1          ;PC0

;TIMING
0001      SKEDG    EQU 1          ;PC0
0020      RTMCT    EQU 20H        ;PC5
0040      SKSET    EQU 40H        ;PC6
00EC      TMCA     EQU 0ECH        ;PORT A
00ED      TMCB     EQU 0EDH        ;PORT B
00EE      TMCC     EQU 0EEH        ;PORT C
00EF      TMCIL    EQU 0EFH        ;CONTROL
0004      INT      EQU 4          ;PC2
0002      SGLVL    EQU 2          ;PC1

;DATA CHANNELS
0093      VTMCD    EQU 93H        ;A, B IN; CH OUT, CL IN
009B      DTMCD    EQU 9BH        ;ALL INPUTS
00DF      DTCH     EQU 0DFH        ;DATA HOR CTL
00BF      DTCV     EQU 0BFH        ;DATA VERT CTL
00DC      DTCHF    EQU 0DCH        ;HOR FINE, PORT A
00DD      DTCHC    EQU 0DDH        ;HOR COARSE, PORT B
00BC      DTCVF    EQU 0BCH        ;VERT FINE, PORT A
00BD      DTCVC    EQU 0BDH        ;VERT COARSE, PORT B
00BE      SYCTL    EQU 0BEH        ;SYSTEM CONTROL PORT C
00BF      DTCR     EQU 0BFH        ;PORT C, REF
0010      PLLBT    EQU 10H
13A0      STACK    EQU 13A0H

;
;RAM DATA STORAGE
      ORG 1000H
1000      DS 2
1002      BYCTR:   DS 1          ;CONTINUOUS BYTE COUNTER
1003      DS 1
1004      FRCTR:   DS 1          ;CONTINUOUS FRAME COUNTER
1005      BYCT:    DS 1          ;0-9 COUNTER

```

BEST AVAILABLE COPY

1006	BGNCT: DS 1	;INITIALIZATION BYTE--SYNCH
1007	ABYTE: DS 1	;FRAME SYNCH (SECURE)
1008	ABYTS: DS 1	;FRAME SYNCH SIGNAL
1009	SDTBL: DS 8	;STORAGE TABLE FOR 8 SYNCH DATA EL
1011	SYDEL: DS 1	;BCD MSEC FOR SYNCH DELAY
1012	SYBYT: DS 1	;BYTE # OF SYNCH EDGES DURING SYN
1013	RFBFA: DS 1	;REF A
1014	RFBFB: DS 1	;REF B
1015	RFBFC: DS 1	;REF C
1016	RFBFD: DS 1	;REF D
1017	RFBFF: DS 1	;REF E
1018	RFBFF: DS 1	;REF F
1019	HRBFA: DS 3	;HOR A, RAW COAR, COAR/FINE
101C	HRBFB: DS 3	;HOR B
101E	HRBFC: DS 3	;HOR C
1022	HRBFD: DS 3	;HOR D
1025	HRBFF: DS 3	;HOR E
1028	HRBFF: DS 3	;HOR F
102B	VTBFA: DS 3	;VERT A, RAW COAR, COAR/FINE
102E	VTBFB: DS 3	;VERT B
1031	VTBFC: DS 3	;VERT C
1034	VTBFD: DS 3	;VERT D
1037	VTBFF: DS 3	;VERT E
103A	VTBFF: DS 3	;VERT F
103D	TCMWD: DS 1	;TIMING COMM WORD
103F	SYCTR: DS 1	;SYNCH COUNTER
103F	SYSCM: DS 1	;SYSTEM CONTROL WORD
1040	TEMP: DS 4	
1044	CTMOD: DS 1	;SYNCH COUNT MODE SWITCH

;BORESITE CONSTANTS

ORG 10A0H

CONST:

10A0	HCCOR: DS 1	;HORIZ COAR CORR
10A1	VCCOR: DS 1	;VERT COAR CORR
10A2	DS 62	

;64 BYTES

ORG 800H

:

;A C MARSHALL APR 16, 1976

:

;INITL

;INITIALIZE -- ENTERED ONCE AT SYSTEM TURN ON.

; HAS EQUATES AND RAM STORAGE ALLOCATION

:

0800	DI	;DISABLE INTERRUPTS
0801	MVT A,0C3H	;JUMP INSTRUCTION
0803	STA 13PDH	
0806	LXI H,INTPR	;TRANSFER ADDR
0809	MOV A,H	
080A	STA 13FFH	
080D	MOV A,L	
080E	STA 13FEH	
0811	XRA A	;CLEAR ACCUM
0812	STA ABYTE	
0815	STA ABYTS	
0818	STA BYCT	
081B	STA BGNCT	;SET FOR SYNC FIRST
081E	STA CTMOD	
0821	STA SYSCM	
0824	LXI H,BYCTR	

BEST AVAILABLE COPY

0827 77
 0828 2B
 0829 77
 082A 2B
 082B 77
 082C 21 04 10
 082D 77
 0830 2B
 0831 77
 0832 3E FF
 0834 32 12 10
 0837 B6 0F
 0839 32 3D 10

MOV M,A
 DCX H
 MOV M,A
 DCX H
 MOV M,A
 LXI H,FRCTR
 MOV M,A
 DCX H
 MOV M,A
 MVI A,-1
 STA SYBYT
 ANI LSR
 STA TCMWD

BEST AVAILABLE COPY

083C 31 80 13

;STACK SETUP
 SSTAK:LXI SP,STACK
 ;IO SETUP

;INITIALIZE STAK PTR

083F 3E 01
 0841 D3 F7
 0843 D3 FF
 0845 3E 0F
 0847 D3 DF
 0849 3E 03
 084B D3 BF

SIOPT:MVI A,WNMOD
 OUT WNCTL
 OUT TMCTL
 MVI A,DTMOD
 OUT DTCH
 MVI A,VTMOD
 OUT DTCV

;WANG
 ;TIMING
 ;DATA
 ;VERT AND SYS CON

084D 3A 3D 10
 0850 EF 60
 0852 D3 FF
 0854 EF 60
 0856 D3 FF
 0858 FF
 0859 76

;SETUP TIMING

CLRIM: LDA TCMWD
 XRI BTMCT XOR SKSET
 OUT TMCC
 XRI BTMCT XOR SKSET
 OUT TMCC
 EI
 HLT

;RESET SYNCH TIME
 ;ENABLE INT
 ;WAIT FOR INTERRUPT

085A F5
 085B F5
 085C C5
 085D D5
 085F 3A 06 10
 0861 B7
 0862 CA 23 09
 0865 CD 77 08
 0869 3A 05 10
 086B FF 05
 086D CC 76 08
 0870 D1
 0871 C1
 0872 F1
 0873 F1
 0874 FB
 0875 C9

;INTPR: PUSH H ;SAVE H

PUSH PSW
 PUSH R
 PUSH D
 LDA BGNCT
 ORA A

;SAVE A,FIGS
 ;SAVE B,C
 ;SAVE D,E
 ;GET FLAG
 ;SET CONTROL

MAIN: CALL BYTPR

JZ SYNCH
 LDA BYCT
 CPI 5

;IN SYNCH ROUTINE
 ;DO BYTE PGM

CZ FRPR2

;END OF LAST TRANSMITTER?
 ;YES DO FRAME PGM

POP D

;REST D,E

POP B

;REST B,C

POP PSW

;REST A,FIGS

POP H

;REST H

EI

;ENABLE INT

RET

;RETN TO INT'D PGM

0876 C9

FRPF2: RET ;DUMMY

;BYTE PROCESSOR

;BYTPR

;A C MARSHALL APR 16,1976

;A CONTROL PROGRAM FOR EACH INTERRUPT - 100 MSEC

0877 CD 06 08
 087A 3A 05 10

BYTPR: CALL INCB
 LDA BYCT

;INCREMENT BYTE NUMBER
 ;BYTE COUNTER

087D EF 06
087F DC B4 08
0892 CD FC 09

```

CPI 6          ;>LAST BYTE?
CC DTSTR       ;NO, INPUT AND STORE DATA
CALL WANGO     ;TRANSFER DATA TO WANG
CALL PLTDT     ;GET PLOT DATA
CALL PLOT      ;PLOT IT
CALL PRINT     ;PRINT OUTPUT
RET

```

0885 C9

```

;A C MARSHALL APR 16, 1976
;INCP--INCREMENT BYTE COUNTER AND HOUSEKEEPING
;

```

0886 21 02 10
0889 06 00

```

INCEC: LXI H, BYCTR      ;CONTINUOUS COUNTER

```

088B 7E

MVI B, 0

088C 3C

MOV A, M

088D 27

INR A ; INCREMENT

088E 77

DAA ; DEC ADJ

088F 2B

MOV M, A ; STORE

0890 78

DCX H

0891 8E

MOV A, B

0892 27

ADC M ; ADD WITH CARRY TO NEXT DIGIT

0893 77

DAA

0894 2B

MOV M, A

0895 78

DCX H

0896 8E

MOV A, B

0897 27

ADC M

0898 77

DAA

0899 3A 05 10

MOV M, A

089C 3C

LDA BYCT

; 0-9 COUNTER

089D EF 0A

INR A

089F C2 A3 08

CPI 10

08A2 AF

JNZ INCB1

08A3 32 05 10

XRA A ; RESET TO 0

08A6 C0

INCB1: STA BYCT

08A7 21 04 10

RNZ ; END EXCEPT BYTE 0

08AA 7E

INCFR: LXI H, FRCTR ; GET FRAME COUNTER

08AB 3C

MOV A, M

08AC 27

INR A ; INCREMENT

08AD 77

DAA

08AF 2B

MOV M, A

08AF 78

DCX H

08B0 8E

MOV A, B

08B1 27

ADC M

08B2 77

DAA

08B3 C9

MOV M, A

RET

```

;
;A C MARSHALL -- MAY 17, 1976
; STORES AND INPUTS ANGLES
; CALLS AMBIG
;

```

08B4 3A 2F 10

DTSTR: LDA SYSCM ; SYSTEM COMMAND WORD

08B7 EF 10

XRI PLLBT ; MAKE PC4 LO - HOLD

08B9 03 EF

OUT SYCTL ; OUTPUT CMD WD

08BB DB EF

IN DTOR ; IN REF BYTE

08BD 2F

CMA ; SIGN CHANGE

08BE 21 05 10

LXI H, BYCT ; GET BYTE COUNT

08C1 5E

MOV E, M

08C2 16 00

MVI D, 0

08C4 D5

PUSH D

08C5 21 13 10

LXI H, RFBPA

08C8 19

DAD D

BEST AVAILABLE COPY

08C9 77
08CA 5F
08CB 3F 9A
08CD 93
08CE 87
08CF 27
08D0 5F
08D1 32 41 10
08D4 DB DC
08D6 2F
08D7 83
08D8 27

08D9 57
08DA DB DD
08DC 2F
08DD 83
08DE 27

08DF 4F
08E0 3A A0 10
08E3 91
08E4 27
08E5 4F
08E6 CD 43 9A
08E9 42
08EA D1
08EB D5
08EC 21 19 10
08EF 19
08F0 19
08F1 19
08F2 71
08F3 23
08F4 77
08F5 23
08F6 70
08F7 3A 41 10
08FA 5F
08FB DB DC
08FD 2F
08FE 93
08FF 27
0900 57
0901 DB DD
0903 2F
0904 83
0905 27
0906 4F
0907 3A A1 10
090A 91
090B 27
090C 4F
090D CD 43 9A
0910 42
0911 D1
0912 21 2B 10
0915 19
0916 19
0917 19

BEST AVAILABLE COPY

MOV M,A ;STOR REF
MOV E,A ;9'S COMP OF REF
MVT A,9AH
SUB E ;REMOVE REF
ORA A ;CLEAR CARRY
DAA ;DEC ADJ
MOV E,A
STA TEMP+1
IN DTCHP ;INPUT HOR FINE
CMA ;CHG SIGN
ADD E ;REMOVE REF
DAA
MOV D,A
IN DTCHC
CMA
ADD E ;REMOVE REF
DAA
MOV C,A ;PUT IN C
LDA HCCOR ;ADD BORESIT CORR
ADD C
DAA
MOV C,A
CALL AMBIG ;RESOLVE
MOV B,D ;SAVE FINE
POP D
PUSH D
LXI H,HRBPA
DAD D
DAD D
DAD D
MOV M,C ;RAW COARSE
INX H
MOV M,A ;RESOLVED COARSE
INX H
MOV M,B ;STOR FINE
LDA TEMP+1
MOV E,A
IN DTCVF ;INP VERT FINE
CMA ;CHG SIGN
ADD E ;REMOVE REF
DAA ;DEC ADJ
MOV D,A
IN DTCVC ;INP VERT COARSE
CMA ;CHG SIGN
ADD E ;REMOVE REF
DAA ;DEC ADJ
MOV C,A
LDA VCCOR ;ADD BORESIT CORR
ADD C
DAA
MOV C,A
CALL AMBIG ;RESOLVE
MOV B,D ;FINE
POP D ;GET INCREMENT
LXI H,VTBPA
DAD D
DAD D
DAD D

B7

0018 71
0019 23
001A 77
001B 23
001C 70
001D 3A 3F 10
0020 D3 RF
0022 C9

MOV M,C ;RAW COAR
INX H
MOV M,A ;RESOLVED COARSE
INX H
MOV M,B ;FINE
LDA SYSCM ;TURN PLL ON
OUT SYCTL
RET

;A C MARSHALL APR 16, 1976

;:
;SYNCH--SYNCHRONIZATION ROUTINE
;OPFRATES ONLY ONCE ON INITIALIZATION
;CALLED BY INITL
;

0023 CD 86 08
0026 DB FF
0028 E6 01
002A CA F5 09
002D 21 05 10
0030 3A 12 10
0033 BF
0034 C2 C8 09
0037 DB FC
0039 47
003A 3A 3E 10
003D 4F
003F 21 09 10
0041 85
0042 6F
0043 70
0044 79
0045 3C
0046 32 3F 10
0049 3A 44 10
004C B7
004D 79
004E CA 09 09
0051 FF 07
0053 C2 F2 09
0056 21 09 10
0059 0E 00
005B 06 07
005D 7F
005F 23
005F 86
0060 DC FA 09
0063 05
0064 C2 5F 09
0067 16 03
0069 B7
006A 47
006B 79
006C 1F
006D 4F
006E 78
006F 1F
0070 15
0071 C2 69 09
0074 4F
0075 CD FC 09

SYNCH: CALL INCRC
IN TMCC ;GET STATUS
ANI SKFDG ;EDGE?
JZ SRET2 ;NO
LXI H,BVCT
LDA SYBYT
CMP M ;SAME BYTE?
JNZ SYNC4 ;NO
SYNC3: IN TMCA ;GET DATA
MOV B,A ;SAVE DATA
LDA SYCTR ;
MOV C,A ;SAVE SYCTR
LXI H,SDTBL ;TABLE ADDR
ADD L ;INDEX ADDR
MOV L,A
MOV M,B ;SAVE DATA
MOV A,C ;RETN TO SYCTR
INR A
STA SYCTR ;INCREMENT COUNTER
LDA CTMOD
ORA A ;CSET COND BITS
MOV A,C ;RESTR SYCTR
JZ SYNC5
CPI 7 ;8EDGES?
JNZ SRET1 ;NO
LXI H,SDTBL ;YES, AVE 8 MEAS
MVI C,0 ;INCR STORAGE
MVI B,7 ;ADD 8 ELEMENTS
MOV A,M ;GET FIRST
SLOP1: INX H ;ADDR NEXT
ADD M ;ADD ELEM
CC SYCRY ;CARRY
DCR B ;NO
JNZ SLOP1 ;DO NEXT
MVI D,3 ;DIV BY 8
SYROT: ORA A
MOV B,A
MOV A,C
RAR
MOV C,A
MOV A,B
RAR
DCR D
JNZ SYROT
SYNC2: MOV C,A ;SAVE N
CALL SRTMC ;RESET TIME COUNTER

BEST AVAILABLE COPY

BEST AVAILABLE COPY

B8

0078 32 06 10
0079 79
007C 06 10
007F 27
007F 47
0080 32 11 10
0083 3E 0A
0085 00
0086 B7
0087 27
0088 06 87
008A 05
008B C2 8A 09
008F 3C
009F 27
0090 C2 88 09
0093 3A 3D 10
0096 EE 60
0098 D3 EE
009A EE 60
009C D3 EE
009E 3A 11 10
00A1 EE 0A
00A3 3E EE
00A5 0A A9 09
00A9 3C
00AA 32 02 10
00AC 32 05 10
00AF AF
00B0 32 01 10
00B3 32 04 10
00B6 EB
00B7 C3 2B 00
00BA 0C
00BB C9
00BC 3A 3D 10
00BF EE 20
00C1 D3 EE
00C3 EE 20
00C5 D3 EE
00C7 C9
00C9 3A 44 10
00CB B7
00CC C2 F2 09
00CF 32 3F 10
00D2 7E
00D3 32 12 10
00D6 C3 F2 09
00D9 EE 03
00DB C2 F2 09
00DE 2F
00DF 32 44 10
00E2 CD BC 09
00E5 D1
00E6 D1
00E7 D1
00E8 D1
00E9 D1
00EA EB
00EB 76

STA BGNCT ;SET BEGIN MAIN SWITCH
MOV A,C ;DELAY
ADI 10H ;CALC (10 PLUS N)MOD 100
DAA ;MOD 100
MOV B,A ;BCD DELAY
STA SYDEL ;NR OF MSEC DELAY
MVI A,9AH
SUB B
ORA A ;CLEAR CARRY
DAA ;DEC ADJ
SLOP2: MVI B,135 ;1MSEC EACH LOOP
SLOP3: DCR B ;2.44USEC
JNZ SLOP3 ;4.88USEC
INR A
DAA
JNZ SLOP2
LDA TCMWD
XRI SKSET XOR RTMCT ;RESET TIMING
OUT TMCC
YRI SKSET XOR RTMCT
OUT TMCC
DLTST: LDA SYDEL
CPI 10 ;LESS THAN 10 MSEC?
MVI A,0FFH
JC NOINC ;YES, SAME BYTE
INR A
NOINC: STA BYCTR
STA BYCT
XRA A
STA BYCTR-1
STA PRCTR
EI ;ENABLE INT
JMP GETCM ;GO TO NON BACKGROUND
SVCRY: INR C
RPT
SRTMC: LDA TCMWD ;RESET TIME COUNTER
XRI RTMCT
OUT TMCC
XRI RTMCT
OUT TMCC
RPT
SYNC4: LDA CTMOD
ORA A ;COUNT MODE?
JNZ SRET1 ;NO, IGNORE EDGE
STA SYCTR ;ZERO SYCTR
MOV A,M ;GET BYTE CTR
STA SYBYT
JMP SRET1 ;NO
SYNC5: CPI 3 ;3 EDGES?
JNZ SRET1 ;NO
CMA ;YES
STA CTMOD ;SET MODE
SRET1: CALL SRTMC
SPET2: POP D ;RESET STAK PTR
POP D
POP D
POP D
POP D
EI ;ENABLE INT
HLT ;WAIT FOR INTERRUPT

09EC D3 F6
 09FE F6 02
 09F0 32 40 10
 09F3 C3
 09F4 21 00 10
 09F7 16 42
 09F9 7F
 09FA 2F
 09FB D3 F5
 09FD 3E FF
 09FE D3 F6
 0A01 FF 10
 0A03 D3 F6
 0A05 06 07
 0A07 CD 17 0A
 0A0A 23
 0A0B 15
 0A0C C2 F9 09
 0A0F CD 1C 0A
 0A12 C3 29 0A

0A15 06 05
 0A17 05
 0A18 C2 17 0A
 0A1B C9
 0A1C 3F 14
 0A1E 06 37
 0A20 05
 0A21 C2 20 0A
 0A24 3D
 0A25 C2 1F 0A
 0A28 C9

0A29 21 A0 10
 0A2C 16 20
 0A2F 0F F4
 0A30 2F
 0A31 77
 0A32 3F 0F
 0A34 D3 F6
 0A36 0F 20
 0A38 D3 F6
 0A3A CD 15 0A
 0A3D 23
 0A3E 15
 0A3F C2 2F 0A
 0A42 C9

```

;
; AC MARSHALL, MAR 3, 1976
; WANG IO ROUTINE
; OPERATES DURING INTERRUPT;
; WANG - SYSTEM
WANG0: IN WNGIO      ;GET CPB
        ANI CPB
        STA TEMP
        RZ           ;RETN IF ZERO
        LXI H,1000H;INPUT ARRAY
        MVI D,66     ;ARRAY SIZE +2
B2:     MOV A,M       ;GET DATA
        CMA          ;INVERT
        OUT WNGIO    ;OUTPUT IT
        MVI A,0FFH XOR IBS ;STROBE IBS
        OUT WNGIO
        XRI IBS      ;NEXT ADDR
        OUT WNGIO    ;DONE?
        MVI B,7      ;75 USEC REP RATE
        CALL VDEL1
        INX H         ;NO, LOOP
        DCR D         ;DONE?
        JNZ B2        ;NO, LOOP
        CALL DELAY
        JMP WANG1

```

```

;
DEL1: MVI B,5        ;SHORT DELAY
VDEL1: DCR B
        JNZ VDEL1
        RET
DELAY: MVI A, 20
DLP2:  MVI B,135
DLP1:  DCR B
        JNZ DLP1
        DCR A
        JNZ DLP2
        RET

```

```

; AC MARSHALL, MAR 3, 1976
; WANG IO ROUTINE
; OPERATES DURING INTERRUPT;
; SYSTEM - WANG
WANG1: LXI H,CONST;OUTPUT ARRAY
        MVI D,20H ;ARRAY SIZE
INPT1: IN WNGIO   ;INPUT
        CMA
        MOV M,A   ;STORE BYTE
        MVI A,0FFH XOR ACK;STROBE ACK
        OUT WNGIO
        XRI ACK
        OUT WNGIO
        CALL DEL1 ;60USEC REP RATE
        INX H
        DCR D     ;DONE?
        JNZ INPT1 ;NO, LOOP
        RET

```

```

; AMBIGUITY RESOLUTION SUBROUTINE
; ENTRY AND CALL
;     MOV D,REGM (FINE 2 DIGIT DATA)
;     MOV C,REGM (COARSE 2 DIGIT DATA)
;     CALL AMBIG

```

BEST AVAILABLE COPY

B10

```

;      USES A,B,C,D,H,L,FF'S
;      EXIT COARSE IN A, FINE IN D
;      PAW COARSE IN C
;
0A43 06 04      AMBIG: MVI    B,FOUR      ;SET COUNTER
0A45 79          MOV    A,C            ;GET COARSE
0A46 05      LOOP1: DCR    B            ;CTR-1
0A47 0F          RRC                  ;ROTATE RIGHT 1 BIT
0A48 C2 46 0A    JNZ    LOOP1          ;4 TIMES?
0A4B E6 0F      ANI    LSD            ;YES, C1 IN LSD POS
0A4D 67          MOV    H,A            ;SAVE C1
0A4F 7A          MOV    A,FINE         ; GET FINE
0A4F 06 04      MVI    B,FOUR         ;SET COUNTER
0A51 05      LOOP2: DCR    B            ;CTR-1
0A52 0F          RRC                  ;ROTATE RIGHT 1 BIT
0A53 C2 51 0A    JNZ    LOOP2          ;4 TIMES?
0A56 E6 0F      ANI    LSD            ;MASK FOR LSD
0A58 67          MOV    L,A            ;SAVE F1 IN LSD
0A59 79          MOV    A,C            ;GET COARSE
0A5A E6 0F      ANI    LSD            ;C0 IN LSD
0A5C 95          SUB    L              ;C0-F1
0A5D D2 64 0A    JNC    POS            ;ANS IS POSITIVE
0A60 2F      NEG:   CMA                  ;2'S COMP OF ANS FOR ABS
0A61 3C          INR    A              ;MASK
0A62 E6 0F      ANI    LSD            ;MASK
0A64 EF 05      POS:  CPI    FIVE       ;COMPARE WITH FIVE
0A66 DA 77 0A    JC     SAME           ;ABS VAL <5
0A69 79          MOV    A,C            ;GET COARSE , ABS VAL>=5
0A6A E6 0F      ANI    LSD            ;C0 IN LSD
0A6C EF 05      CPI    FIVE           ;C0 >=5?
0A6E 7C          MOV    A,H            ;NO, GETC1 IN LSD
0A6F D2 79 0A    JNC    INC1          ;YES
0A72 C6 09      DEC1: ADI    9          ;NO, C2=C1-1
0A74 C3 7A 0A    JMP    EXIT
0A77 7C      SAME:  MOV    A,H          ;GET C1 IN LSD
0A78 C9          RET                  ;C2=C1
0A79 3C      INC1:  INR    A            ;C2-C1+1
0A7A 27      EXIT:  DAA                  ;ADJ DEC
0A7B E6 0F      ANI    LSD            ;C0 IN LSD
0A7D C9          RET
;
END

```

BEST AVAILABLE COPY

SYMBOL TABLE

ABYTE	1007	ABYTS	1008	ACK	0020	AMBIG	0A43
ASAVE	13F2	B2	09F9	BGNCT	1006	BYCT	1005
YCTR	1002	BYTPP	0877	CLRTM	084D	CONST	10A0
CPB	0002	CTMOD	1044	DEC1	0A72	DEL1	0A15
DELAY	0A1C	DL21	0A20	DL22	0A1E	DLTST	099F
DOPB	0001	DTCH	00DF	DTCHC	00DD	DTCHF	00DC
DTCR	00DE	DTCV	00BE	DTVCV	00BD	DTCVF	00BC
DTMOD	0003	DTSTR	08B4	EXIT	0A7A	FINE	0002
FIVE	0005	FOUR	0004	FRCTR	1004	FRPR2	0876
GETCM	002B	HCCOR	10A0	HRBFA	1019	HRBFB	101C
HRBFC	101B	HRBFD	1022	HRBFF	1025	HRBFF	1028
IPS	0010	TNC1	0A79	TNCB1	08A3	INCB	0886
INCB	08A7	INITL	0800	INPT1	0A2E	TNT	0004
INTPR	085A	LOOP1	0A46	LOOP2	0A51	LSAVE	13F3
LSR	000F	LSO	000F	MAIN	0865	MSB	00F0
MSTAK	13ED	NEG	0A60	NOINC	09A9	PLLBT	0010
POS	0A64	PSAVE	13F5	RFBFA	1013	RFBFB	1014
RFBFC	1015	RFBFD	1016	RFBFE	1017	RFBFF	1018
RTMCT	0020	SAME	0A77	SDTBL	1009	SGLVL	0002
STOPT	083F	SKEDG	0001	SKSET	0040	SLOP1	095E
SIOP2	0988	SIOP3	098A	SPET1	09E2	SRET2	09E5
SPTMC	09BC	SSAVE	13F7	SSTAK	083C	STACK	13A0
SVBYT	1012	SYCRY	09BA	SYCTL	00BE	SYCTR	103E
SYDEL	1011	SYNC2	0974	SYNC3	0937	SYNC4	09C8
SYNC5	09D9	SYNCH	0923	SYROT	0969	SYSCM	103F
TCMWD	103D	TEMP	1040	TMCA	00EC	TMCB	00ED
TMCC	00EE	TMCTL	00EE	VCCOR	10A1	VDEL1	0A17
VTBFA	102B	VTBFB	102E	VTBFC	1031	VTBFD	1034
VTBFF	1037	VTBFF	103A	VTMOD	0093	WANGI	0A29
WANGO	09EC	WNCTL	00F7	WNGIO	00F6	WNIDT	00F4
WNMOD	0091	WNOUT	00F5	ZERO	0000		

BEST AVAILABLE COPY

APPENDIX C
Perspective Display Program

APPENDIX C. PERSPECTIVE DISPLAY PROGRAM

```
5  DIM A(12,6),A0(6,12),A1(6,6),A2(6,6),A3(6),B(12),E(6),R(2,3),P(6,2),P1(6,3),  
    H(6),V(6)  
10  DIM B0$64,C$32  
12  DIM P2(6,2),P3(6,3)  
15  C$ = HEX(0000567890ABCDEFFEDCBA9876543210112233445566778899AABBCCDDEEFF34)  
20  T$ = HEX(A2002020)  
25  U$ = HEX(8600C6402020)  
30  INPUT "L/W RATIO",L  
35  INPUT "HEX PATTERN WIDTH RATIO",W  
  
45  INPUT "INITIAL THETA,BETA,PHI",H0,E0,I0  
50  INPUT "INITIAL X,Y,Z",X0,Y0,Z0  
55  INPUT "DISTANCE TO SCREEN (MM)",D  
60  G = 0  
65  INPUT "G FACTOR",G  
66  INPUT "G-H,V",G1,G2  
70  PACK (####)STR(C$,1,2)FROM G  
75  R(1,1) = COS(E0)*COS(I0)  
80  R(1,2) = COS(E0)*SIN(I0)  
85  R(1,3) = -SIN(E0)  
90  R(2,1) = SIN(H0)*SIN(E0)*COS(I0) - COS(H0)*SIN(I0)  
95  R(2,2) = SIN(H0)*SIN(E0)*SIN(I0) + COS(H0)*COS(I0)  
100 R(2,3) = SIN(H0)*COS(E0)  
105 P(1,1),P(3,1),P2(1,1),P2(2,1),P2(3,1) = 1  
110 P(2,1) = W  
115 P(4,1),P(6,1),P2(4,1),P2(5,1),P2(6,1) = -1  
120 P(5,1) = -W
```



```
125 P(1,2),P(4,2),P2(1,2),P2(4,2) = L
130 P(2,2),P(5,2),P2(2,2),P2(5,2) = 0
135 P(3,2),P(6,2),P2(3,2),P2(6,2) = -L
140 MAT P1 = P*R

145 FOR I1 = 1 TO 6
150 P1(I1,1) = P1(I1,1) + X0

155 P1(I1,2) = P1(I1,2) + Y0

160 P1(I1,3) = P1(I1,3) + Z0

165 A(2*I1-1,1) = (P1(I1,1)/P1(I1,2))

170 A(2*I1,1) = (P1(I1,3)/P1(I1,2))

175 NEXT I1

180 FOR I2 = 1 TO 6
185 H(I2) = A(2*I2-1,1)*D*64/161
190 V(I2) = A(2*I2,1)*D*16/108
195 NEXT I2

200 H8 = R(2,1)/R(2,2)*D*64/161
205 V8 = R(2,3)/R(2,2)*D*16/108
210 IF COS(E0) = 0 THEN 230
215 IF I0 = 0 THEN 240
220 H9 = TAN(I0/ABS(I0)*PI/2-I0)*D*64/161
```



```
225 GO TO 255
230 E0 = E0-ABS(E0)/E0*1E-5
235 GO TO 215
240 H9 = 1E16
245 V9 = -H9*TAN(E0)
250 GO TO 260
255 V9 = -SIN(E0)/(COS(E0)*SIN(I0))*D*16/108
260 M = (V9-V8)/(H9-H8)
265 PRINT HEX(03)
270 FOR I3 = (31.5-H8) TO -(31.5+H8) STEP -1
275 V7 = V8 + M*I3
280 IF V7 <= -8.5 THEN 320
285 IF V7>7.5 THEN 320
290 PRINT HEX(01)
295 IF V7>6.5 THEN 315
300 FOR I4 = 1 TO (-V7 + 7.5) :PRINT :NEXT I4
305 PRINT TAB(I3 + H8 + 31.5); "-"; HEX(0C)
310 GO TO 320
315 PRINT TAB(I3 + H8 + 31.5); "-"
320 NEXT I3
325 FOR I5 = 1 TO 6
330 IF V(I5) <= -8.5 THEN 375
335 IF V(I5)>7.5 THEN 375
340 IF H(I5)<-31.5 THEN 375
345 IF H(I5)>=32.5 THEN 375
350 PRINT HEX(01)
355 IF V(I5)>6.5 THEN 370
```



```

360 FOR I6 = 1 TO (-V(I5) + 7.5) :PRINT :NEXT I6
365 PRINT TAB(H(I5) + 30.5); I5;HEX(OC) :GO TO 375
370 PRINT TAB(H(I5) + 30.5); I5
375 NEXT I5
380 PRINT HEX(01)
382 PRINT X0,Y0,Z0
384 PRINT H0,E0,I0
386 PRINT HEX(01)
400 $GIO READ /07B (U$,N$)B0$
410 $GIO WRITE /07B (T$,Q$)C$
420 UNPACK(#####)STR(B0$,26,9) TO A(1,2),A(3,2),A(5,2)
430 UNPACK(#####)STR(B0$,44,9) TO A(2,2),A(4,2),A(6,2)
440 UNPACK(#####)STR(B0$,35,9) TO A(7,2),A(9,2),A(11,2)
450 UNPACK(#####)STR(B0$,53,9) TO A(8,2),A(10,2),A(12,2)
460 FOR I7 = 1 TO 11 STEP 2
470 B(I7) = -(A(I7,2)-1000*INT(A(I7,2)/1000)-G1):IF B(I7)<-500 THEN 900:IF B(I7)>500 THEN 910
475 B(I7) = B(I7)/3000-ARCTAN(A(I7,1))
480 A(I7,1),A(I7,2),A(I7,3) = 0
490 NEXT I7
492 FOR I7 = 2 TO 12 STEP 2
494 B(I7) = -(A(I7,2)-1000*INT(A(I7,2)/1000)-G2):IF B(I7)<-500 THEN 920:IF B(I7)>500 THEN 930
495 B(I7) = B(I7)/3000-ARCTAN(A(I7,1))
496 A(I7,1),A(I7,2),A(I7,3) = 0
498 NEXT I7
500 H4 = SIN(E0)*COS(I0)*COS(H0) + SIN(I0)*SIN(H0)
505 H5 = SIN(E0)*SIN(I0)*COS(H0) - COS(I0)*SIN(H0)
510 H6 = COS(E0)*COS(H0)
515 E1 = -COS(I0)*SIN(E0)
520 E2 = -SIN(I0)*SIN(E0)
525 E3 = -COS(E0)
530 E4 = SIN(H0)*COS(I0)*COS(E0)
535 E5 = SIN(H0)*SIN(I0)*COS(E0)
540 E6 = -SIN(H0)*SIN(E0)
545 FOR I8 = 1 TO 6
550 U1 = X0 + P(I8,1)*R(1,1) + P(I8,2)*R(2,1)

```



```

555 V1 = Y0 + P(I8,1)*R(1,2) + P(I8,2)*R(2,2)
560 S1 = V1+2
565 A(2*I8-1,1) = 1/V1
570 A(2*I8-1,2) = -U1/S1
575 A(2*I8-1,3) = 0
580 A(2*I8-1,4) = (V1*H4 - U1*H5)*P(I8,2)/S1
585 A(2*I8-1,5) = (V1*(P(I8,1)*E1+P(I8,2)*E4) - U1*(P(I8,1)*E2+P(I8,2)*E5))/S1
590 A(2*I8-1,6) = (-V1*(P(I8,1)*R(1,2)+P(I8,2)*R(2,2)) - U1*(P(I8,1)*R(1,1)+P(I8,2)*R(2,1)))/S1
595 NEXT I8
600 FOR I9 = 1 TO 6
605 U1 = Z0 + P(I9,1)*R(1,3) + P(I9,2)*R(2,3)
610 V1 = Y0 + P(I9,1)*R(1,2) + P(I9,2)*R(2,2)
615 S1 = V1+2
620 A(2*I9,1) = 0
625 A(2*I9,2) = -U1/S1
630 A(2*I9,3) = 1/V1
635 A(2*I9,4) = (V1*H6 - U1*H5)*P(I9,2)/S1
640 A(2*I9,5) = (V1*(P(I9,1)*E3+P(I9,2)*E6) - U1*(P(I9,1)*E2+P(I9,2)*E5))/S1
645 A(2*I9,6) = -U1*(P(I9,1)*R(1,1)+P(I9,2)*R(2,1))/S1
650 NEXT I9

700 MAT A0 = TRN(A)
710 MAT A1 = A0*A
720 MAT A2 = INV(A1),D1
730 MAT A3 = A0*B
740 MAT E = A2*A3

```



```
750 X0 = E(1) + X0
760 Y0 = E(2) + Y0
770 Z0 = E(3) + Z0
780 H0 = E(4) + H0
785 H0 = H0-2*PI*INT(H0/(2*PI))
790 E0 = E(5) + E0
795 E0 = E0-2*PI*INT(E0/(2*PI))
800 I0 = E(6) + I0
805 I0 = I0-2*PI*INT(I0/(2*PI))
810 GO TO 75
900 B(I7) = B(I7) + 1000:GO TO 475
910 B(I7) = B(I7) - 1000:GO TO 475
920 B(I7) = B(I7) + 1000:GO TO 495
930 B(I7) = B(I7) - 1000:GO TO 495
```




MISSION *of* **Rome Air Development Center**

RADC plans and conducts research, exploratory and advanced development programs in command, control, and communications (C³) activities, and in the C³ areas of information sciences and intelligence. The principal technical mission areas are communications, electromagnetic guidance and control, surveillance of ground and aerospace objects, intelligence data collection and handling, information system technology, ionospheric propagation, solid state sciences, microwave physics and electronic reliability, maintainability and compatibility.